TL.114-61/02

CANADIAN GOVERNMENT PROGRAM
FOR THE AVROCAR
PHASE 1

PROPULSIVE SYSTEM ANALYSIS

500/INT AERO/421

AVRO AIRCRAFT LIMITED

500/INT.AERO/421

CANADIAN GOVERNMENT PROGRAM FOR THE AVROCAR

PHASE I

PROPULSIVE SYSTEM ANALYSIS

February 1961

Issued by:

Avro Aircraft Limited
Malton, Ontario, Canada

Under

Contract TB No. 570345
Serial No. 9BXO-8

Written by:

F.L. Gilbertson
F.L. Gilbertson
Avro Aircraft Limited

Approved by:

T.D. Earl
T.D. Earl
Chief Aerodynamicist
Avro Aircraft Limited

TABLE OF CONTENTS

TABLE OF CONTENTS (cont'd)

List of Illustrations

List of Illustrations (cont'd)

List of Illustrations (cont'd)

List of Illustrations (cont'd)

List of Illustrations (cont'd)

SUMMARY

This report is divided into three main sections: the first dealing with re-engined variants of the existing Avrocar; the second with the design of a lower powered GETOL aircraft; and the third with a heavier and more powerful VTOL version.

The General Electric T 58, both as a shaft driven unit and as a gas generator is considered as a replacement for the J 69 engines of the Avrocar. The three systems are compared with respect to various operating assumptions.

Two elliptic planform GETOL vehicles, powered by two Astazou II engines, are considered next: one propelled by the annular jet deflected aft; and the other by separate propellers. Emphasis is placed on the fan propeller combination in which the fan system provides the ground cushion and the propeller provides the cruising thrust.

Lastly, two verions of VTOL vehicles, similar to the Avrocar but using J 85 engines, are examined: a centrifugal fan version, and a lower pressure ratio axial fan version employing a central jet. Emphasis is placed on the latter which was found to be the best.

A summary of salient propulsive system details is found in Table I, following Section 5.

1.0 INTRODUCTION

This report presents the propulsive system analysis conducted under Phase I of the Canadian Government Program for the Avrocar. Both VTOL and GETOL developments of the Avrocar are considered.

The main body of the report is broken down into separate sections for different families of designs, the three engined versions, the Astazou powered GETOL aircraft, and the J 85 powered VTOL design.

Illustrations of all the configurations to be considered are found in Figs. 1.1 to 1.7.

There is an Appendix to this report in which will be found an outline of the methods followed in the calculation and a detailed consideration of the effects of fan and nozzle size, fan pressure ratio, duct loss, etc. on typical lifting fan systems. The methods used are obtained from Ref. 1 and Ref. 2.

2.0 T 58 POWERED VERSIONS

2.1 Alternative Powerplants

Two suggestions for re-engining the Avrocar have been compared to the present arrangement. The method has been to work out basic values of thrust and specific fuel consumption as functions of Mach No. for each configuration. Many assumptions have to be made to arrive at these basic curves, so the effect on the curves of changes in these assumed parameters is next studied. Although the parameters are varied one at a time, the cumulative effect of several variations can be easily estimated.

Cases will be described by a letter and a number such as "B-3", where "B" refers to the powerplant being considered (see below) and "3" refers to the operating assumption (see Section 2.2). Examples are given in Fig. 2.1.

The following powerplants and associated fan drive systems were considered:

Case "A" 3 Continental J69-T-9 discharging into 95% efficient 'tusks' leading to an 80% efficient tip turbine. The turbine exhaust mixes with the fan flow. The engines weigh 364 lb. each.

Case "B" 3 General Electric T58-GE-6 driving the fan through a 95% efficient set of shafts and gears. The engines exhaust separately from the fan flow. Each engine weighs 271 lb. and its gearbox 75 lb.

Case "C" 3 General Electric T58-GE-6 with their output turbines removed so that the engine becomes a simple jet engines. Performance estimates were made from model spec. E-1012 assuming that the efficiency of the removed turbine was 90%. The engines discharge into 95% efficient 'tusks' leading to an 80% efficient tip turbine. The turbine exhaust mixes with the fan flow. The engines, stripped of their output turbines, weigh about 250 lb. each.

2.2 Alternative Operating Assumptions

The following operating assumptions were considered for each powerplant. The number indicating each condition applied to the graphical presentation as stated in Section 2.1.

1. The basic case - Sea Level. 100% ram recovery at fan and engine intakes. Duct loss coefficient K = 0.3. The fan is 85% efficient and operates at 1.10 pressure ratio. Fig. 2.2 compares the basic cases for the 3 alternative powerplants.

2.2 Alternative Operating Assumptions (cont'd)

2. The fan pressure ratio is 1.20. Otherwise the same as the basic case.

3. The fan and engine intake pressure recovery is reduced to values measured on the 1/5th scale Avrocar model.

4. Only 90% of the gross thrust at the nozzle is considered useable.

5. 20,000 ft. altitude.

6. Supercharged engines. That is, the engine intake is relocated inside the duct. No loss is assumed between the fan and the engine.

2.3 Discussion of Operating Assumptions

(a) Fan Efficiency = 85%

Orenda Engines Limited in their design of the Avrocar fan, show its peak efficiency to be 89%. 85% allows for a small amount of off design operation.

(b) Tip Turbine Efficiency = 80%

Orenda Engines Limited estimated the maximum efficiency to be 83.4%.. Again 80% allows for a measure of off design operation.

(c) Duct Loss $K = 0.3 = \frac{\Delta P}{q_{fan}}$

That is to say that the total pressure loss between the fan and nozzles is .3 times the dynamic pressure immediately behind the fan. This is what would be expected from a cleaned up Avrocar. It would be conservative if there was a large central jet.

(d) Tusk Efficiency = 95%

Tests have shown an average total pressure loss of 5% through the tusk-shaped duct delivering engine exhaust gas to the tip turbine.

2.3 Discussion of Operating Assumptions (cont'd)

(e) T58 As a Gas Generator

General Electric has confirmed the feasibility of removing the output free turbine from the T58 to convert it to a jet engine. The total temperature of the jet can be found from the JPT, HP, and air flow of the standard engine. The efficiency of the output turbine was estimated to be 90%. The total pressure of the jet is then determined.

Note that the standard engine considered was the 1050 HP model. A 1250 HP model will be available shortly and this engine will give 19% more power with a slightly lower SFC and only 4 lb. more weight.

(f) Equating Total Pressures behind Fan and Turbine

This is only an approximation made to simplify calculations for tip turbine configurations. In fact when fan and turbine exhaust flows meet, the static pressures must be equal and the turbine exhaust total pressure will be slightly greater than the total pressure in the fan flow. The approximation makes the results for cases A and C (cases with tip turbine) slightly optimistic, but the error is not significant. However, since these cases assume complete mixing of the hot and cold flows before the nozzle, which is unlikely in practice, the result is again optimistic.

(g) Equating Nozzle Static and Atmospheric Pressures

This assumption is valid in free air but yields slightly optimistic results in the ground cushion where the static pressure at the nozzles is above atmospheric.

(h) Supercharging.

This is discussed in some detail in Section 2.5.

2.4 Performance with Various Operating Assumptions

The curves of thrust and SFC vs Mach number for the three basic cases, A-1, B-1, and C-1, are shown in Fig. 2.2.

Figs. 2.3 to 2.7 show the performance of the J69 (case A) version operating under its basic condition compared with operation under the other five conditions described in Section 2.3.

2.4 Performance with Various Operating Assumptions (cont'd)

It is anticipated that if more than one variation of the basic case is to be considered at the same time, an idea of the result can be had by taking the sum of the variations, from the basic case. However, Fig. 2.8 has been included to give a more accurate combination of operating conditions 2, 3 and 4, which make up a typical case.

Figs. 2.9 to 2.13 show the performance of the T58 shaft drive version (case B) with various operating assumptions.

Figs. 2.14 to 2.18 show the performance of the T58 gas generator verions (case C) with various operating assumptions.

As noted in Section 2.3, cases A and C may be slightly optimistic.

Note that case B has a rather different shape of curve to A and C, falling off more with forward speed. This has two causes:

(i) The separate exhaust for the turboshaft engine is a fixed size. It provides some static thrust but at high speed has a negative net thrust.

(ii) Heating the fan flow, as in cases A and C, increases the velocity at the nozzle and improves net thrust, particularly at speed.

The leveling of the thrust curve at high speed in case A may not be significant since data for these speeds was extrapolated.

In summary, the advantage of using the T58 as in cases B and C is its better SFC and lower weight. Its lower thrust is not significant due to the more powerful version available.

The advantages of a gas generator, as in cases A and C are:

(i) Less fall off in thrust at high speed due to heating of the fan flow.

(ii) No gearbox with its weight, lubrication, load sharing, and engine out problems.

The advantages of shaft drive, as in case B, are:

(i) More static thrust due to the use of a 90% efficient, close tolerance reaction, turbine instead of the 80% impulse design tip turbine.

2.4 Performance with Various Operating Assumptions (ont'd)

(ii) A minimum of hot ducts to insulate and cool.

(iii) A growth potential by merely strengthening the shafts and gears whereas the gas generator versions would require new tusks and tip turbine.

2.5 Engine Supercharging

It will be noted in the following sections that there is a slight gain to be had by supercharging the engines, that is, by locating their intakes in the flow from the fan. However, recall that no loss has been assumed between the fan and the engine. This might be a fair approximation for case B-6, where the installation could look like:

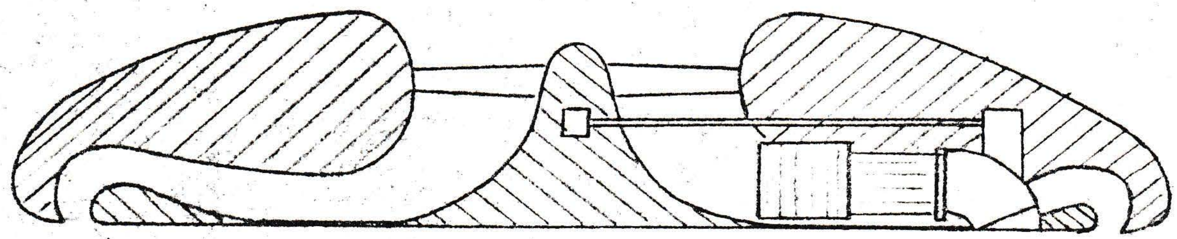

But for cases A and C there seems to be little alternative to a layout like the early Avrocar, represented by A-6:

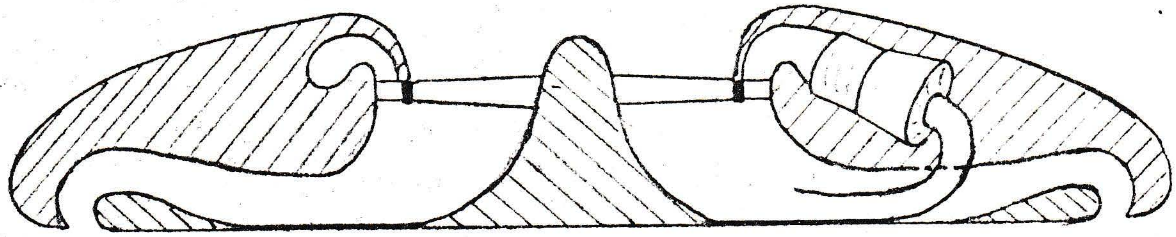

The loss in this arrangement can hardly be negligible.

2.5 Engine Supercharging (cont'd)

An earlier calculation on supercharging the Avrocar indicated 108% of normal thrust when there was no loss between the fan and engine. Allowing for anticipated duct loss this fell to 104-1/2%. Considering an additional 20°C temperature rise in the duct, the thrust became 96-1/2% of the thrust available when the engines were breathing from outside. Therefore, some gain can be obtained from supercharging but not enough to justify compromising other features of the design. The use of intake ducts with significant loss or with heat transfer into them may more than cancel any gain.

3.0 GETOL TYPE VEHICLES

In order to provide true VTO performance along with useful payload, speed, and range, the designs grew to be of the order of 10,000 lb. AUW. A new approach was sought that would make the vehicle lighter, simpler, and cheaper to build and operate. The key to this approach is the use of a ground cushion for take-off and landing. This reduces the power required and the powerplant weight. The smaller engines are more efficient at cruise power settings and so the fuel load is much less. The final design weighed less than 7,000 lbs.

The initial design was for a circular planform vehicle with a wing area of 314 sq.ft. However, in order to reduce the induced drag for short take-off, the planform was changed to a 353 sq.ft. elliptic wing having the same effective diameter (20 ft.) and hence the same ground cushion performance.

3.1 Axial Fan versus Centrifugal Fan

Early layouts of the GETOL vehicle featured a centrifugal impeller. This was considered attractive because its radial delivery allowed installation in a thin wing and simplified the ducts to the peripheral nozzle. However, such an impeller is not as efficient as a corresponding axial fan, and its ability to provide a large pressure rise in a single stage is not an advantage for this type of vehicle where only low pressures are required.

Fig. 3.1 compares the two types of compressor when driven by 1044 HP. The axial fan was considered to be 85% efficient and to have a duct loss coefficient, K, of .30. The centrifugal impeller is less efficient (80%) but has less duct loss (K = .20). The axial fan is shown to be superior as long as the fan (and ducts) can be made reasonably large.

3.2 Power Required

From first layouts involving 2 Astazou turbo-shaft engines of 360 HP each, the design was shown to be underpowered. Finally, the Astazou II was selected. This engine is rated at 522 HP, has a better SFC and weighs no more than the 360 HP version. With 1044 HP installed in a 4,400 lb. vehicle the take-off distance to clear 50 ft. is about 600 ft.

It should be noted that there is a wide variety of engines available that can produce the required HP, or slightly more, so there is every prospect of a HP stretch or a powerplant weight reduction if required. The Astazou II and some of the alternatives are compared below:

3.2 Power Required (cont'd)

No. of Engines	Type	SFC	Total HP at T/O	Total Weight
2	Astazou II	.66	1044 HP	550 lb.
1	Bastan V	.68	1000 HP	482 lb.
2	Artouste III	.65	1100 HP	820 lb.
1	Turmo IIIC	.68	1100 HP	-
1	T58-GE-6	.64	1050 HP	271 lb.
1	T58-GE-8	.61	1250 HP	285 lb.
2	Boeing 520-6	.65	1100 HP	520 lb.
2	Continental	.67	1000 HP	490 lb.
2	P & W PT6-A-2	.69	1000 HP	500 lb.

3.3 Selection of Fan Pressure Ratio and Fan Area

The lower the fan pressure ratio the greater can be the thrust produced by a fixed amount of horsepower. There are, however, two factors imposing a lower limit to feasible pressure ratios. First, low pressure ratios mean high mass flows and great sensitivity to duct loss; i.e. they can only be used in conjunction with large fans and large clean ducts. Second, the momentum of the large intake airflow must be efficiently converted into pressure energy and recovered at the nozzle to avoid a crippling momentum drag in forward flight.

The performance objectives required 2400 lb. of nozzle thrust statically to give an adequate hovering height plus a thrust for 0.2g acceleration. From Figs. A.3 and A.4 of Appendix 'A', assuming a value of the duct loss factor K between .3 and .4, A_e/HP would be about 2.1, allowing for a thrust loss of about 5%. The fan drive efficiency is taken as 97% so that the fan area would be 2.1 x 1044 x .97 = 2130 sq.in. On this basis, a fan area of 15 sq. ft. (1160 sq.in.) was chosen. Although the optimum fan pressure ratio would be about 1.055, pressure ratios of 1.05 to 1.065 would give almost equal hover performance with take-off power.

However, if the engines are throttled back the fan rpm and hence pressure ratio will decrease. Similarly, in forward flight where the ram pressure tends to increase the density of the air in the ducts, if the nozzles are not restricted the fan pressure ratio will fall. Then to achieve maximum performance there must be some method of uniformly making small adjustments to the nozzle areas.

3.4 Evaluation of Duct Losses

A comprehensive set of data for the determination of pressure losses in duct components is found in Ref. 3.

3.4.1 Intake Pressure Recovery

While hovering, $\Delta P/_q$ is assumed to be about .10 which results in a pressure recovery of .9972.

At M = .4 the air should flow into the intake quite smoothly giving a pressure recovery of .985. However, below M = .4 the pressure recovery will involve a combination of the above two conditions, as assumed in Fig. 3.2.

3.4.2 90° Bend Below Fan

For minimum duct loss in this section, the arrangement shown in Fig. 3.3 would be recommended. It consists of splitting the duct into four segments and adding an annular guide vane. This immediately improves the radius ratio - $\frac{\text{(duct radius)}}{\text{duct width}}$ while maintaining a reasonable aspect ratio for each section of the duct. Based on this geometry a duct loss $\frac{\Delta P}{q_{fan}}$ = .086 could be expected.

3.4.3 Wing Ducting

This consists of 36 straight walled ducts leading to the exit nozzle assemblies. Based on diffusion angle the average $\frac{\Delta P}{q}$ = .027, or .021 based on fan dynamic pressure. In most of the ducts a bend is required at the entrance to the exit nozzle assemblies. Considering cascades to be installed in bends exceeding 20° the average $\frac{\Delta P}{q}$ = .0893, or .048 based on fan dynamic pressure.

3.4.4 Exit Nozzle

Due to wing structure, the nozzle exit assembly is restricted to a depth of about 5 inches which requires a small radius bend. The resulting small ratio of bend radius to passage depth would give a high duct loss but an improvement may be gained by adding a turning vane to increase the radius ratio. Still further improvement would be gained by adding splitter plates to reduce the aspect ratio of the individual ducts. With this arrangement, which is shown in Fig. 3.4, a duct loss $\Delta P/_q$ = .16 could be achieved.

3.5 Operating Assumptions

Powerplants: Two Astazou II engines rated at 522 SHP (take-off power).

Note: The information available for the Astazou II engine is limited to take-off and maximum continuous power settings. Data from the T58 was used as a guide for determining the fuel flow corresponding to various percentages of maximum continuous power.

Power transmission efficiency		=	97%
Engine intake efficiency		=	100%
Fan intake efficiency		=	85%
Fan area	= 15 sq. ft.	=	2160 sq.in.
Total duct loss factor	$\frac{\Delta P}{q_{fan}}$	=	0.32

Total nozzle exit area :

1950 sq.in.	at M	=	0
1200 sq.in.	at M	=	.1
940 sq.in.	at M	=	.2
800 sq.in.	at M	=	.3
740 sq.in.	at M	=	.4

Gross thrust recovery = 95%

3.6 Performance

Considering the sea level case at take-off power for a range of pressure ratios, we obtain the thrust curves shown in Fig. 3.5. Optimum thrust occurs at fan pressure ratios ranging from 1.055 at M = 0 to 1.14 at M = .9. However, this range of pressure ratios is too great for the fan to accept. Therefore, we have selected the variation of areas as shown in Fig. 3.6 which results in the variation of fan pressure ratio from 1.06 at M = 0 to 1.094 at M = .4, for take-off power. The selected variation of nozzle exit area with Mach number is shown replotted in Fig. 3.7. This variation of exit area is not affected by reduced power or altitude.

On the basis of these exit areas, the thrust for a range of power settings and Mach numbers at sea level was calculated as shown plotted against fan pressure ratio in Fig. 3.8. In Fig. 3.9 the sea level thrust is replotted against Mach number for a range of power settings. The drag curve is included in Fig. 3.9.

3.6 Performance (cont'd)

Specific fuel consumption $\frac{\text{lb. fuel/hr}}{\text{thrust horsepower}}$ for various power settings and at sea level is shown in Fig. 3.10. Figs. 3.11, 3.12, and 3.13 show thrust, drag and specific fuel consumption at 10,000 feet.

Residual engine thrust has been added to the basic fan thrust for all speeds except M = 0. From Fig. 3.9 and 3.12 we see that the cruise speed will vary from M = .33 at sea level to M = .36 at 10,000 ft. The top speed at sea level is 268 mph.

3.7 Propeller Version

Looking at the thrust curves of the preceding paragraphs, one is struck by how small the thrust horsepower is, at speed, compared to the engine horsepower.

For example, at 268 mph, $THP = T \times \frac{V}{550} = 800 \times \frac{268}{550} \times \frac{5280}{3600} = 572$ HP

whereas the two engines are producing about 1170 HP. That is, the efficiency of the energy transfer from the engines to the air is 49%. With a propeller we can expect an 80% efficient transfer, assuming 5% mechanical loss and an 85% efficient propeller. Of course, this 80% does not apply right down to zero speed. It has been assumed that the static thrust is limited to 3.5 lb. per engine HP.

The thrust of a propeller driven vehicle at take-off and maximum power is given at various altitudes in Fig. 3.14. The corresponding fuel consumption is shown in Fig. 3.15. Figs. 3.16 to 3.19 show the thrust and SFC for a wide range of power settings.

3.8 Comparison of Fan and Propeller Version

A comparison of Fig. 3.9 and 3.16 shows the propeller version to be far superior to the fan version. The fan version can produce only about 60% of the thrust of the propeller version. However, due to higher weight of the propeller version (6,600 lb.), the drag is higher for this vehicle. Based on the estimated drags, the power required for cruise is given for each vehicle in Fig. 3.20. The lower drag of the fan version partially compensates the higher thrust of the propeller version, so that the latter is not very much faster at take-off power. But for typical cruise speeds the propeller version needs up to 16% less power and so will have much improved range.

4.0 VTOL TYPE VEHICLES

These vehicles were of circular planform and powered by two J85 engines rated at 2700 lb. static thrust at sea level.

For the first vehicle, considered in Sections 4.1 and 4.2, the engines were mounted so as to exhaust into a common duct to drive a turbine. The turbine was geared to a centrifugal fan operating at a pressure ratio of 1.5. Although the centrifugal fan has a lower efficiency than the axial fan, there is a reduction in duct loss since the 90° bend necessary below the axial fan is eliminated, (i.e. with the peripheral jet arrangement used).

In addition, the free turbine may be designed to a higher efficiency than a tip turbine (approximately 88%, as opposed to 80%) allowing a greater HP to be extracted from the engine flow. As was pointed out in para 3.1, the advantages of the less efficient centrifugal fan are not realized at low fan pressure ratios. Hence, the compromise pressure ratio of 1.5 was selected. On this basis the low pressure ratio axial fan will be much superior at low speeds, but the centrifugal fan will give better performance at high speeds due to the lower fan flow and momentum drag.

The axial fan version which employs a central jet is considered in Sections 4.3 to 4.5.

A third vehicle, briefly considered in the design stage, was similar to the axial fan version employing the J85 powered axial fan system for hover and low speeds only. Two T58 engines, with power turbines removed, powered the vehicle in cruising flight. Thus fuel consumption in cruise was reduced considerably. However, such a design would involve additional weight and expense, and have a slightly lower speed. The design was therefore discontinued.

4.1 Operating Assumptions - Centrifugal Fan Version

Engine intake pressure recovery	=	100%
Turbine efficiency	=	88%
Turbine pressure ratio		set arbitrarily at 2.3:1 (with take-off power, the resulting turbine exit total pressures range from 15.5 psi at M = 0 to 21.9 psi at M = .9)

4.1 Operating Assumptions - Centrifugal Fan Version (cont'd)

Power extracted from turbine (Sea Level):

8500 HP	at M =	0
8670 HP	at M =	.2
9310 HP	at M =	.4
10320 HP	at M =	.6
13650 HP	at M =	.9

Fan drive efficiency = 95%

Fan intake pressure recovery as per 1/5th scale Avrocar model tests, extended as a quadratic (Fig. 4.1)

Fan operating efficiency = 80%

Fan exit area = 1000 sq. in.

Duct losses:

Peripheral nozzles $P/q_{fan} = K = 0.2$

Jet pipe = 98% total pressure recovery from turbine

Gross thrust recovery = 95% at all speeds

Total pressure loss, = 5% (engine thrust case)

4.2 Performance - Centrifugal Fan Version

Maintaining a constant fan pressure ratio of 1.5 with military power produces the variation of nozzle exit area with forward speed as shown in Fig. 4.2.

The performance at sea level and 20,000 ft. with military power is given in Figs. 4.3 and 4.4 which show net thrust vs Mach number. Residual engine thrust has been added to all forward speed fan thrusts. For the hover case it is assumed that this residual thrust will be spoiled in some manner since to divert it downward to increase hover thrust would impose control problems. The approximate drag curves have been shown which indicate a sea level top speed of about 583 mph.

It was considered if it would be practical to close the fan down and operate on engine thrust alone during high speed flight From Figs. 4.3 and 4.4 it can be seen that the increase in sea level top speed would be about 50 mph while at altitude the gain would be even greater. However, the drag rise Mach number for such a vehicle would probably occur at about M = .65. Taking this into account, the sea level top speed with the fan operating would be about 535 mph and the gain in using engine thrust directly would be negligible. In addition, the weight and complication of incorporating a jet pipe diverter valve and a device for fairing over the fan intake make the use of direct engine thrust unattractive. A further disadvantage is that the control system, which depends upon the gyro stabilization of the impeller, would have to be changed.

4.3 Axial Fan Version

This vehicle employs two J85's as gas generators driving a turborotor. A central jet is employed both for hovering and forward flight, supplementing the peripheral nozzles. Exit guide vanes incorporated on the central jet reduce the exit area as they are rotated from the vertical hover positions to the forward flight position. The aft peripheral nozzle arrangement consists of vertical nozzles (hover) and horizontal nozzles (forward flight). During transition from hover to forward flight the aft hover nozzles are shut off and the horizontal nozzles opened. In addition, the forward peripheral nozzles are closed down by means of transition vanes which alter the focussing properties to reduce drag and optimize exit areas with forward flight conditions.

During transition the division of airflow to the central jet and peripheral nozzles is altered due to the changing exit areas.

4.4 Operating Assumptions - Axial Fan Version

Fan intake pressure recovery

Static	=	1.0
M = .2	=	.9938
M = .4	=	.985
M = .6	=	.970
M = .9	=	.949

Engine intake pressure recovery	=	100%
Turbine tusk pressure recovery	=	95%
Turbine efficiency	=	80%
Fan efficiency	=	85%

Duct Losses: $\frac{\Delta P}{q_{fan}}$ (from Ref. 3)

Forward peripheral nozzle	=	.30
Central jet	=	.10
Aft peripheral nozzle	=	.35 (hover)
Aft peripheral nozzle	=	.25 (forward flight)

These duct losses have been confirmed by tests reported in Ref. 4.

Gross thrust recovery

Hover	=	100%
Forward flight	=	95%
Engine residual	=	95%

Fan area	=	3800 in.^{2}

4.4 Operating Assumptions - Axial Fan Version (cont'd)

Central jet exit area:

Hover	=	2300 $in.^2$
Forward flight	=	1310 $in.^2$

Peripheral nozzle exit area (total)

Hover	=	1730 $in.^2$
Forward flight	=	1400 $in.^2$

Turbine exhaust duct loss $\frac{P}{q}$	=	.20
Exhaust exit area	=	457 $in.^2$

4.4.1 Engine Analysis

Engine data for the civil version of the J85 used was limited. However, existing data does include sea level power settings down to corrected values of 85% rpm. For power settings below 85% the non-dimensional curves were extended with the aid of data from a previous version of the J85.

For the sea level static case a turborotor turbine exit total pressure equal to 18 psi was selected and an exhaust exit area = 457 $in.^2$ was established on the basis of output from two J85's operating at 100% rpm. This exit area was then applied to all operating conditions to determine the HP absorbed by the turbine (and fan). Figs. 4.5 and 4.6 show HP vs Mach number for a range of power settings at sea level and 20,000 ft. The residual net thrust is given in Figs. 4.7 and 4.8. Fuel flows are given in Figs. 4.9 and 4.10.

4.5 Performance - Axial Fan Version

4.5.1 Hovering

With 60% of the fan flow going to the central jet, Figs. 4.11 and 4.12 show that optimum hover performance would be had with a central jet area of 2640 $in.^2$ and a peripheral jet exit area of 2130 $in.^2$. However, for design purposes the central jet area was reduced to 2300 $in.^2$ which gives a corresponding peripheral jet exit area of 1730 $in.^2$ While not giving optimum performance, an almost equal thrust is obtained, as shown in Fig. 4.11. In addition, with full power the pressure ratio of 1.12 is compatible with that required for normal cruise power.

To simplify the analysis, the peripheral flow duct losses were combined.

4.5 Performance - Axial Fan Version (cont'd)

4.5.2 Forward Flight

During forward flight, the aft peripheral hover nozzle is closed off and the horizontal thrust nozzle opened along with a reduction in area of the forward nozzle. Also, the central jet guide vanes are deflected aft giving an area of 1310 in.^{2}. Based on this central jet area and 100% engine rpm, fan thrusts were calculated for a range of fan pressure ratios and flight Mach numbers. This is shown in Fig. 4.11. The corresponding peripheral nozzle exit areas are given in Fig. 4.13.

In previous work it was shown that the peak in the thrust curve for a particular flight speed will be produced with a fixed exit area regardless of the horsepower delivered to the fan. Therefore, selecting the optimum areas from Figs. 4.11 and 4.13 will give a schedule of exit areas with flight speed. However, in selecting the exit areas consideration must be given to fan pressure ratio and the actual advantage of varying the areas with regards to thrust. If the area was scheduled to give peak thrust at all speeds (M = .2 to .9) pressure ratios of 1.16 to 1.22 would have to be produced by the fan for 100% rpm. The higher pressure ratios would be difficult to attain with an axial flow fan. In addition, the wide range of pressure ratios required would introduce problems in fan design.

If a fixed exit area is selected the pressure ratio will reduce with forward speed for a fixed power setting. However, if only enough power is used to overcome drag, the pressure ratio will increase with flight speed and designing the fan for the average pressure ratio will allow quite efficient fan operation throughout the speed range. In Figs. 4.14 and 4.15, thrust is shown plotted against Mach number for sea level and 20,000 ft. for a range of power settings, having assumed a constant exit area of 1400 in.^{2}. The percentage of total fan airflow to the central jet is reduced from 60% at the hover to about 49% with forward speed.

Another alternative in selecting the peripheral jet exit area is to choose a line between the optimum thrust line and the fixed exit area line on Fig. 4.11. As an example, consider a fan pressure ratio of 1.16 for the 100% rpm case. From Fig. 4.13 we again establish the required exit areas which are shown in Fig. 4.16. Based on this schedule of areas the final plot of thrust vs Mach number is shown in Fig. 4.17 for a range of power settings. Decreasing the peripheral jet exit area causes an increase in the percentage of fan airflow going to the central jet as shown below:

Mach No.	Peripheral Jet Exit Area (in.^{2})	Percentage of Fan Airflow to central Jet
.2	1160	53.9
.4	915	59.8
.6	730	64.8
.9	530	71.5

4.5.2 Forward Flight (cont'd)

A comparison of Figs. 4.14 and 4.17 show that the scheduling of the exit area produces a gradual increase in thrust as foward speed increases. The maximum speed at sea level is increased from M = .61 to M = .67. This is clearly shown in Fig. 4.20. Note that the suggested wing surfaces are not expected to influence the propulsive system.

All thrust values in Figs. 4.14, 4.15, 4.17 and 4.20 include the residual engine thrust given in Figs. 4.7 and 4.8. While hovering it is assumed that the residual engine thrust will be either deflected to the sides of the vehicle to cancel itself out or spoiled to reduce its value. At the present time no means have been devised by which this residual thrust may be used usefully during hover.

4.5.3 Effect of Reducing Flow to the Central Jet

From recent model tests it appears that for hover, an 80% fan flow to the peripheral nozzle would be required for best stability. In Fig. 4.18 thrust is given for the full range of central jet flows. From this we see that for 20% fan flow to the central jet, a thrust of 10,730 lb. could be obtained with full power - a thrust reduction of 600 lb. from the assumed case. The corresponding exit areas are given in Fig. 4.19 for the range of central jet flows which show that a central jet exit area of 690 sq. inches should be used.

As before, the nozzle areas required for forward flight will be dictated by the central jet area during hover. That is, the central jet flow must be deflected aft and in doing so the area is reduced by rotation of the guide vanes. Although the central jet area was taken as 1310 sq.in. for the forward flight cases, the new area would be about 350 sq. in. Consequently, the optimum thrust would be reduced since the higher loss peripheral duct system would be handling the major part of the fan flow. However, the thrust loss would be partially compensated by reduced momentum drag due to the optimum thrust occurring at higher fan pressure ratios for all speeds and power settings.

4.5.4 Warming the Fan Intake Flow

The flow from the turbine is exhausted to atmosphere at the upper surface behind the fan. This leads to the possibility of hot air being drawn into the fan during hover, especially if the vehicle is facing downwind. A short investigation of this showed that the thrust loss would not be too significant as long as the hot air did not reach the engine intakes. For example, an average temperature rise of 10^{o} across the fan would result in a thrust loss of less than 1%. The net result is that for a given horsepower input and fan pressure ratio, the temperature reduces the airflow which is partially compensated by a lower duct loss and an increase in jet velocity. It is assumed that the exhausted flow would not re-circulate to the engine intakes placed in the leading edge of the vehicle.

4.6 Comparison of Axial and Centrifugal Fan Versions

Fig. 4.21 shows the variation of thrust with Mach number for the axial fan version, centrifugal fan version, and basic engine thrust case, all using military power. From this we see the advantage of using low fan pressure ratios for hovering and at low speeds. However, at speeds above M = .42 the centrifugal fan version provides better performance than the axial fan version. At speeds greater than M = .57 the direct engine thrust case provides best performance.

As pointed out in Section 4.2 the drag rise will impose strict limits on attainable speeds with the centrifugal fan version and engine thrust case. However, the axial fan version is practically unaffected by the drag rise. Therefore, there is little gain in top speed by choosing the centrifugal fan or by using engine thrust directly. The top speed for the axial fan version if 505 mph, while the attainable speeds for the centrifugal fan version and engine thrust case are 533 mph., and 540 mph, respectively.

The main advantage in choosing the centrifugal fan or engine thrust case lies in the fact that they can operate with a substantially reduced power setting with only slight reduction in speed. For example, if the power setting is reduced to 95% rpm (normal continuous), the engine thrust case would provide a cruise speed of about 510 mph (slightly higher than the axial fan version with military power) with a fuel consumption of about 4300 lb/hr. The axial fan version operating at military power would consume 5320 lb. fuel/hr. However, the difference in fuel consumption would tend to diminish with reduced cruising speed as the required power setting becomes equal for the two cases.

Fig. 4.22 shows how any type of fan could stand to benefit from a shaft drive installation using T58 engines. The performance gain can be attributed to the efficient engine, close tolerance power turbine, and lack of duct loss between them. However, it does not take into account other design problems caused by such an arrangement.

4.7 Recent Intake Tests

Tests are being conducted by Orenda Engines Limited to determine the losses associated with the projected intake designs. The results of these tests are soon to be published in Ref. 4.

The intake pressure recovery for a bell-mouth intake located behind a wide cockpit canopy (see Fig. 1.3), and including the effect of the non-uniform conditions at the fan, is shown in Fig. 4.23. On this curve is also shown the pressure recoveries already assumed in Figs. 3.2 and 4.1 which were based on early tests of a 1/5th scale model. It is seen that the recent Orenda tests anticipate significantly more loss, because they account for the losses through and below the fan due to forward speed as well as the pressure loss in the intake itself.

4.7 Recent Intake Tests (cont'd)

The canopy in front of the fan has the beneficial effect of increasing the bell-mouth lip radius where needed most and the tests showed a large improvement when a canopy, representative of the present design, was added to the basic shape. It is anticipated that development of the canopy shape possibly combined with the introduction of guide vanes above the fan to ensure axial fan entry flow will improve pressure recovery further, so that the original assumption may eventually be achieved.

However, it is interesting to consider the effects of the Orends results on the propulsive system performance results already obtained. The effect on the re-engined Avrocar and on the GETOL developments will be slight because of the lower speed range and because the favoured GETOL development does not use its fan in forward flight. However, significant penalties can be expected for the VTOL developments at high speeds. A comparison showing the effect on maximum power at Sea Level is given in the following table:

Maximum Power at Sea Level

Mach Number	.2	.3	.4	.5	.6
Assumed Pressure Recovery	.996	.992	.986	.978	.968
Calculated thrust (lb)	8,000	6,700	5,650	4,750	3,950
Test pressure recovery	.992	.978	.958	.933	.905
Corrected thrust (lb.)	7,840	6,080	4,390	2,675	880
Percent of calculated thrust	98	91	78	56	22

The reason for the drastic fall off of thrust at the higher speeds is that the intake pressure recovery reduces the gross thrust (a very large number at speed) without reducing the momentum drag (also a large number). Then the difference between these two large terms, the net thrust, can fall off very rapidly.

If the Orenda test results are followed the top speed will be reduced by about 90 knots (to about 345 knots) but at a more typical cruise speed, say M = .3 (200 knots) the engine rpm will have to be increased from 78 to about 82 percent and the fuel flow go up by 11 percent.

However, it is emphasized that the test results whose effect is illustrated above, constitute no more than a spot check on existing intake conditions, with a particular fan, since no attempt was made to develop the design. Further improvement can doubtless be made, possibly to the point of justifying the original assumptions, which were themselves taken from earlier tests, but tests which did not include a fan.

4.8 Gross Thrust Recovery

Full scale tunnel tests with the Avrocar have shown the thrust to be much lower than expected. A low gross thrust recovery could account for the deficiency as shown in Fig. 4.24. However, the assumed gross thrust recovery of 95% can be justified.

The vehicle gross thrust is expected to be less than the sum of the gross thrust of the nozzles because:

(i) the nozzles do not all point straight downstream and so some of the jet momentum is wasted,

(ii) the flow from the front and central jets loses some of its engergy from skin friction drag on the vehicle undersurface.

From the side elevation of the aircraft only the rear peripheral jets are seen to discharge horizontally. The front and central jets, although they discharge 30° downward, will attach to the undersurface of the aircraft and be rotated to a horizontal direction by the Coanda effect. However, in plan view there are some sideways velocity components because the vanes in the rear peripheral jets of the circular vehicle are limited to a 60° deflection and the yaw control in the front peripheral jet will only turn the flow through 45° in the horizontal plane. Then 21% of the total weight flow is misaligned by up to 48° at the ends of the rear peripheral jet, while 12% is misaligned by up to 27° at the ends of the front jet. This part of the thrust recovery factor is the cosine of the angle of misalignment, and for the whole vehilce it averages 97.2%. Although a downward deflection of the rear jets is needed to trim, the thrust loss from this source has been allowed for in an increased induced drag coefficient.

Now account must be taken of the extra drag caused by the high velocity flows from the front and and central jet in contact with the aircraft underside. For example, at $M = .3$ the flow would normally be of the order of 400 ft/sec. (i.e. 14% above freestream velocity) while the flow from the nozzles is at about 600 ft/sec. If we base the drag on a quarter of the profile drag coefficient of the whole aircraft and one half of the wing area, the drag of the lower skin is 29 lb., engines off, and 64 lb. engines on; a drag increase of 35 lb. But the total nozzle thrust is 15,900 lb. at this speed so the gross thrust recovery from this cause is 99.6%.

The overall gross thrust recovery is then $.972 \times .996 = 96.8\%$. Therefore, the adopted value of 95% is slightly conservative.

5.0 CONCLUSION

Table 1 presents a summary of the various vehicles considered. It is difficult to compare the two types since in the case of the GETOL we have a light weight, low powered vehicle requiring only sufficient hover thrust to provide a reasonable ground clearance on take-off and landing; whereas the VTOL vehicle is heavier and must be high powered to enable it to hover out of ground effect. Consequently the GETOL using a propeller for forward thrust has a lower SFC than the VTOL vehicle.

It is seen that for the GETOL aircraft powered by two Astazou II engines, the axial fan and propeller combination is far superior to an axial fan system from the propulsion point of view. Although there is a weight penalty, the overall performance is improved due to the higher operating efficiency of the propeller.

Considering the VTOL vehicles powered by two J85 engines, the axial fan system has far better hover performance than the centrifugal fan system. Also the axial fan system is the more efficient in forward flight up to speeds of about 300 mph giving it the better overall performance. The introduction of a central jet in combination with the peripheral jet increases the performance of the axial fan version over that of a similar vehicle using only peripheral jets.

It is proposed that only 20% of the fan flow will emerge at the central jet but any increase allowed will provide a thrust improvement.

TABLE 1

PROPULSIVE SYSTEMS OF VARIOUS AIRCRAFT

Type of Aircraft	AVROCAR	T58 DEVELOPMENT		GETOL DEVELOPMENT		VTOL DEVELOPMENT	
Engine	Three J69's	Three T 58's		Two Astazou II's		Two J85's	
Propulsive system	tip driven turborotor	shaft drive axial fan	tip driven turborotor	shaft drive axial fan	fan and propellers	centrifugal impeller	tip driven turborotor
Engine Weight (lb.) *	1,090	810	750	550	550	710	710
M = 0, Sea Level							
Max. thrust (lb)	6,650	6,500	5,550	2,430	2,430	7,600	11,300
Fuel flow (lb/hr)	3,160	2,040	2,040	690	690	2,400	2,400
M = .3, Sea Level							
Max. thrust (lb)	3,320	2,560	2,420	930	1,520	6,000	6,600
SFC (lb.fuel/THP hr.)				1.25	.78	1.32	1.19
M = 3, 10,000 ft.							
Max. thrust (lb.)	2,700	1,950	1,950	710	1,150	4,600	5,000
SFC (lb.fuel/THP hr.)				1.23	.77	1.41	1.30

* - these weights are for the engines alone and do not include remainder of the propulsive system.

LIST OF REFERENCES

1.	AVRO GEN/PERF/1 W. Hartley	Simple Momentum Theory Applied to Lifting Fans (Without Ground Effect)
2.	AVRO (unpublished) D.C. Whittley	Simplified Mechanics of the Lifting Fan.
3.	NACA ARR L4F26 J.R. Henry	Pressure Loss Characteristics of Duct Components
4.	ORENDA CT-301	Report on the Canadian Government Program for the Avrocar - Orenda Engines

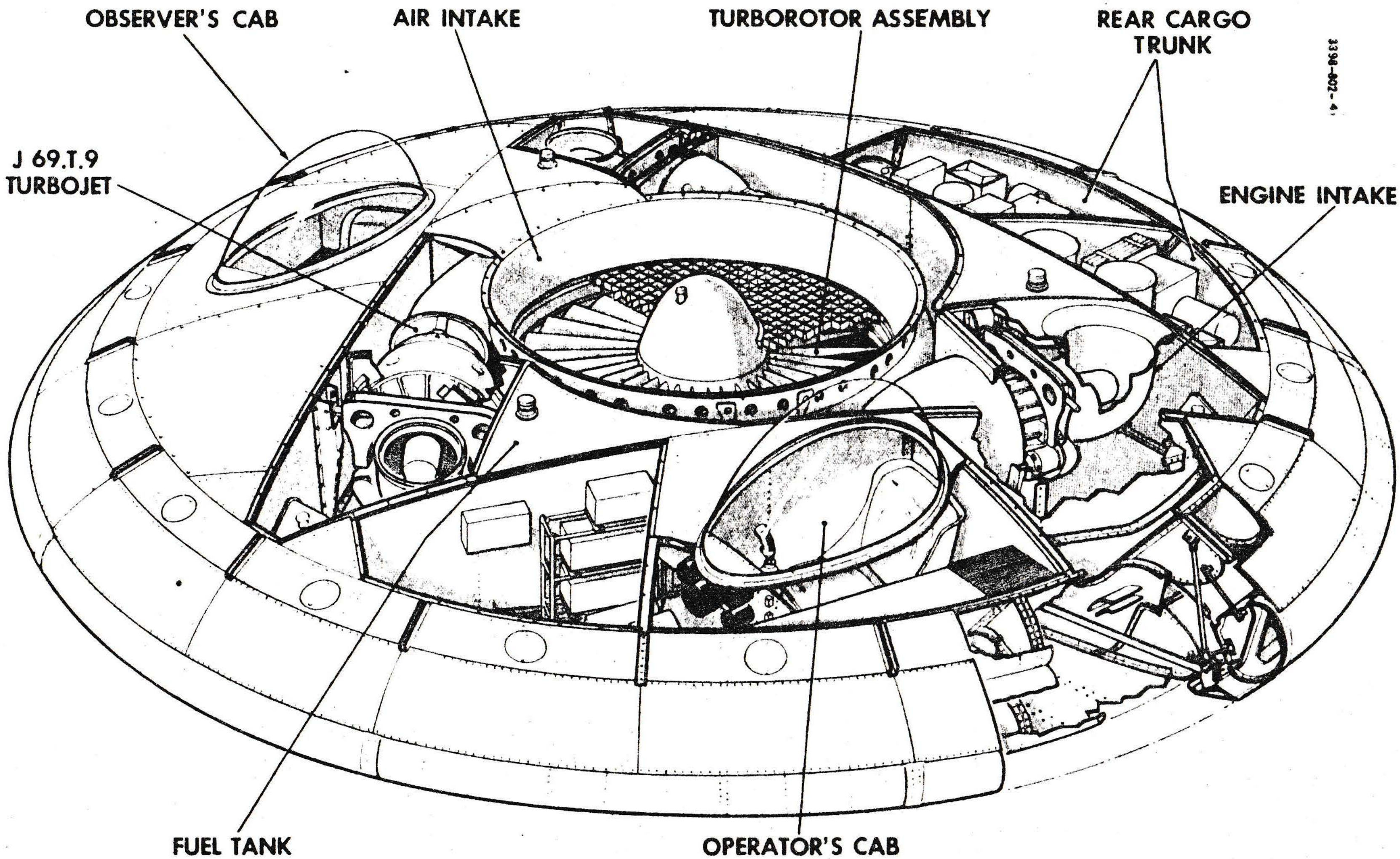

FIG. 14 STRUCTURE CUTAWAY - AVROCAR

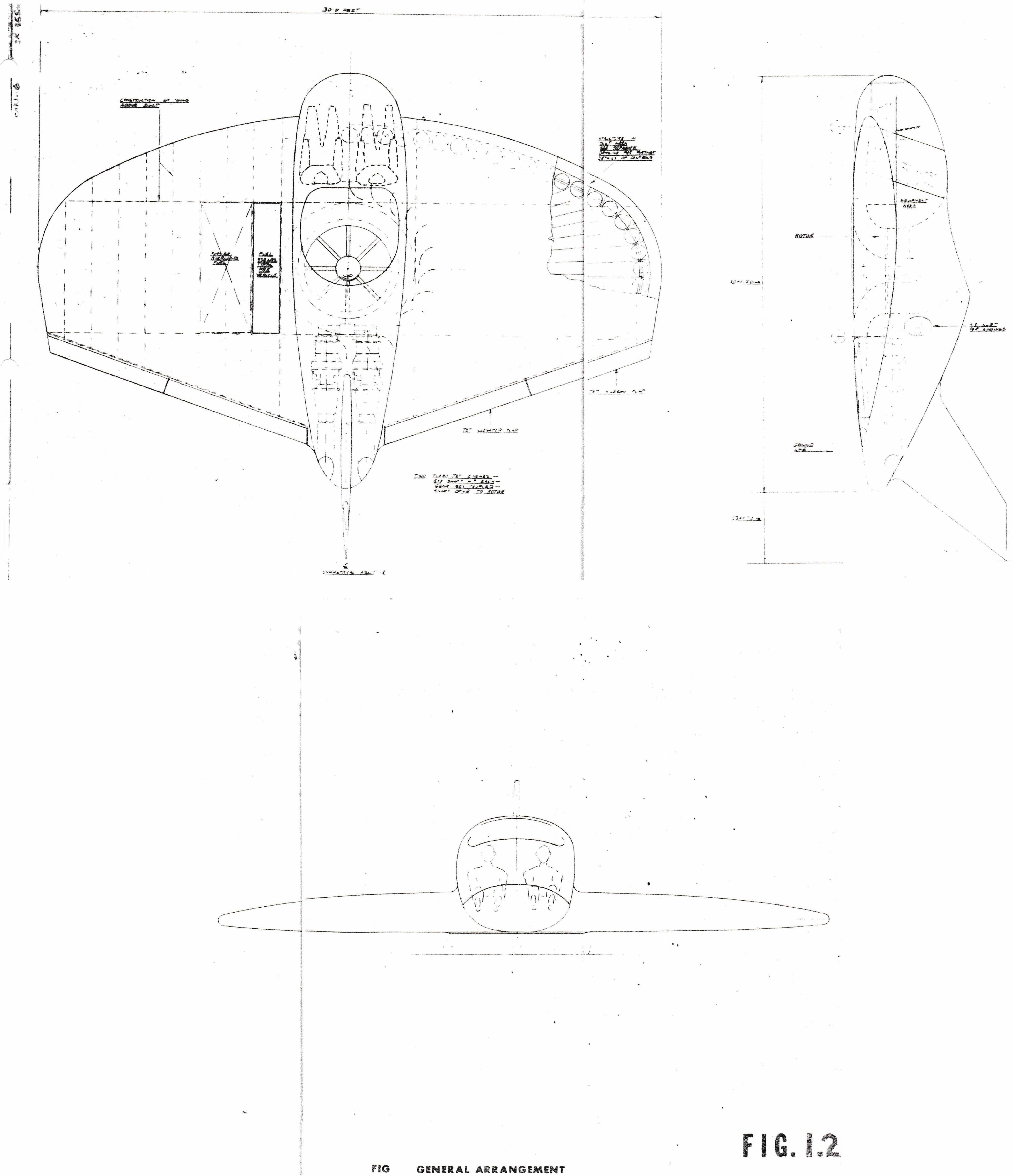

FIG. 1.2

FIG GENERAL ARRANGEMENT

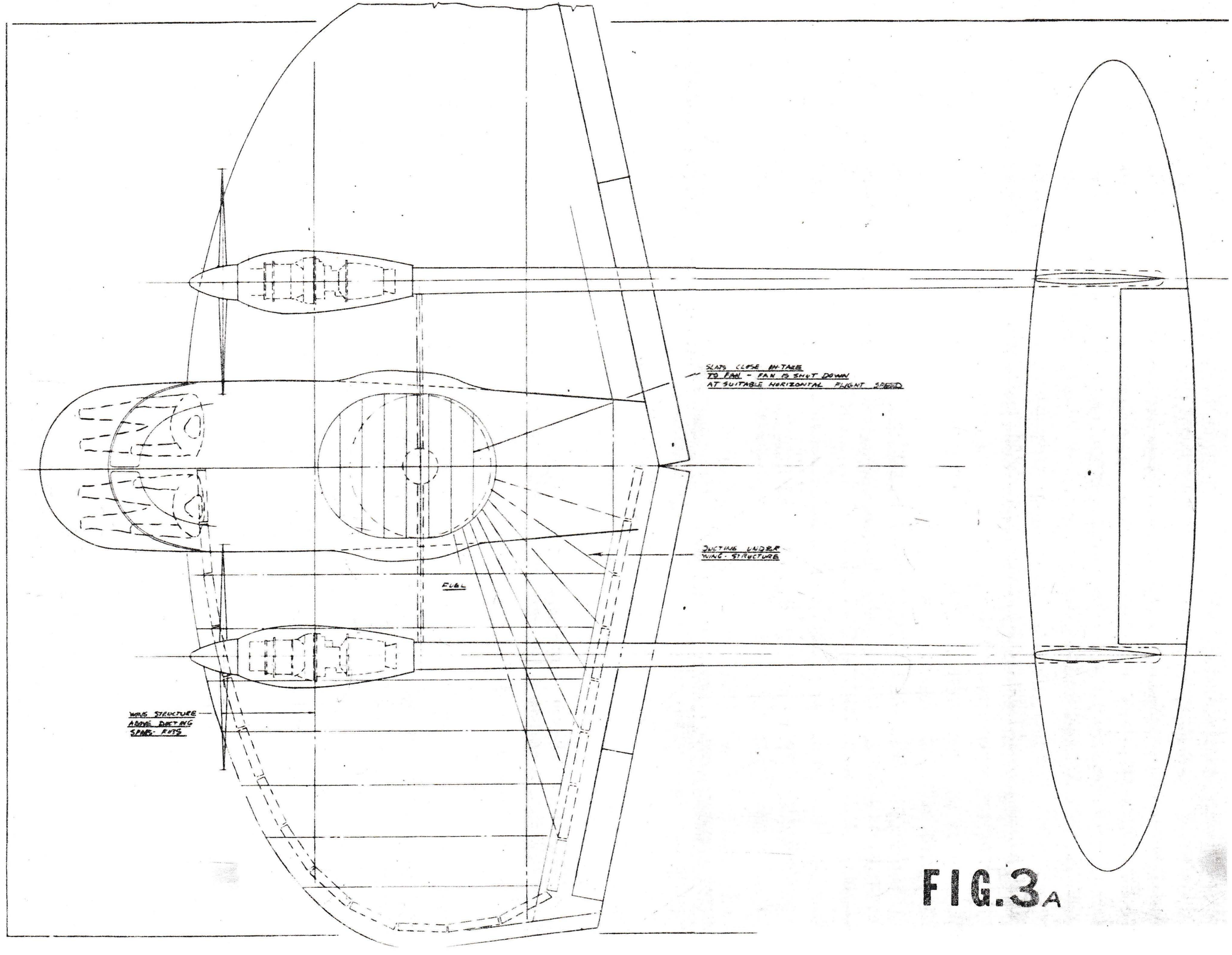
SLATS CLOSE IN-TAKE
TO FAN - FAN IS SHUT DOWN
AT SUITABLE HORIZONTAL FLIGHT SPEED
DUCTING UNDER
WING - STRUCTURE
FUEL
WING STRUCTURE
ABOVE DUCTING
SPARS · RIBS

FIG. 3A

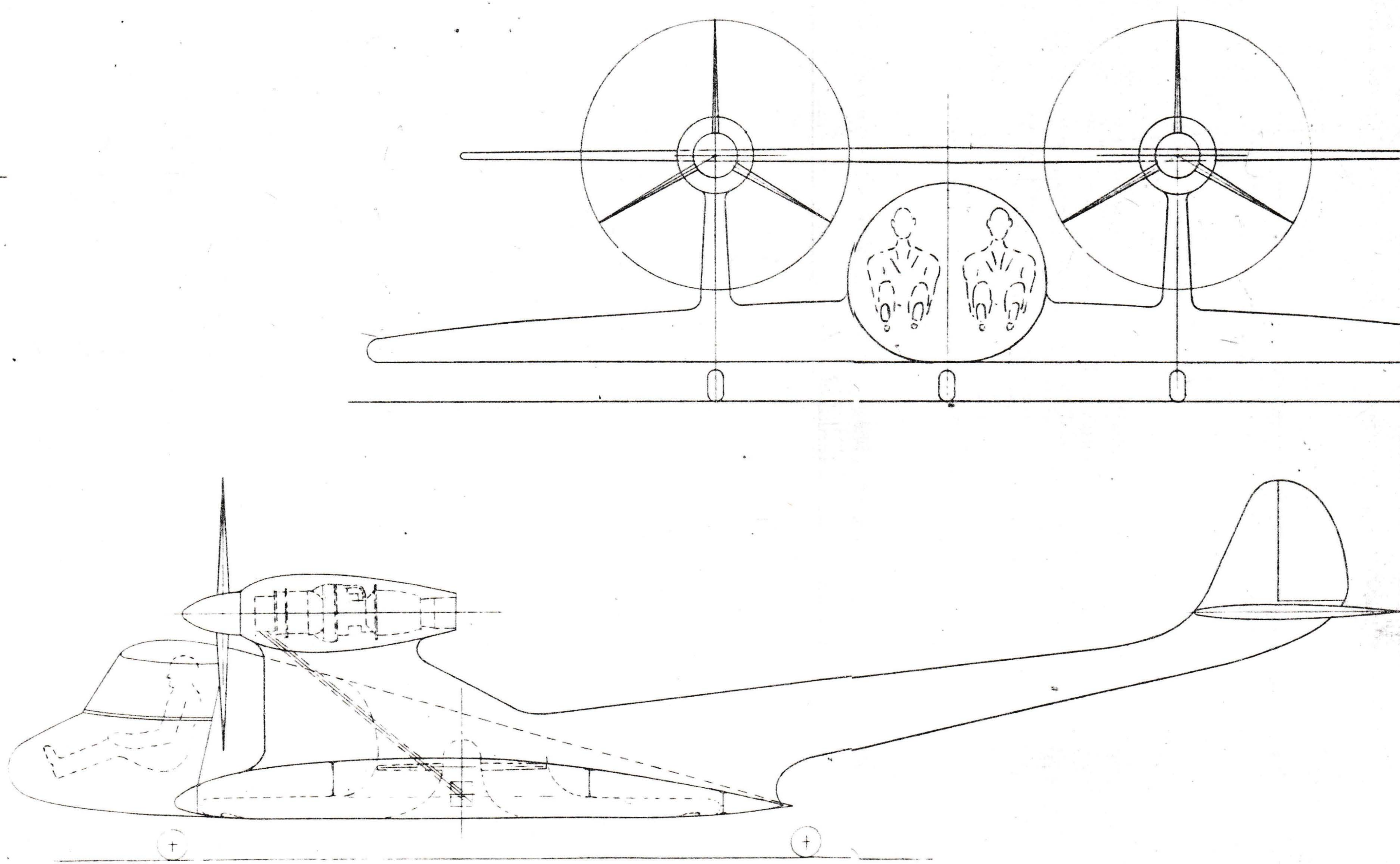

SPAN = 30-0"
O/A LENGTH = 36-5"
C/A HEIGHT = 15-0"
WING AREA = 353 SQ. FT.
WING ASPECT RATIO = [illegible]
T/C WING = 10%
TAILPLANE SPAN = 25-3"
TAILPLANE AREA = 106 SQ. FT
TAILPLANE ASPECT RATIO = 6
T/C TAILPLANE = 8%
2 [illegible] ENGINES - [illegible] EACH
FUEL = 950 LB
PRESSURE RATIO [illegible]
CARGO CAPACITY = [illegible] LB
GROSS WEIGHT = [illegible]

FIG. 3B

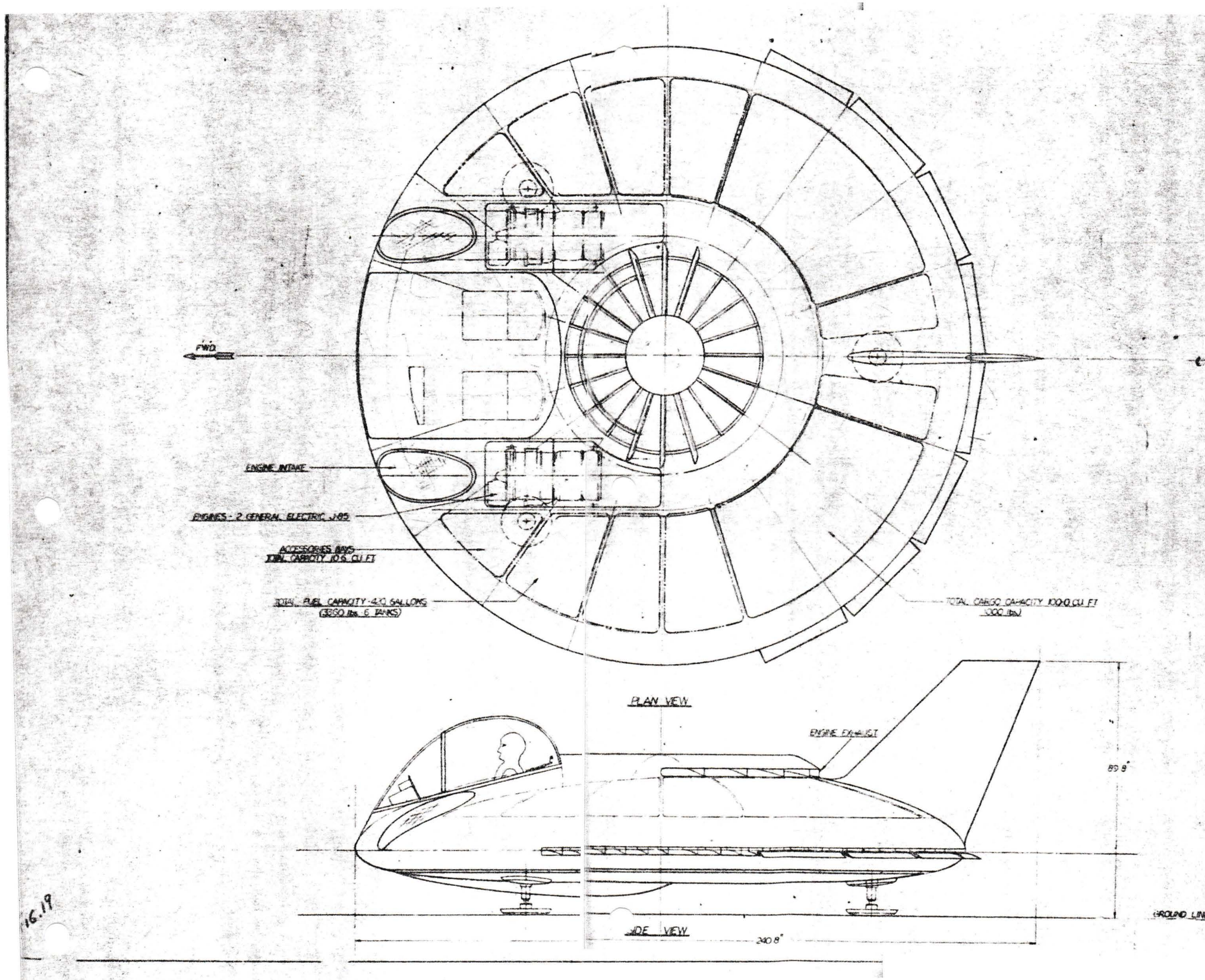
FWD.
ENGINE INTAKE
ENGINES - 2 GENERAL ELECTRIC J-85
ACCESSORIES BAYS
TOTAL CAPACITY 10.6 CU FT
TOTAL FUEL CAPACITY - 420 GALLONS
(3360 lbs. 6 TANKS)
TOTAL CARGO CAPACITY 100.0 CU FT
(1000 lbs.)
PLAN VIEW
ENGINE EXHAUST
89.8"
SIDE VIEW
240.8"
GROUND LINE
IG.19

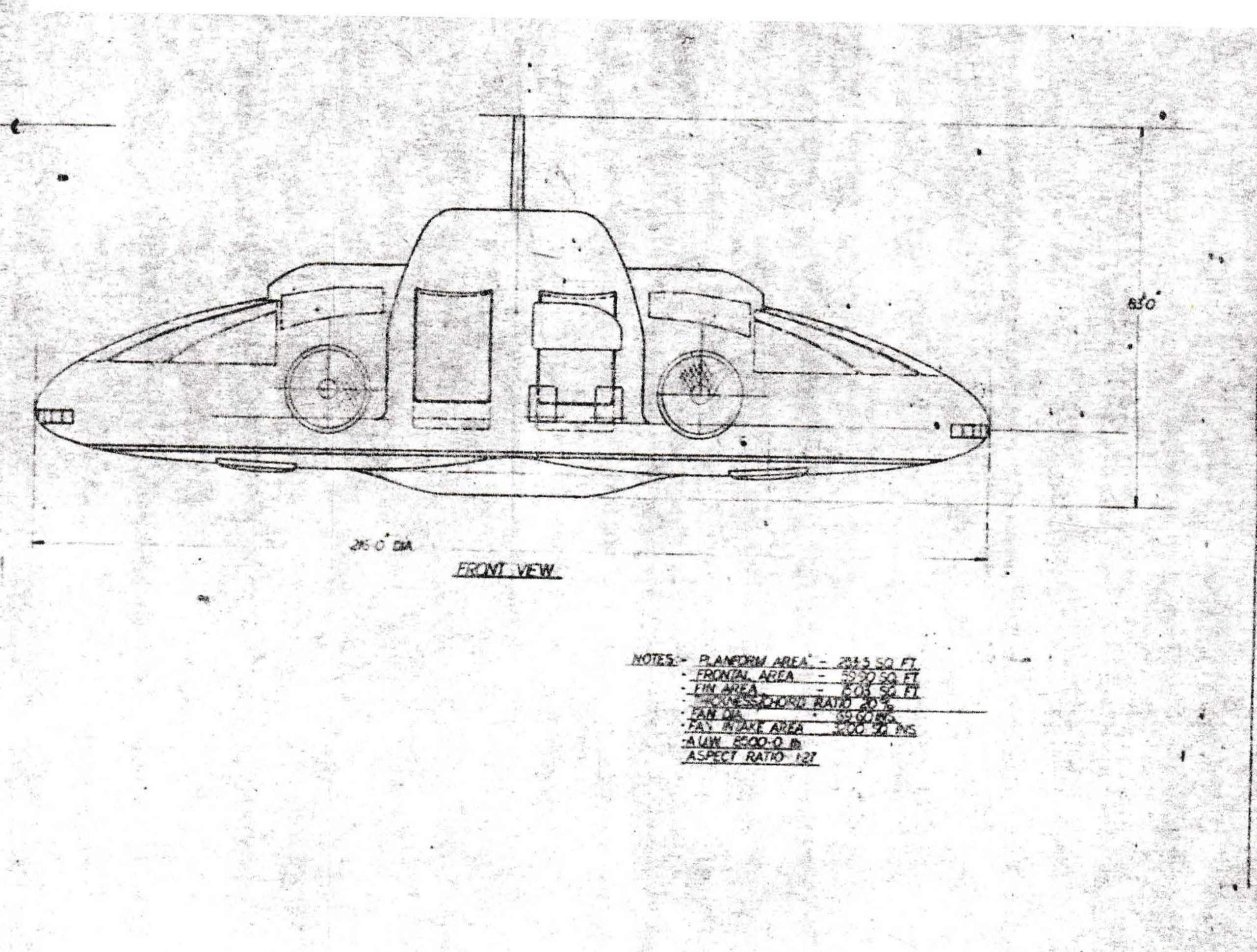
83.0"
216.0" DIA.
FRONT VIEW
NOTES:- PLANFORM AREA - 253.5 SQ. FT.
- FRONTAL AREA - 59.90 SQ. FT.
- FIN AREA - 6.08 SQ. FT.
- THICKNESS/CHORD RATIO 20%
- FAN DIA. - 69.60 INS.
- FAN INTAKE AREA 3200 SQ. INS.
- A.U.W. 8500.0 lb.
ASPECT RATIO 1.27

FIG. I.4

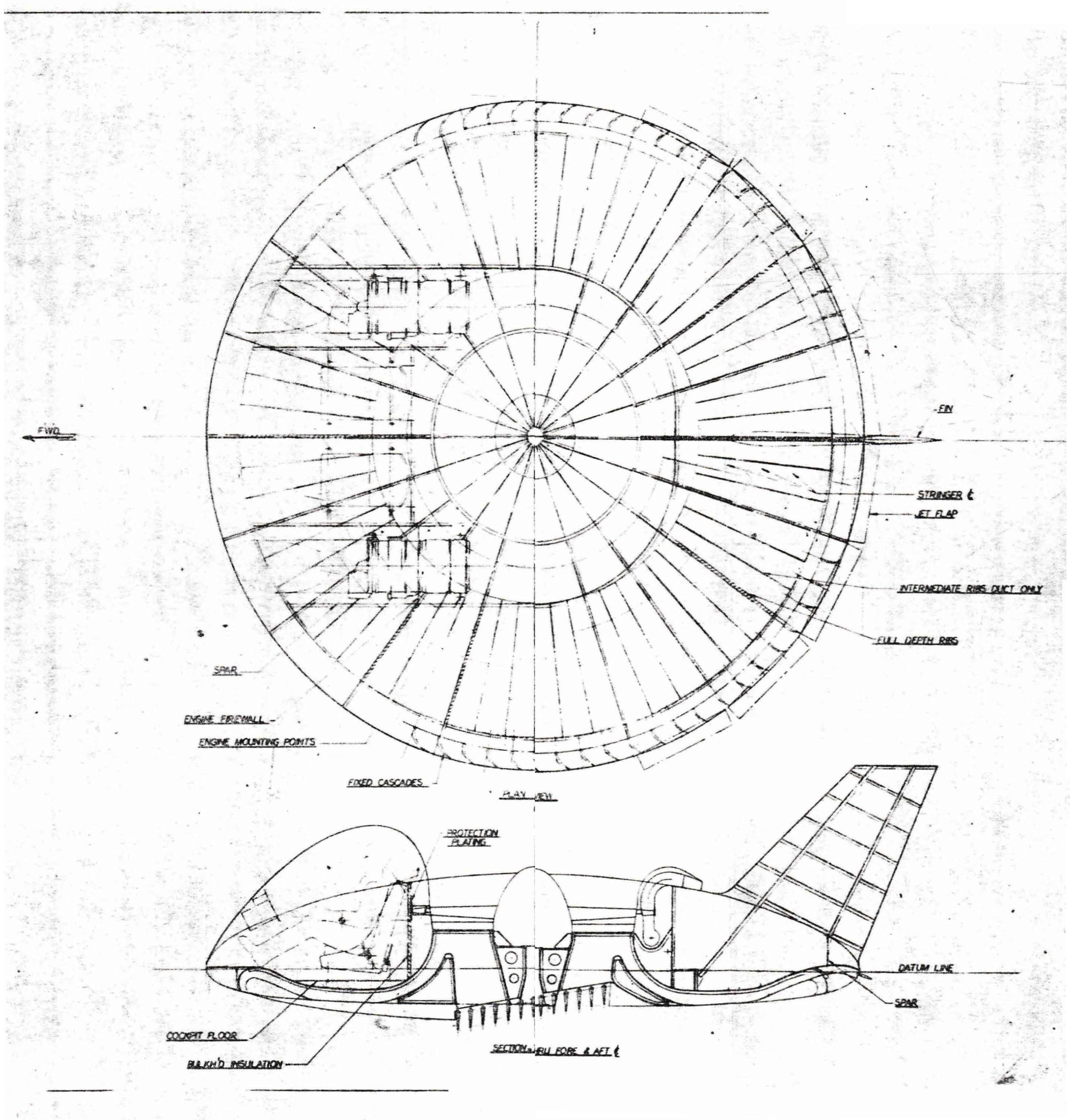
FWD.
FIN
STRINGER ℄
JET FLAP
INTERMEDIATE RIBS DUCT ONLY
FULL DEPTH RIBS
SPAR
ENGINE FIREWALL
ENGINE MOUNTING POINTS
FIXED CASCADES
PLAN VIEW
PROTECTION PLATING
DATUM LINE
SPAR
COCKPIT FLOOR
BULKH'D INSULATION
SECTION
FORE & AFT ℄

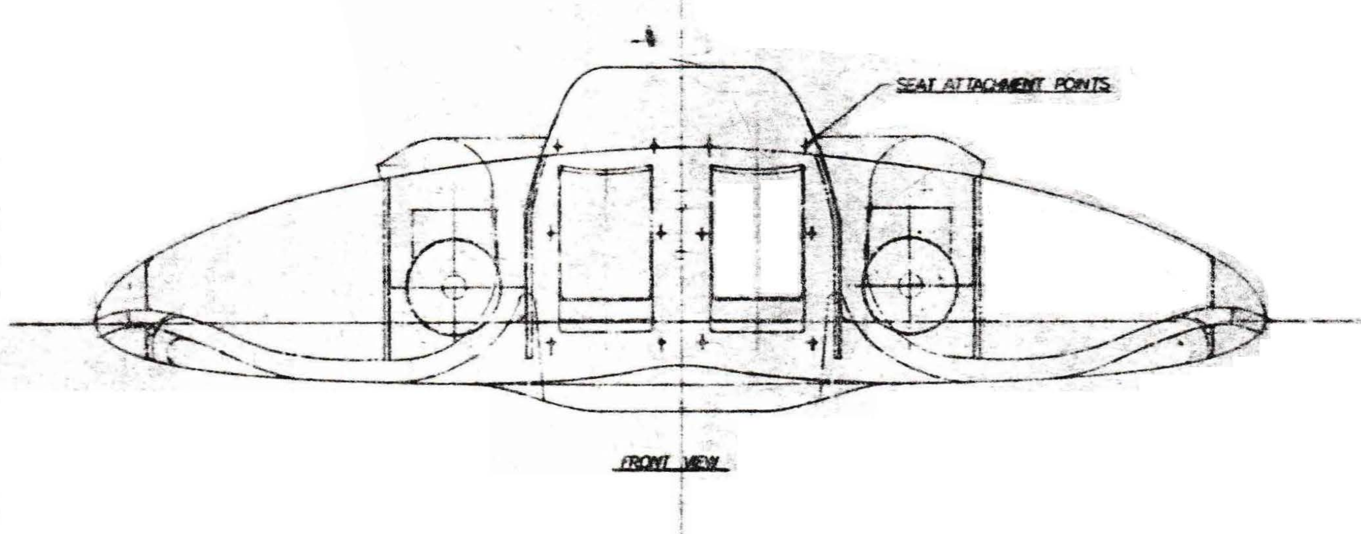
SEAT ATTACHMENT POINTS
FRONT VIEW

FIG.1.5

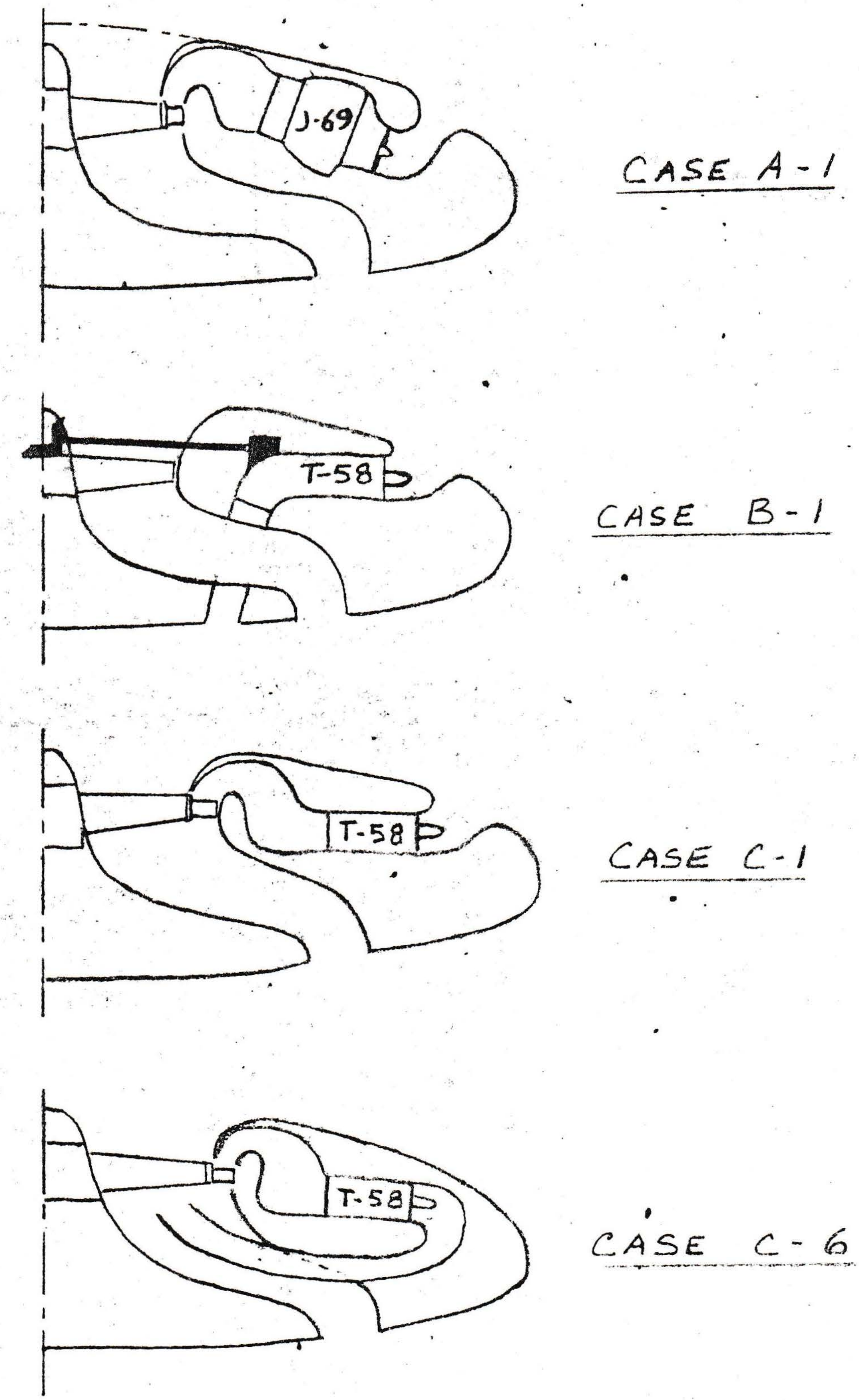

EXAMPLES OF FAN DRIVE SYSTEMS

FIG. 2.1

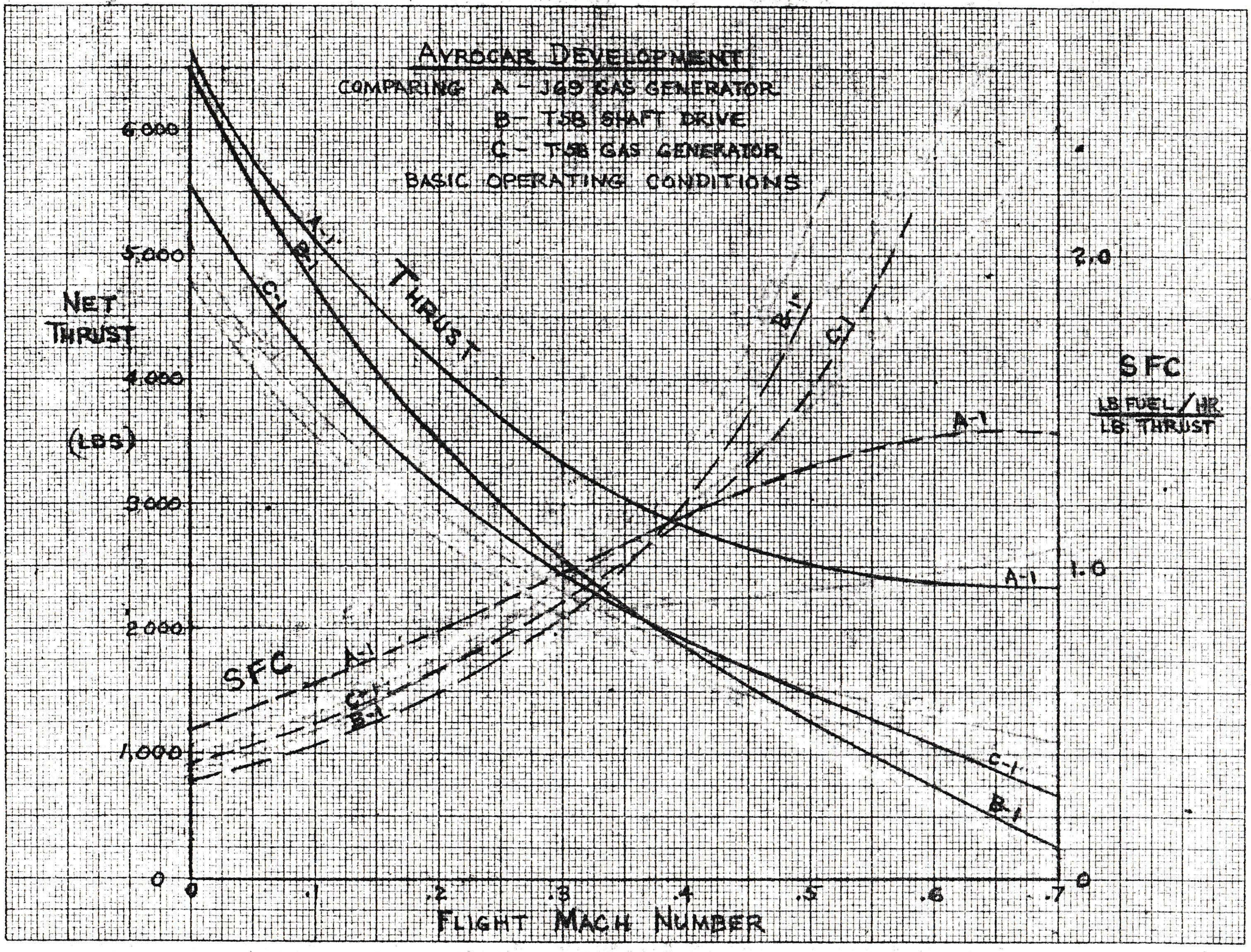
AVROCAR DEVELOPMENT
COMPARING A – J69 GAS GENERATOR
B – T58 SHAFT DRIVE
C – T58 GAS GENERATOR
BASIC OPERATING CONDITIONS
NET THRUST
(LBS)
6,000
5,000
4,000
3,000
2,000
1,000
0
THRUST
A-1
B-1
C-1
SFC
SFC
LB FUEL / HR.
LB. THRUST
2.0
1.0
0
.1
.2
.3
.4
.5
.6
.7
FLIGHT MACH NUMBER

FIG. 2.2

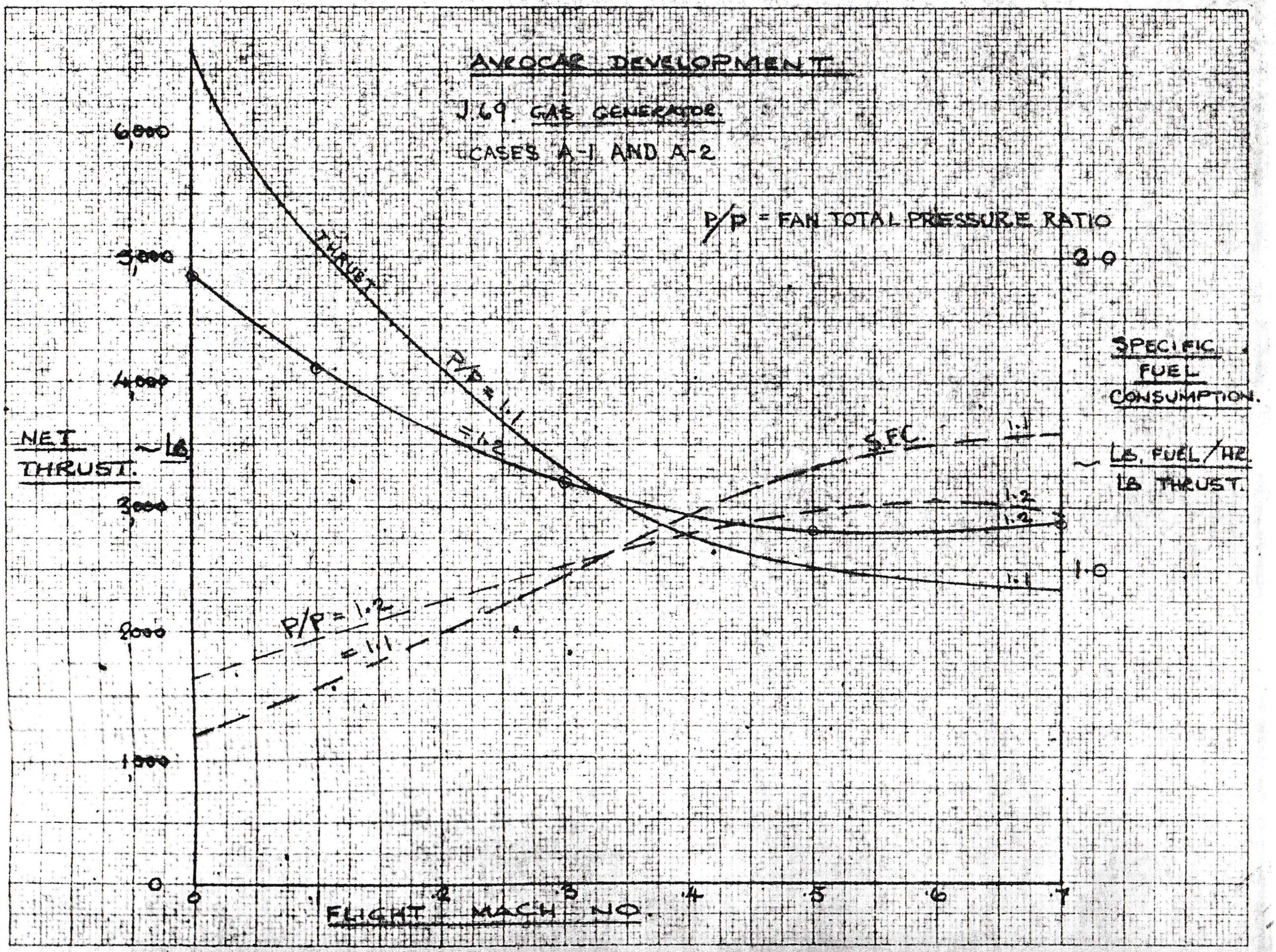
AVROCAR DEVELOPMENT
J.69. GAS GENERATOR.
CASES A-1 AND A-2
P/P = FAN TOTAL PRESSURE RATIO
NET THRUST ~ LB
6000
5000
4000
3000
2000
1000
0
THRUST
P/P = 1.1
= 1.2
S.F.C.
P/P = 1.2
= 1.1
SPECIFIC FUEL CONSUMPTION.
~ LB. FUEL/HR. / LB THRUST.
2.0
1.0
0
.1
.2
.3
.4
.5
.6
.7
FLIGHT MACH NO.

FIG. 2.3

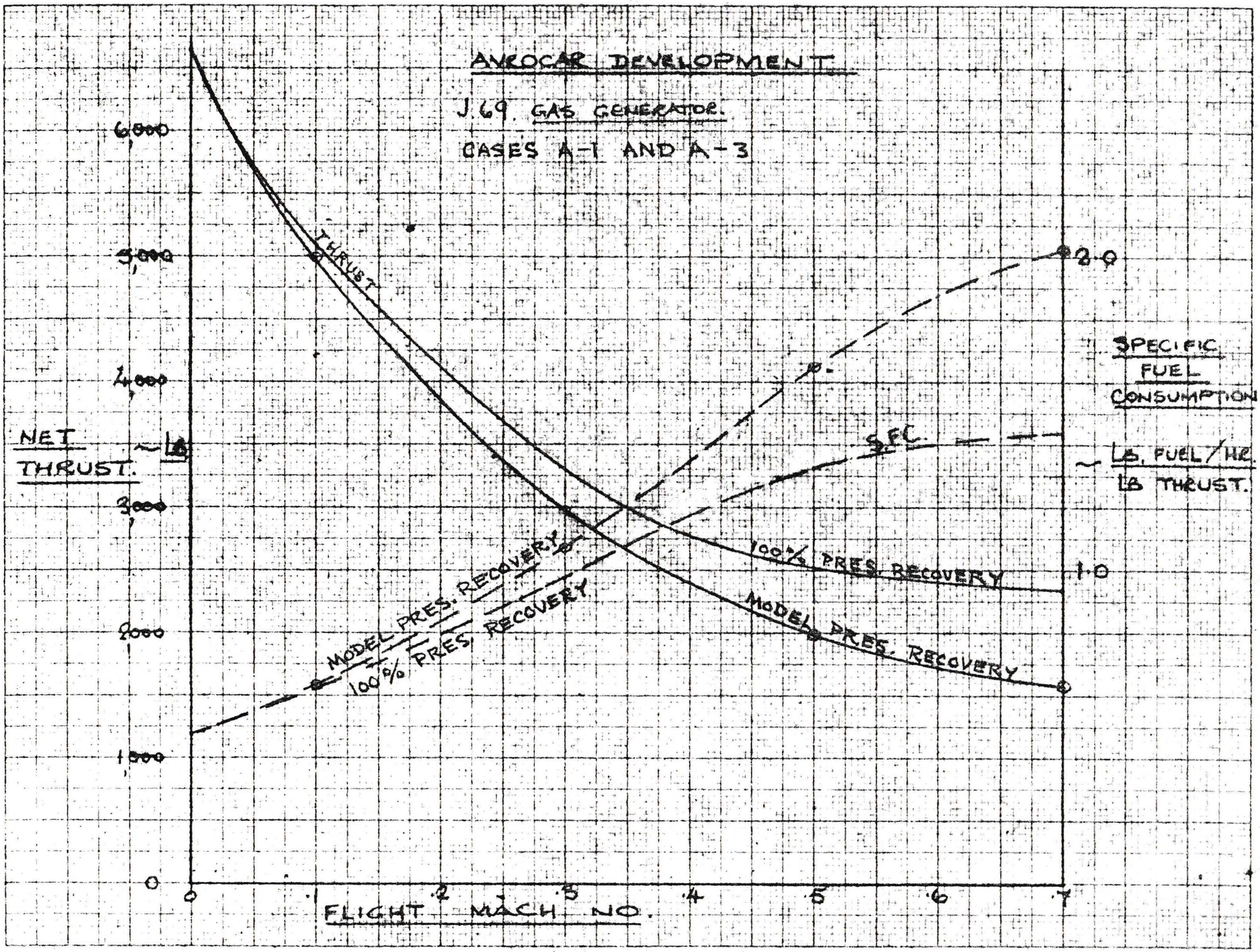
AVROCAR DEVELOPMENT
J.69 GAS GENERATOR.
CASES A-1 AND A-3
NET THRUST ~ LB
6,000
5,000
4,000
3,000
2000
1,000
0
THRUST
S.F.C.
100% PRES. RECOVERY
MODEL PRES. RECOVERY
SPECIFIC FUEL CONSUMPTION.
~ LB. FUEL/HR. / LB THRUST.
2.0
1.0
0
.1
.2
.3
.4
.5
.6
.7
FLIGHT MACH NO.

FIG. 2.4

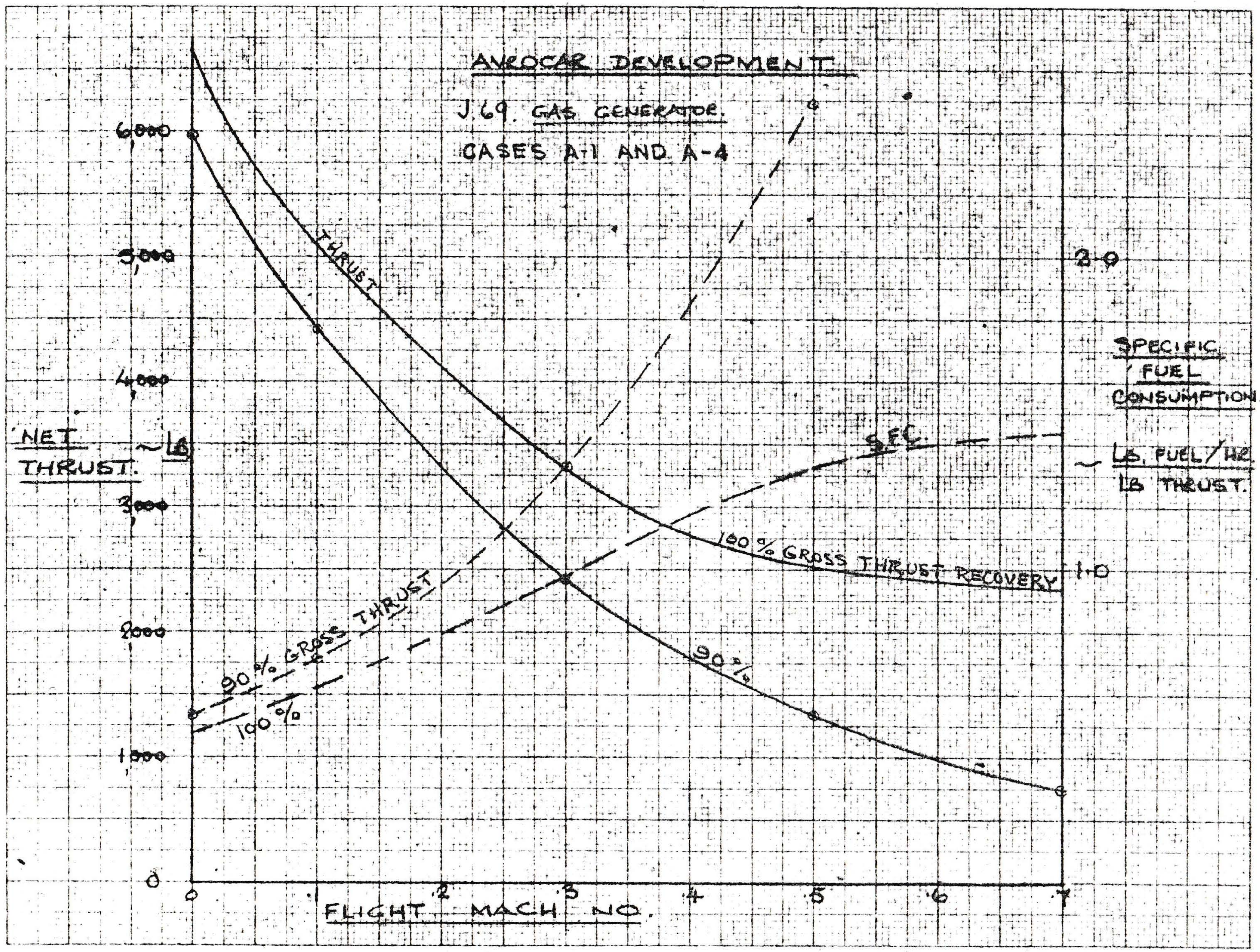
AVROCAR DEVELOPMENT
J.69 GAS GENERATOR
CASES A-1 AND A-4
NET THRUST ~ LB
6000
5000
4000
3000
2000
1000
0
THRUST
100% GROSS THRUST RECOVERY
90%
S.F.C.
90% GROSS THRUST
100%
SPECIFIC FUEL CONSUMPTION
~ LB. FUEL/HR / LB THRUST
2.0
1.0
FLIGHT MACH NO.
0
.2
.3
.4
.5
.6
.7

FIG. 2.5A

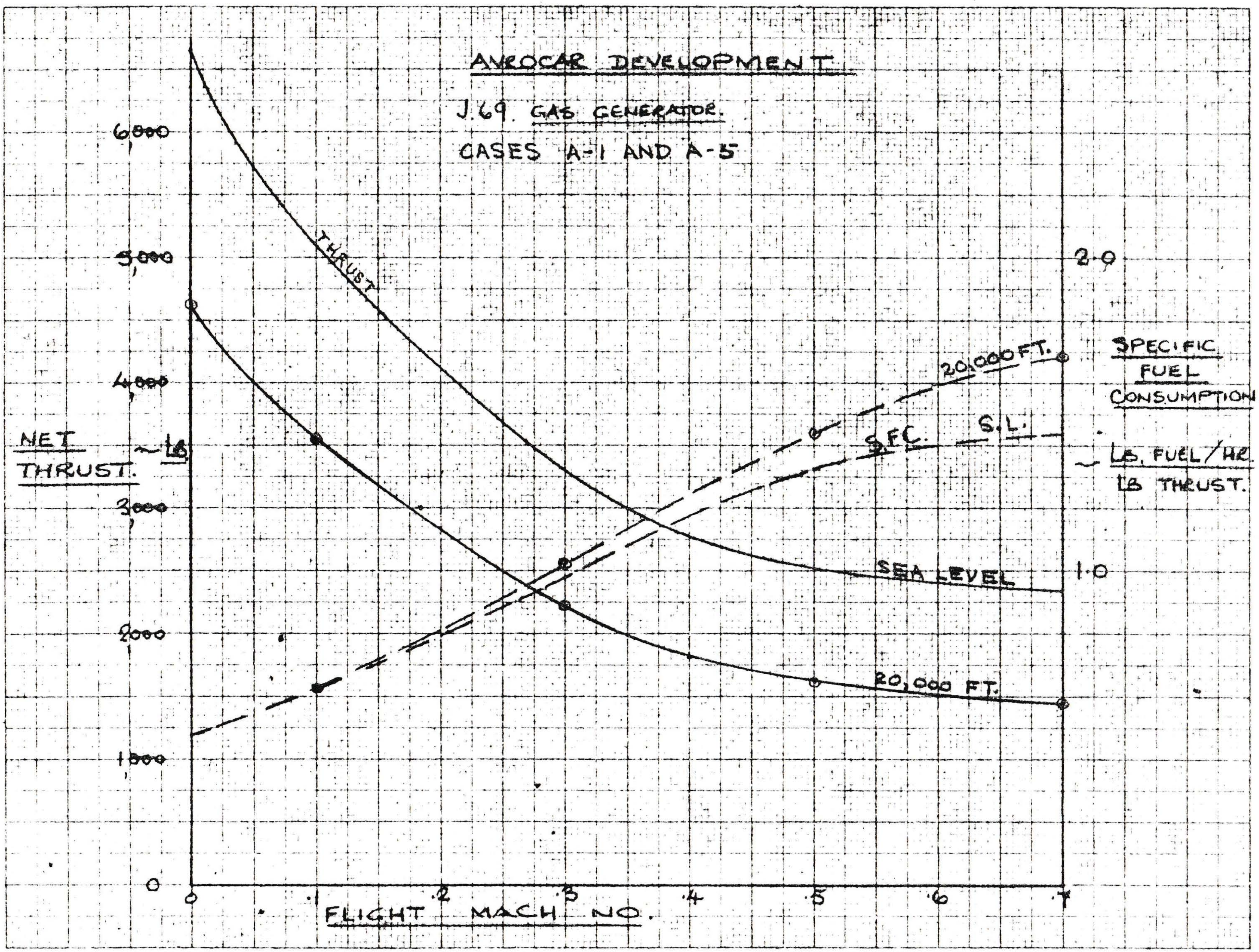
AVROCAR DEVELOPMENT
J.69. GAS GENERATOR.
CASES A-1 AND A-5
NET THRUST. ~ LB
6,000
5,000
4,000
3,000
2000
1,000
0
THRUST
SEA LEVEL
20,000 FT.
20,000 FT.
S.F.C.
S.L.
SPECIFIC FUEL CONSUMPTION.
~ LB. FUEL/HR / LB THRUST.
2.0
1.0
0
.1
.2
.3
.4
.5
.6
.7
FLIGHT MACH NO.

FIG 2.6

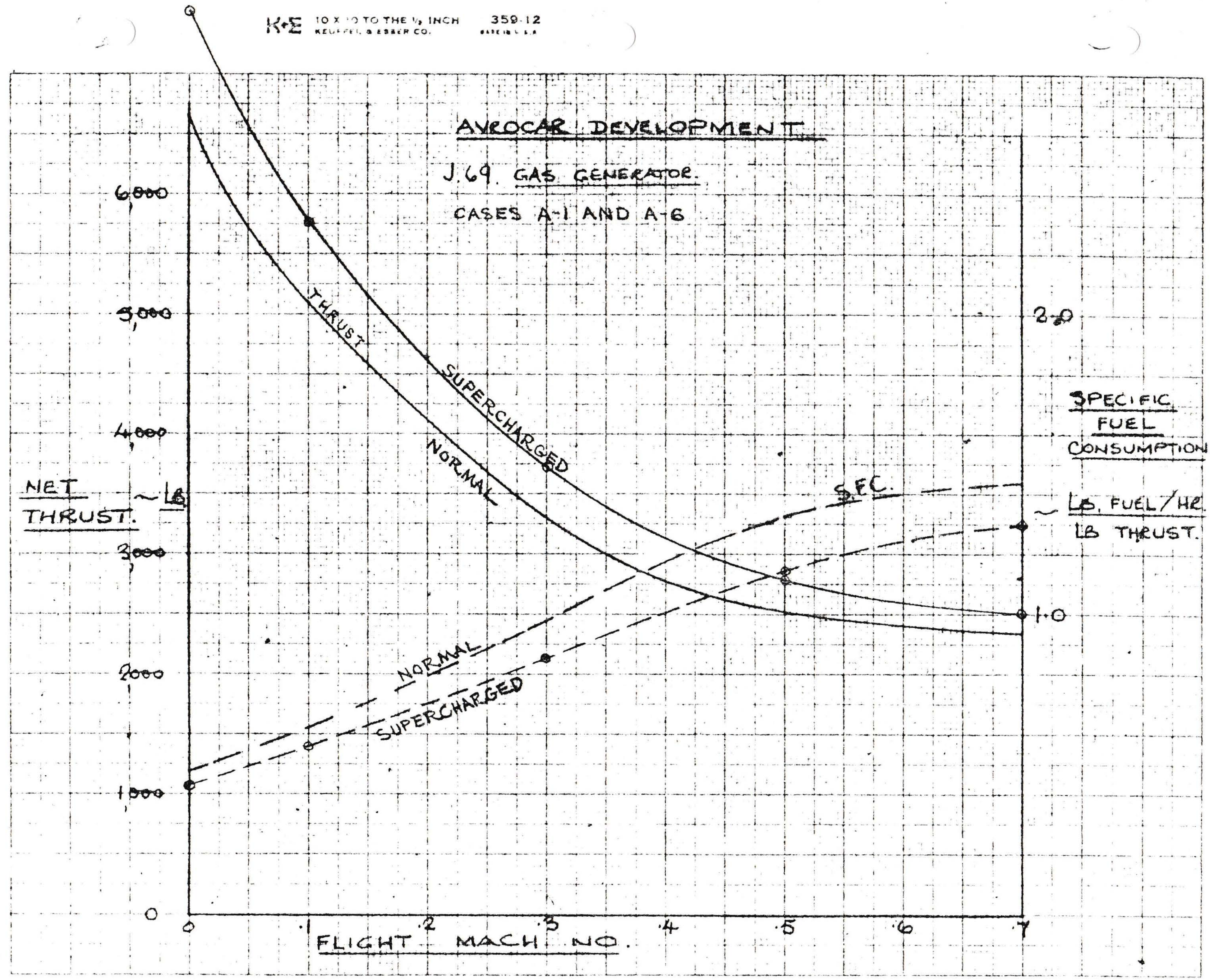
K+E 10 X 10 TO THE ½ INCH 359-12
KEUFFEL & ESSER CO.
AVROCAR DEVELOPMENT.
J.69. GAS GENERATOR.
CASES A-1 AND A-6
NET THRUST. ~ LB.
6000
5000
4000
3000
2000
1000
0
THRUST
SUPERCHARGED
NORMAL
S.F.C.
NORMAL
SUPERCHARGED
SPECIFIC FUEL CONSUMPTION.
~ LB. FUEL/HR. / LB THRUST.
2.0
1.0
0
.1
.2
.3
.4
.5
.6
.7
FLIGHT MACH NO.

FIG. 2.7

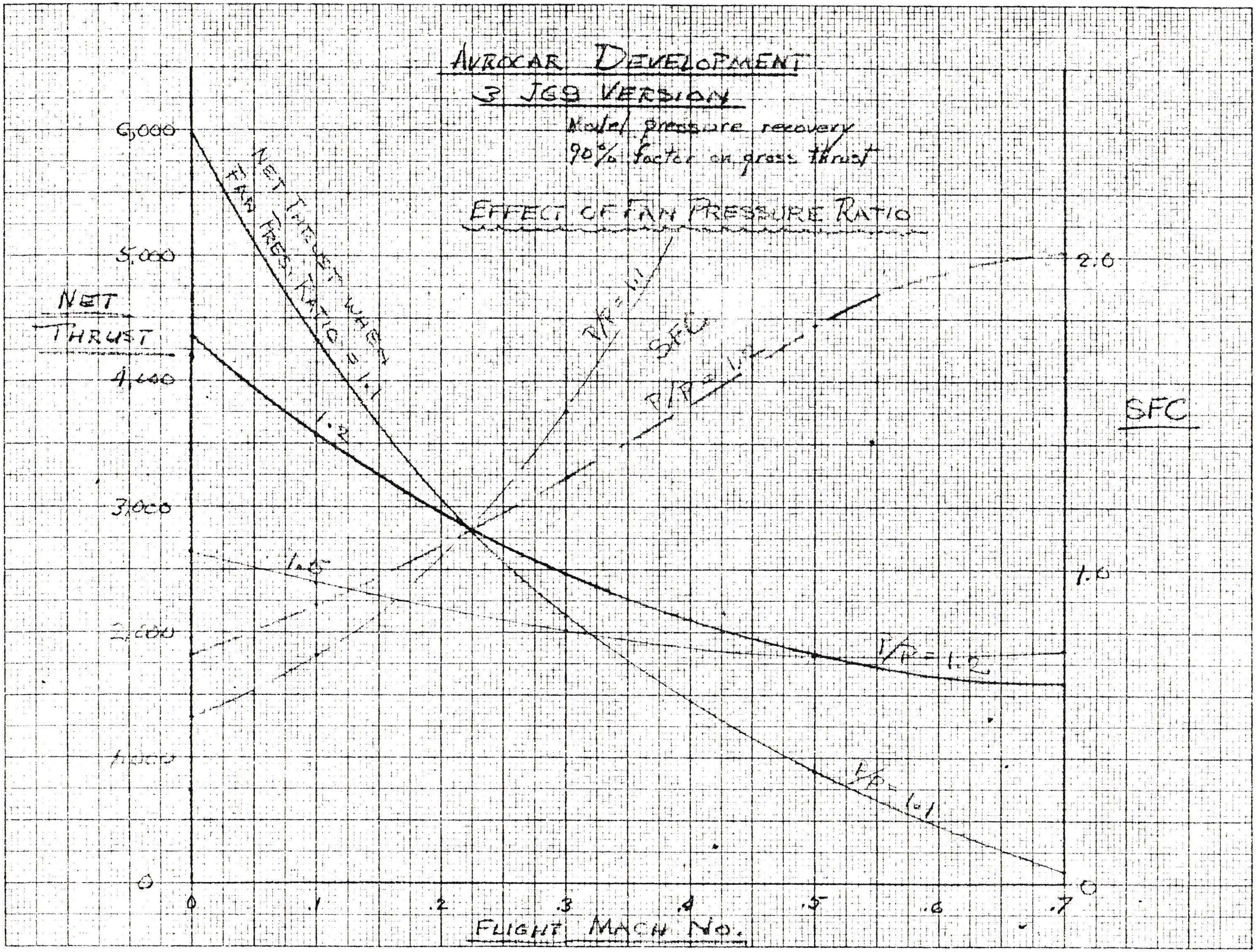

AVROCAR DEVELOPMENT
3 J69 VERSION
Model pressure recovery
90% factor on gross thrust
EFFECT OF FAN PRESSURE RATIO
NET THRUST
6,000
5,000
4,000
3,000
2,000
0
NET THRUST WHEN FAN PRES. RATIO = 1.1
1.2
1.5
P/P = 1.1
SFC
P/P = 1.2
P/P = 1.2
P/P = 1.1
SFC
2.0
1.0
0
0
.1
.2
.3
.4
.5
.6
.7
FLIGHT MACH NO.

FIG. 2.8

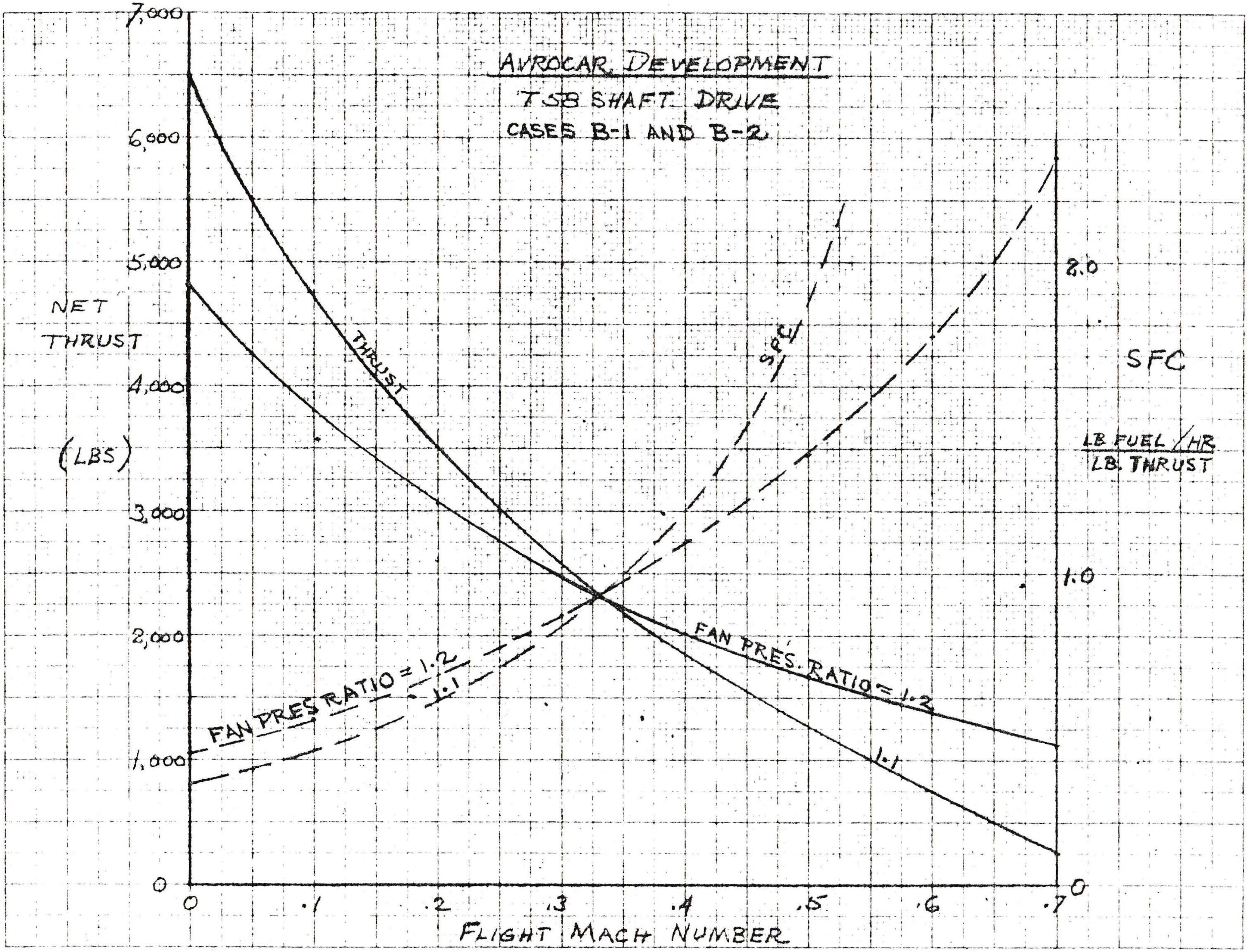
AVROCAR DEVELOPMENT
T58 SHAFT DRIVE
CASES B-1 AND B-2
NET THRUST
(LBS)
7,000
6,000
5,000
4,000
3,000
2,000
1,000
0
THRUST
SFC
FAN PRES. RATIO = 1.2
1.1
FAN PRES RATIO = 1.2
1.1
SFC
LB FUEL / HR
LB. THRUST
2.0
1.0
0
0
.1
.2
.3
.4
.5
.6
.7
FLIGHT MACH NUMBER

FIG. 2.9

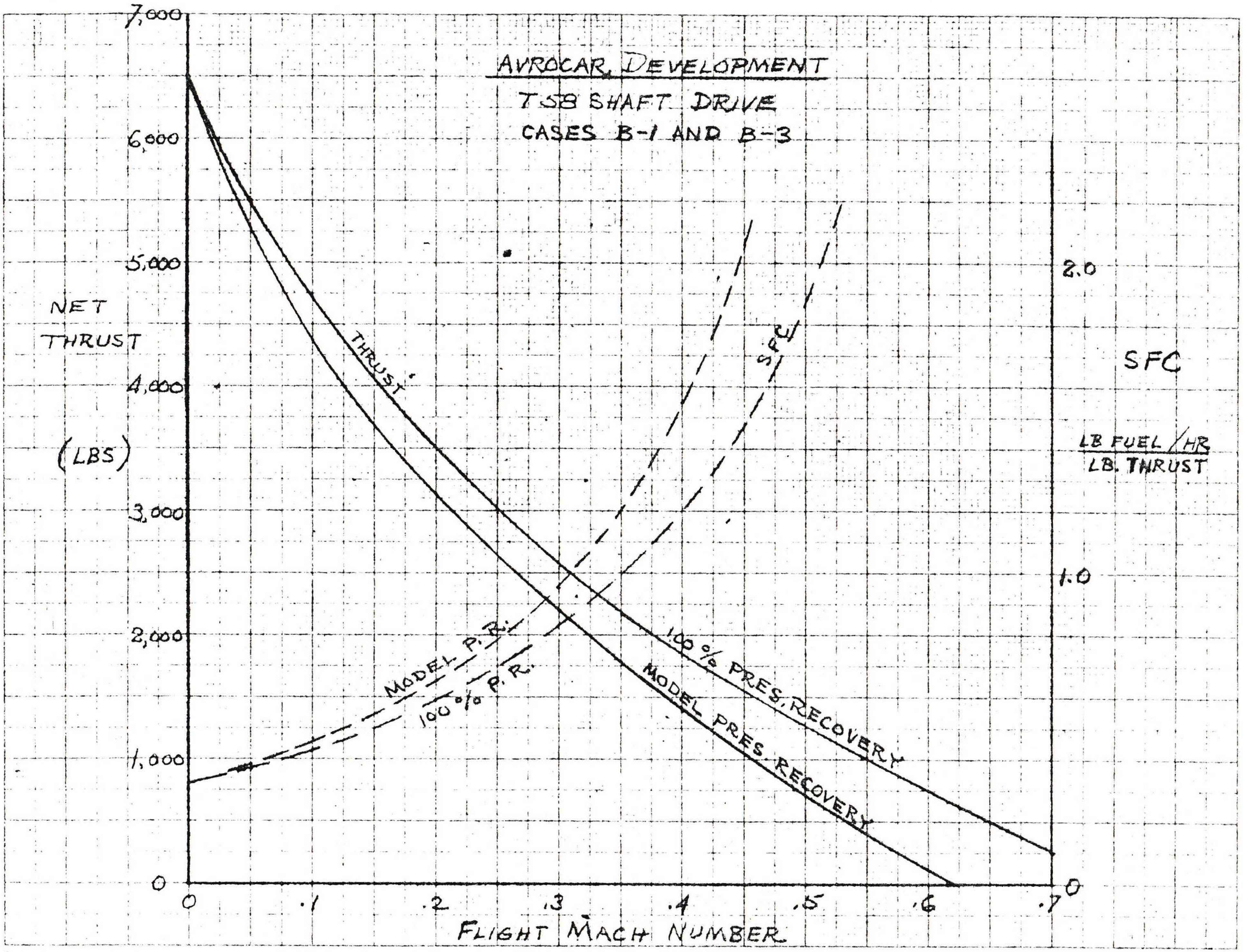
AVROCAR DEVELOPMENT
T58 SHAFT DRIVE
CASES B-1 AND B-3
NET THRUST (LBS)
7,000
6,000
5,000
4,000
3,000
2,000
1,000
0
THRUST
SFC
MODEL P.R.
100% P.R.
100% PRES. RECOVERY
MODEL PRES. RECOVERY
SFC
LB FUEL / HR / LB. THRUST
2.0
1.0
0
.1
.2
.3
.4
.5
.6
.7
FLIGHT MACH NUMBER

FIG. 2.10

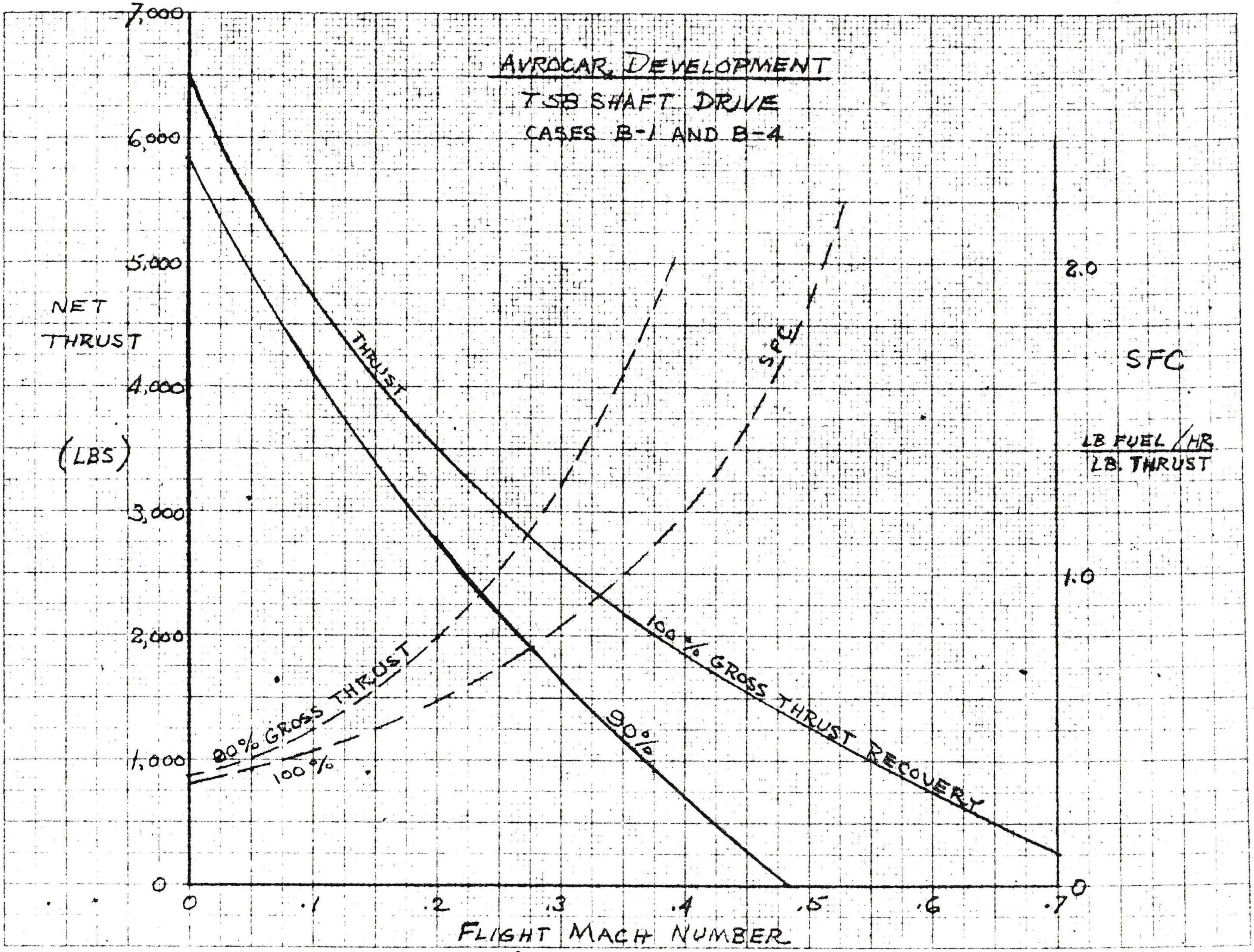
AVROCAR DEVELOPMENT
T58 SHAFT DRIVE
CASES B-1 AND B-4
NET THRUST (LBS)
7,000
6,000
5,000
4,000
3,000
2,000
1,000
0
THRUST
SFC
90% GROSS THRUST
100%
90%
100% GROSS THRUST RECOVERY
SFC
LB FUEL / HR / LB. THRUST
2.0
1.0
0
0
.1
.2
.3
.4
.5
.6
.7
FLIGHT MACH NUMBER

FIG. 2.11

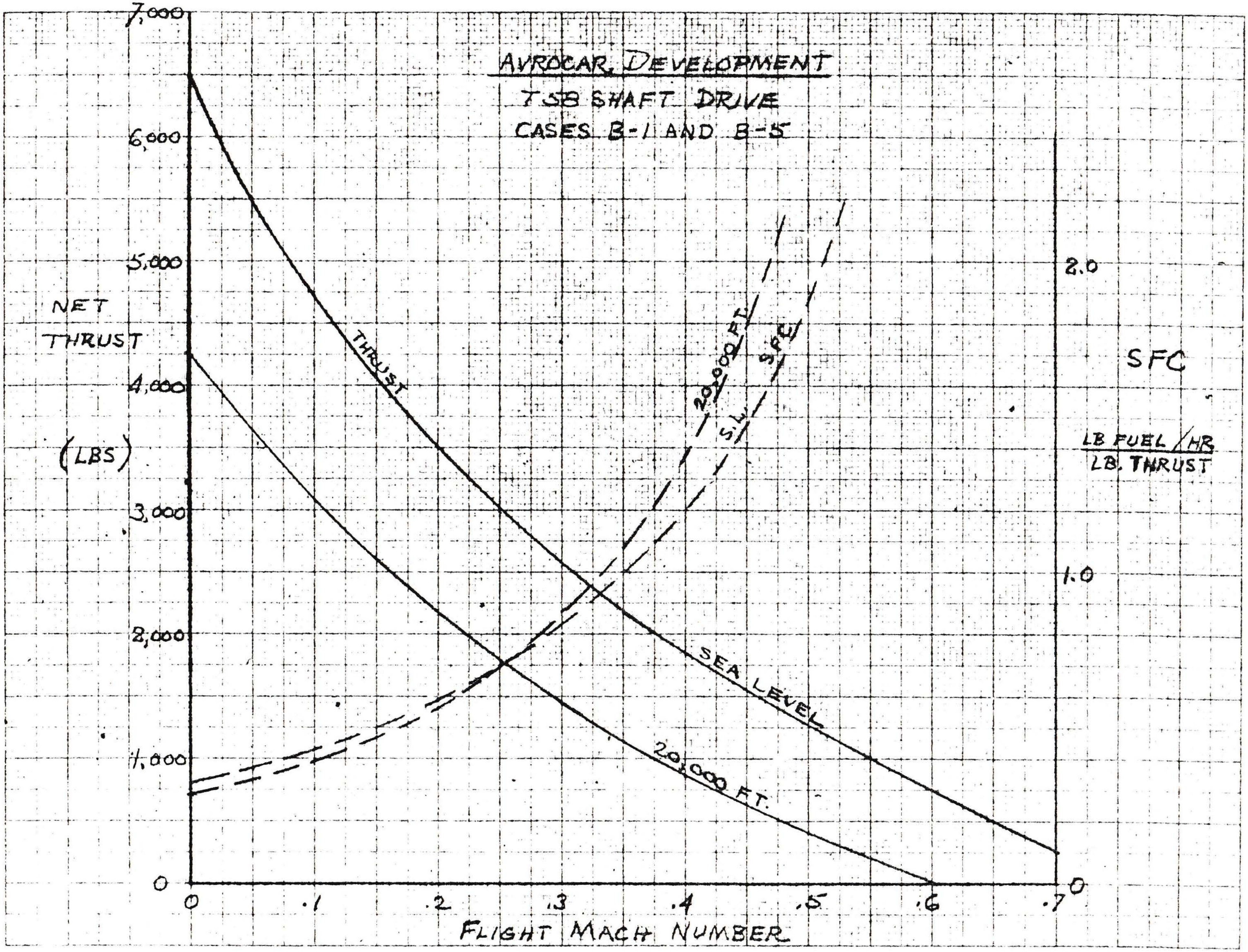
AVROCAR DEVELOPMENT
T58 SHAFT DRIVE
CASES B-1 AND B-5
NET THRUST (LBS)
7,000
6,000
5,000
4,000
3,000
2,000
1,000
0
THRUST
SEA LEVEL
20,000 FT.
20,000 FT.
S.L.
SFC
SFC
LB FUEL / HR / LB. THRUST
2.0
1.0
0
0
.1
.2
.3
.4
.5
.6
.7
FLIGHT MACH NUMBER

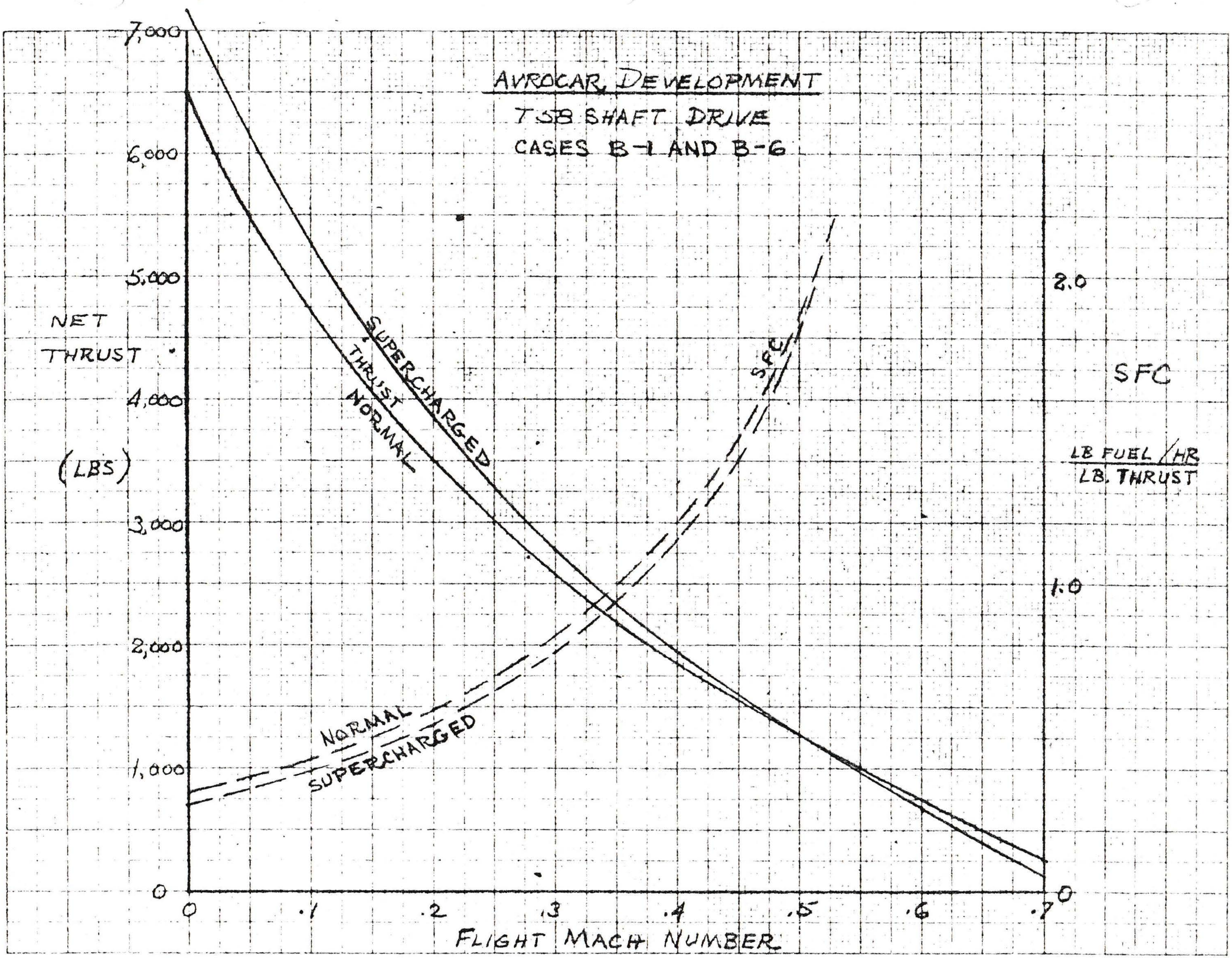
AVROCAR, DEVELOPMENT
T58 SHAFT DRIVE
CASES B-1 AND B-6
NET
THRUST
(LBS)
7,000
6,000
5,000
4,000
3,000
2,000
1,000
0
SFC
LB FUEL / HR
LB. THRUST
2.0
1.0
0
SUPERCHARGED
THRUST
NORMAL
SFC
NORMAL
SUPERCHARGED
0
.1
.2
.3
.4
.5
.6
.7
FLIGHT MACH NUMBER

FIG. 2.13

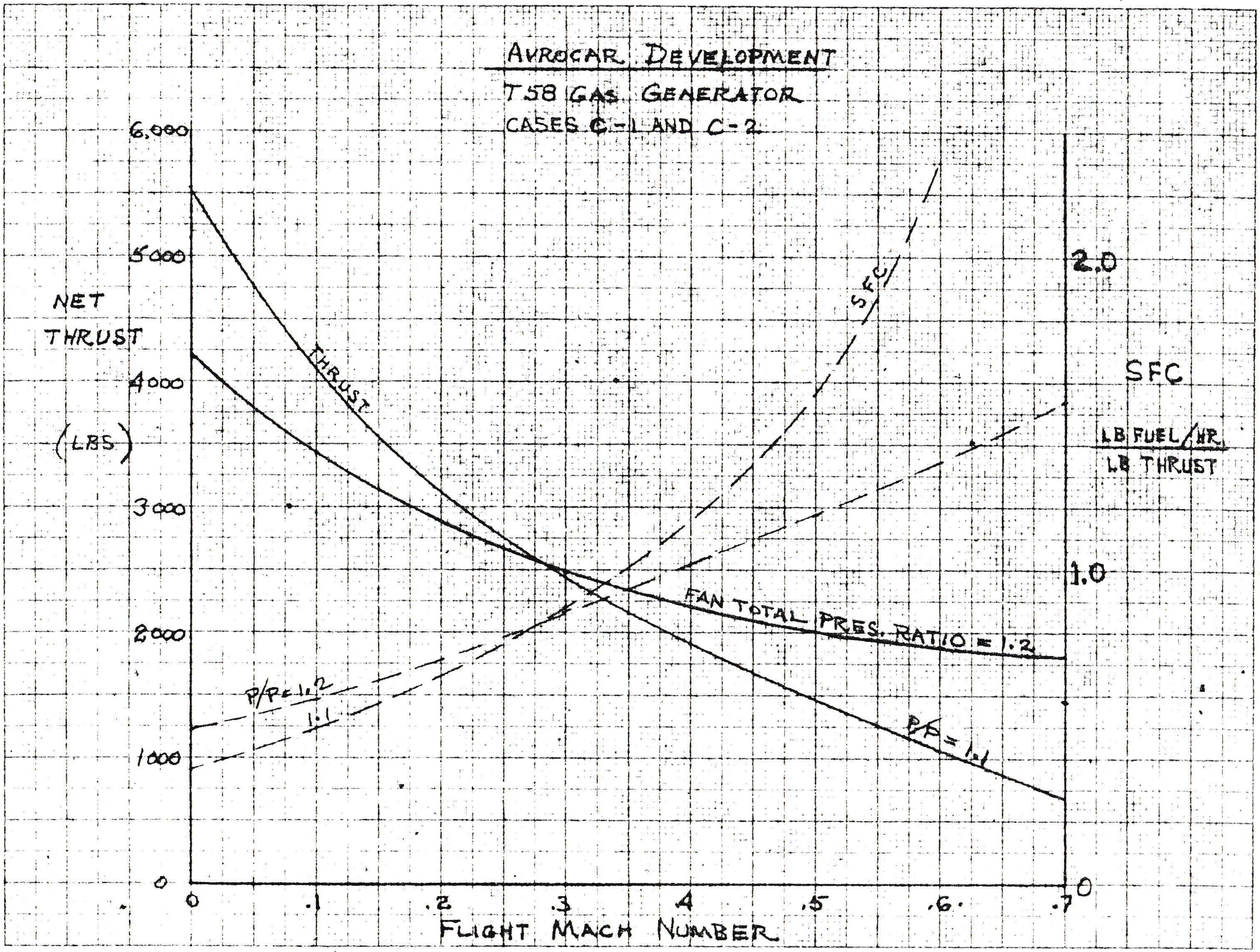
AVROCAR DEVELOPMENT
T58 GAS GENERATOR
CASES C-1 AND C-2
NET THRUST (LBS)
6,000
5000
4000
3000
2000
1000
0
THRUST
SFC
FAN TOTAL PRES. RATIO = 1.2
P/P = 1.1
P/P = 1.2
1.1
SFC
LB FUEL/HR / LB THRUST
2.0
1.0
0
.1
.2
.3
.4
.5
.6
.7
FLIGHT MACH NUMBER

FIG 2.14

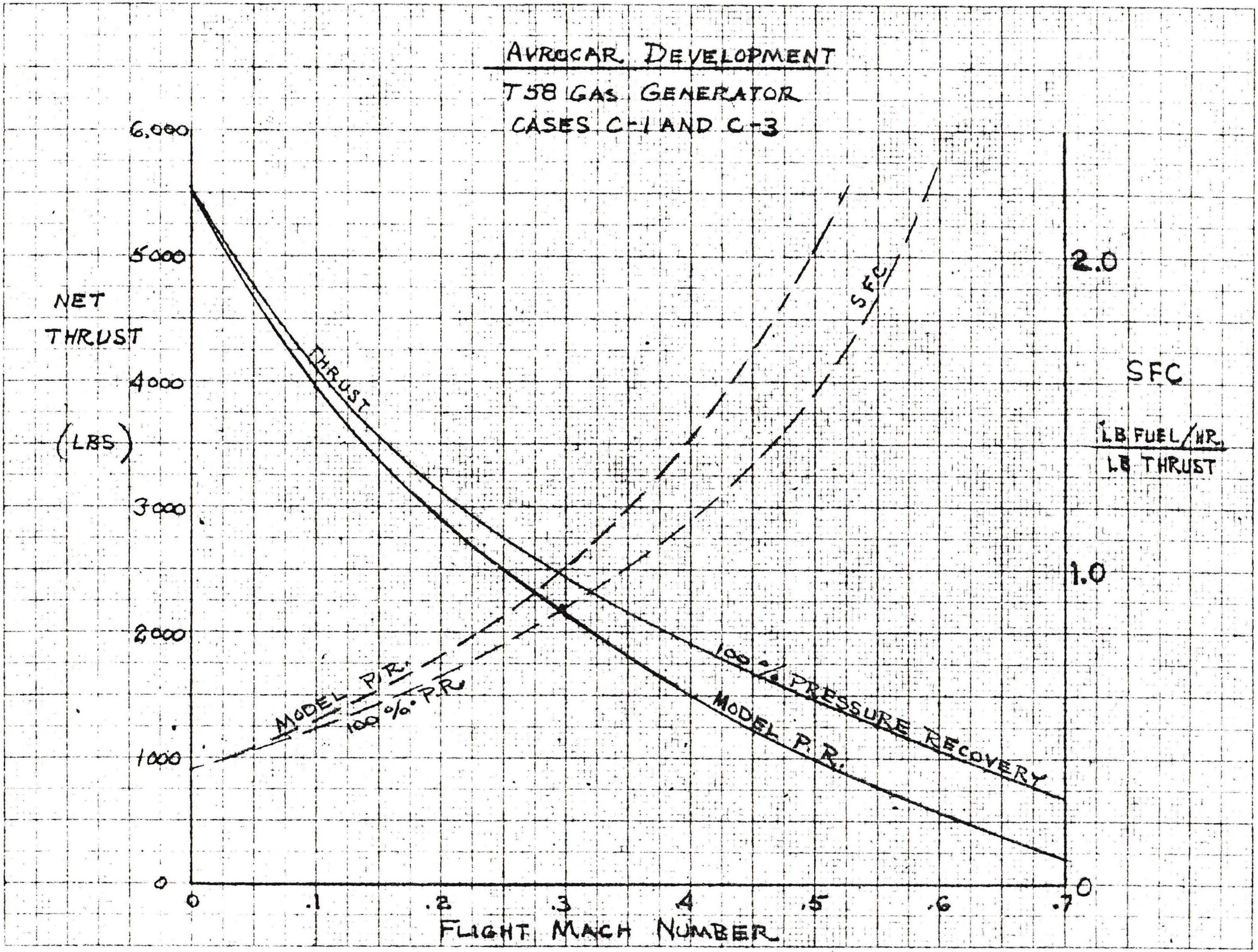
AVROCAR DEVELOPMENT
T58 GAS GENERATOR
CASES C-1 AND C-3
NET THRUST (LBS)
6,000
5000
4000
3000
2000
1000
0
SFC
LB FUEL/HR.
LB THRUST
2.0
1.0
0
THRUST
SFC
MODEL P.R.
100% P.R.
100% PRESSURE RECOVERY
MODEL P.R.
0
.1
.2
.3
.4
.5
.6
.7
FLIGHT MACH NUMBER

FIG. 2.15

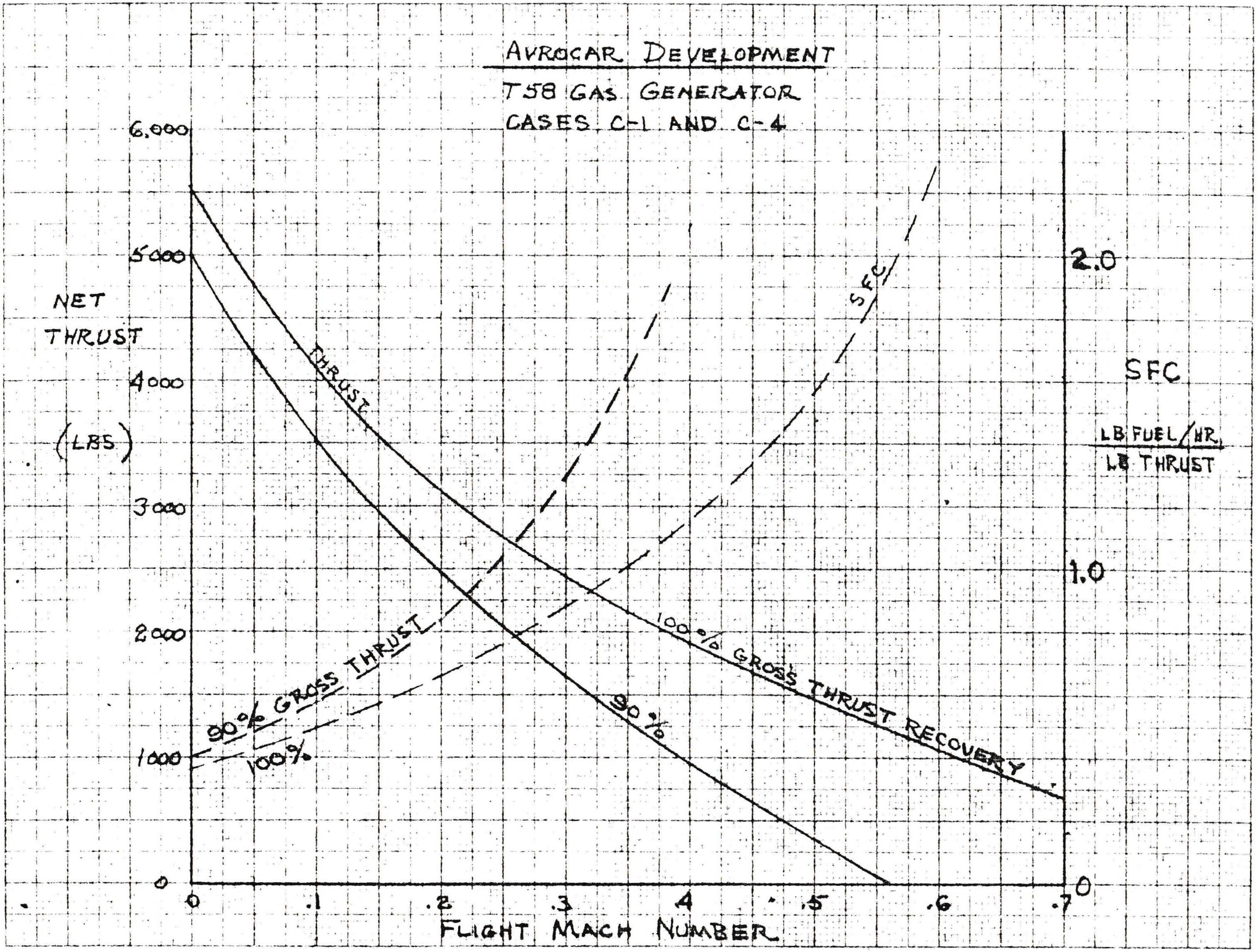
AVROCAR DEVELOPMENT
T58 GAS GENERATOR
CASES C-1 AND C-4
NET THRUST (LBS)
6,000
5000
4000
3000
2000
1000
0
SFC
LB FUEL/HR. / LB THRUST
2.0
1.0
0
THRUST
100% GROSS THRUST RECOVERY
90%
SFC
90% GROSS THRUST
100%
0
.1
.2
.3
.4
.5
.6
.7
FLIGHT MACH NUMBER

FIG. 2.16

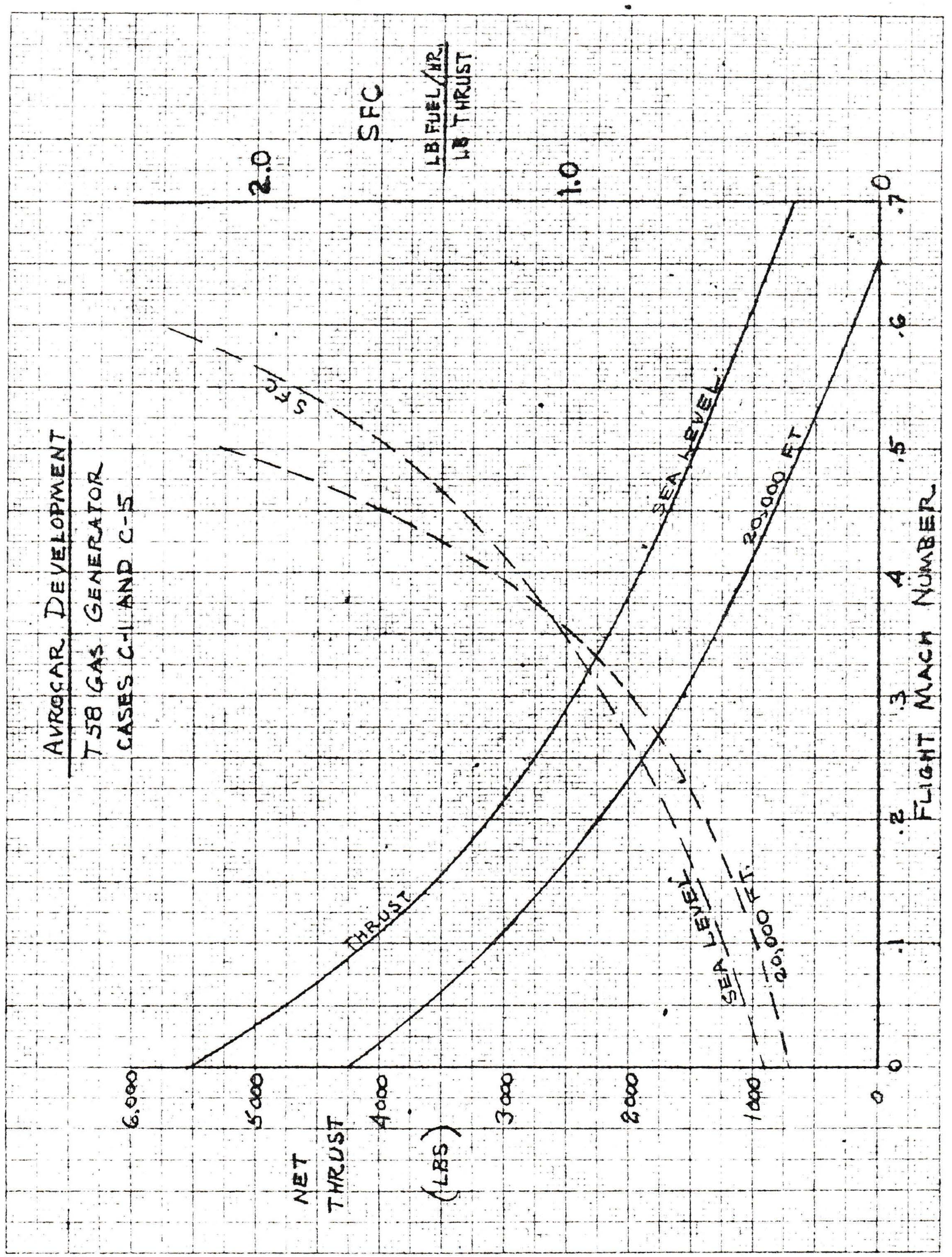
AVROCAR DEVELOPMENT
T58 GAS GENERATOR
CASES C-1 AND C-5
SFC
LB FUEL/HR.
LB THRUST
2.0
1.0
0
NET THRUST
(LBS)
6,000
5000
4000
3000
2000
1000
0
0
.1
.2
.3
.4
.5
.6
.7
FLIGHT MACH NUMBER
THRUST
SEA LEVEL
20,000 FT
SFC
SEA LEVEL
20,000 FT.

FIG. 2.17

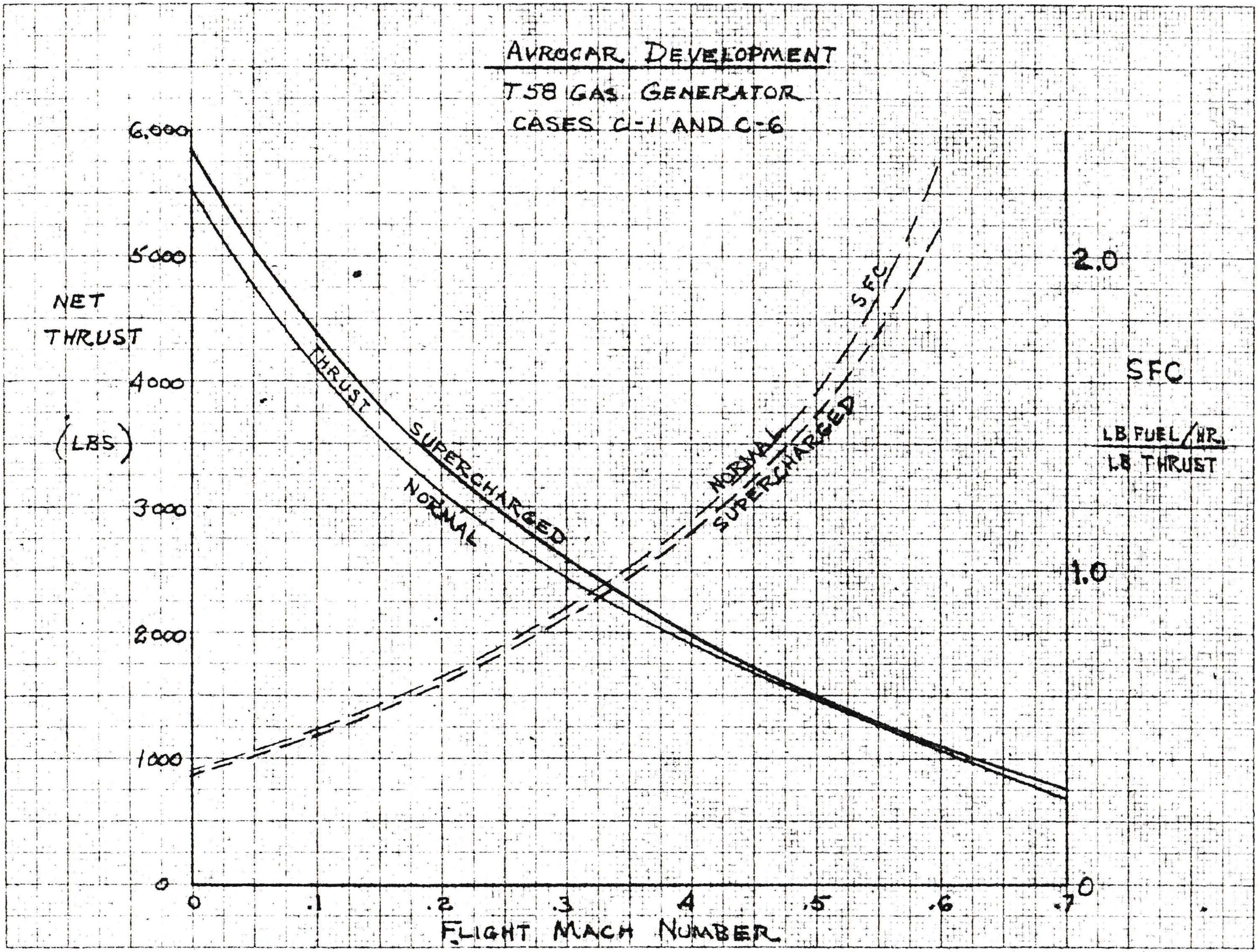
AVROCAR DEVELOPMENT
T58 GAS GENERATOR
CASES C-1 AND C-6
NET THRUST (LBS)
6,000
5000
4000
3000
2000
1000
0
THRUST
SUPERCHARGED
NORMAL
SFC
2.0
1.0
0
LB FUEL/HR.
LB THRUST
0
.1
.2
.3
.4
.5
.6
.7
FLIGHT MACH NUMBER

FIG. 2.18

THRUST & NOZZLE EXIT AREA
VS
FAN AREA

SEA LEVEL STATIC

1044 H.P.
FAN PRESSURE RATIO = 1.07

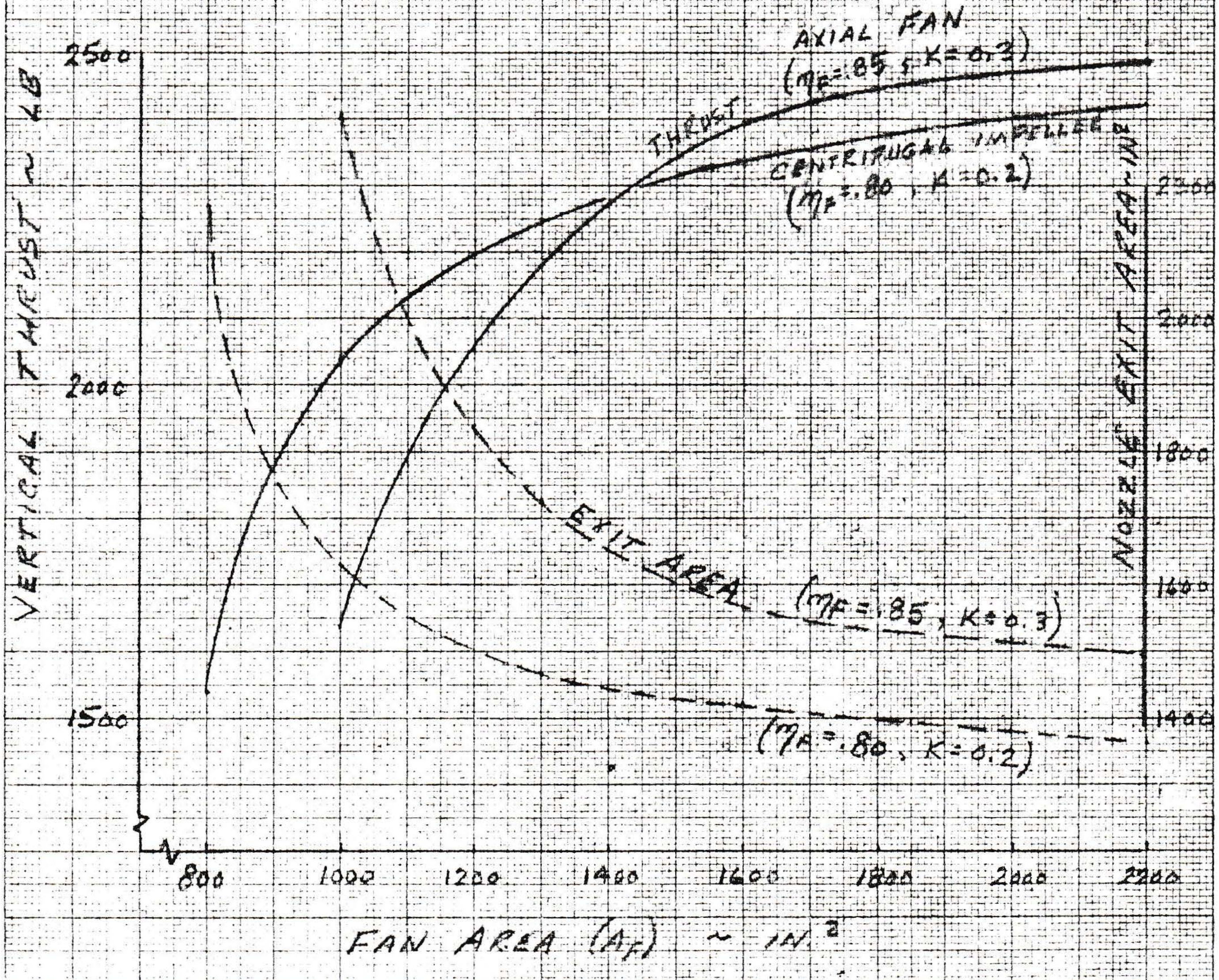

FIG. 3.1

INTAKE PRESSURE RECOVERY

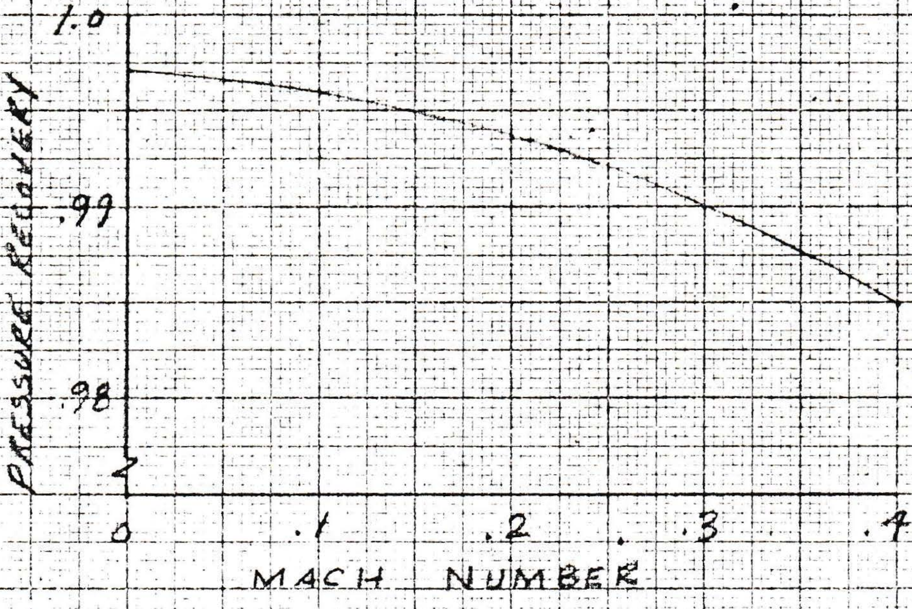

FIG. 3.2

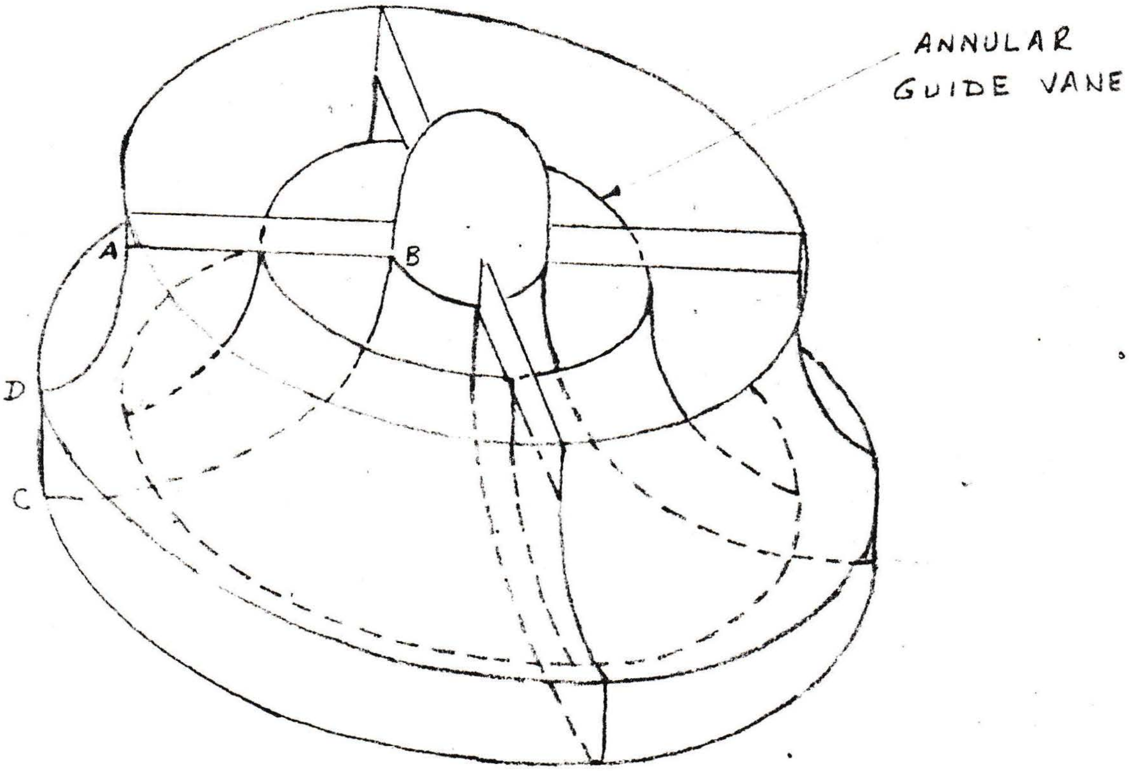

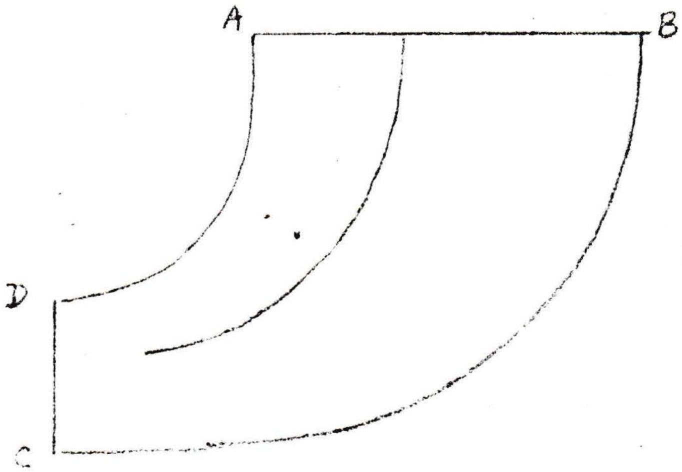

CROSS SECTION
THROUGH DUCT

FAN DUCT DESIGN
(90° BEND BELOW FAN)

FIG. 3.3

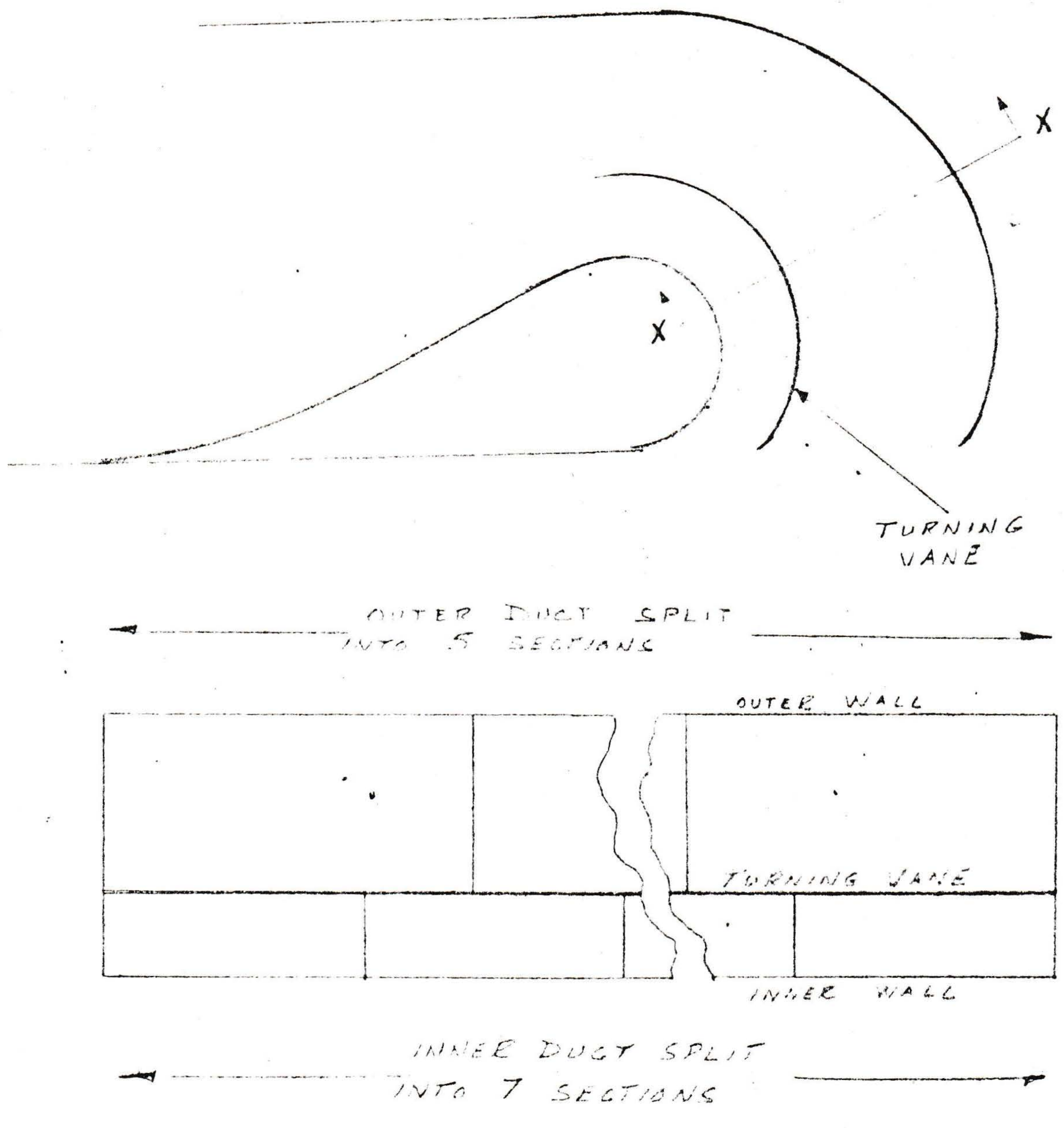

NOZZLE ASSEMBLY DESIGN

THRUST VS FAN PRESSURE RATIO

SEA LEVEL TAKE-OFF POWER

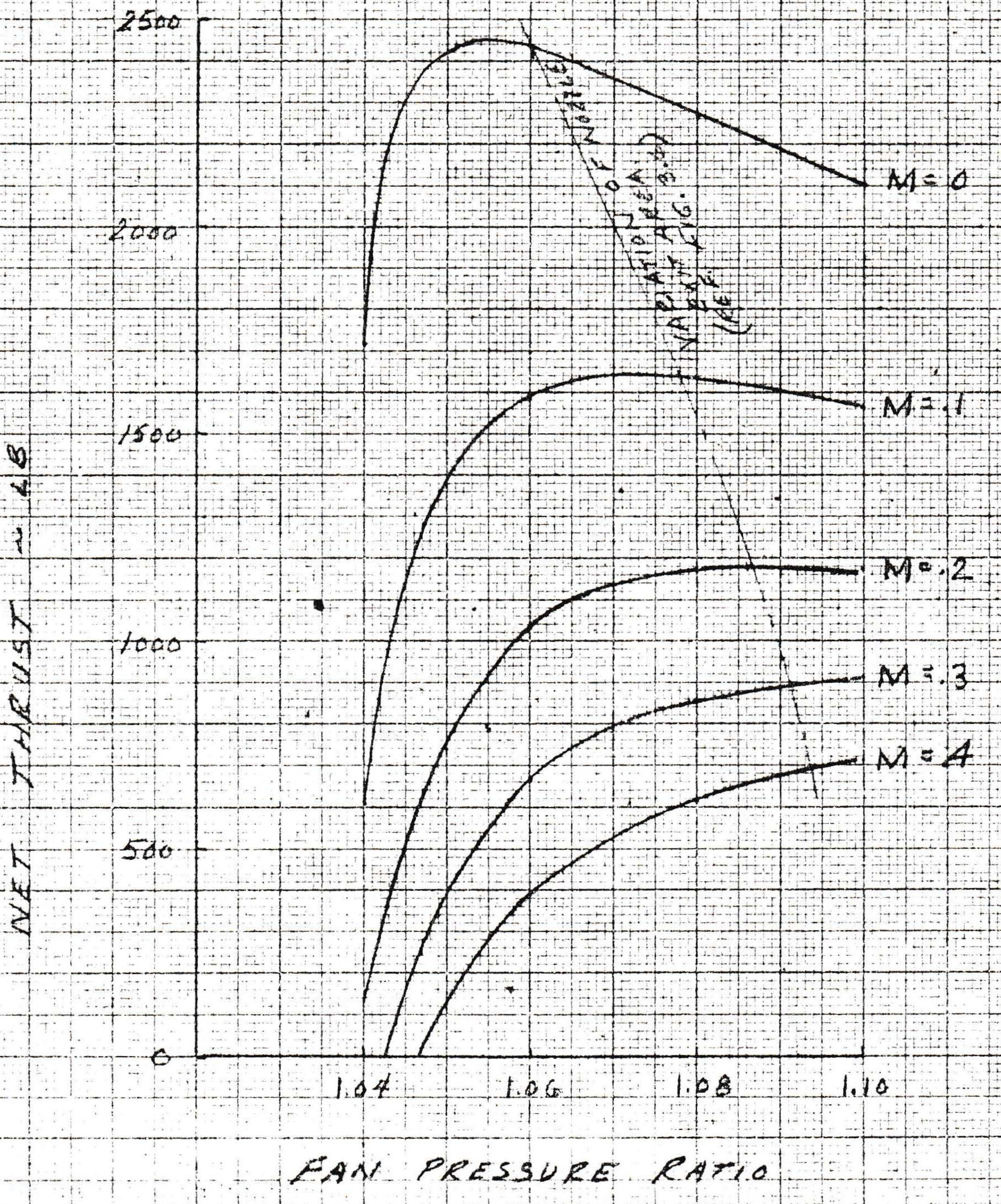

FIG 3.8

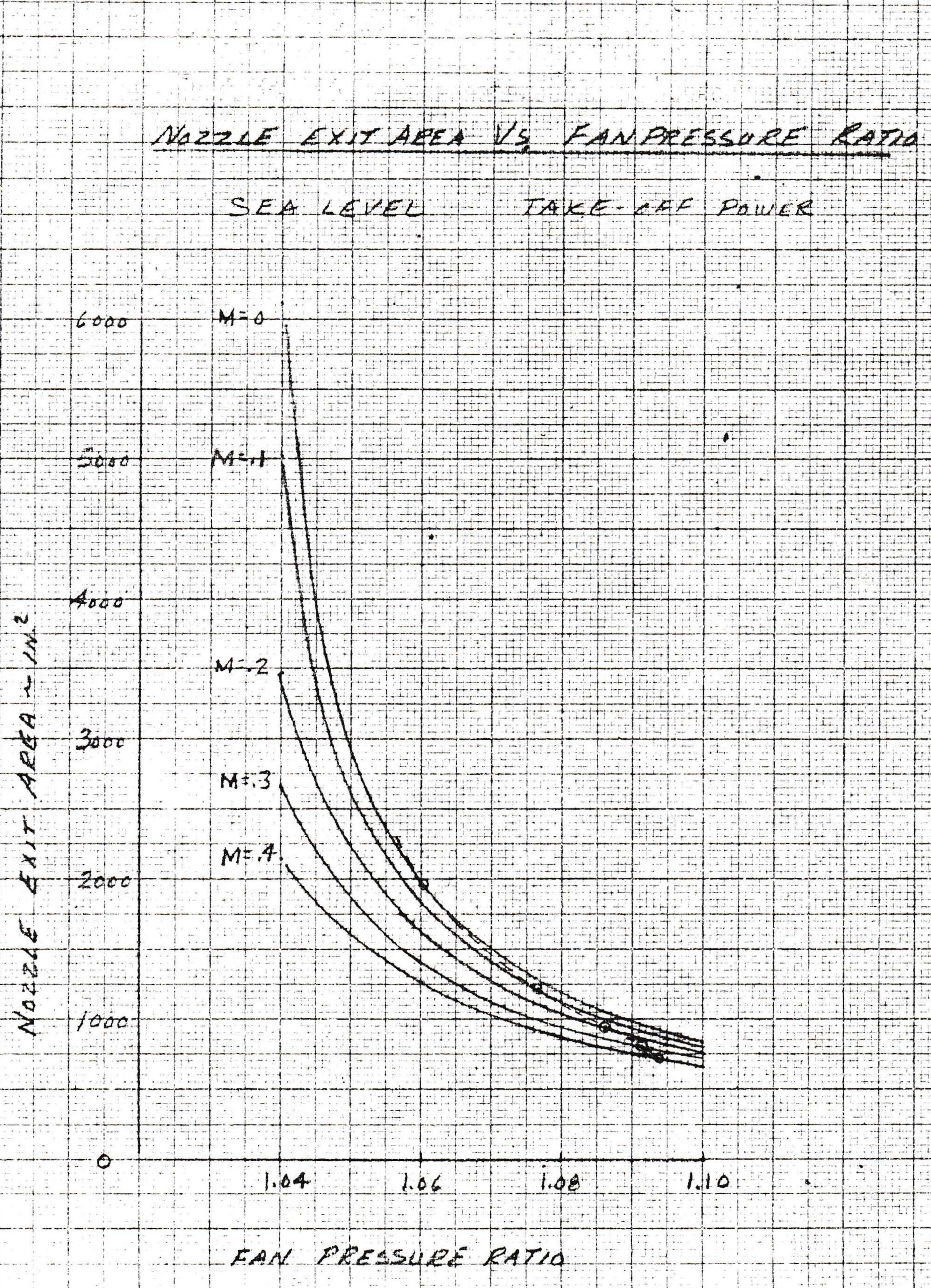
NOZZLE EXIT AREA VS FAN PRESSURE RATIO
SEA LEVEL TAKE-OFF POWER
M=0
M=.1
M=.2
M=.3
M=.4
6000
5000
4000
3000
2000
1000
0
1.04
1.06
1.08
1.10
NOZZLE EXIT AREA ~ IN.^{2}
FAN PRESSURE RATIO

FIG 3.6

VARIATION OF NOZZLE EXIT AREA WITH MACH NUMBER

SEA LEVEL

FAN AREA - 2160 IN²

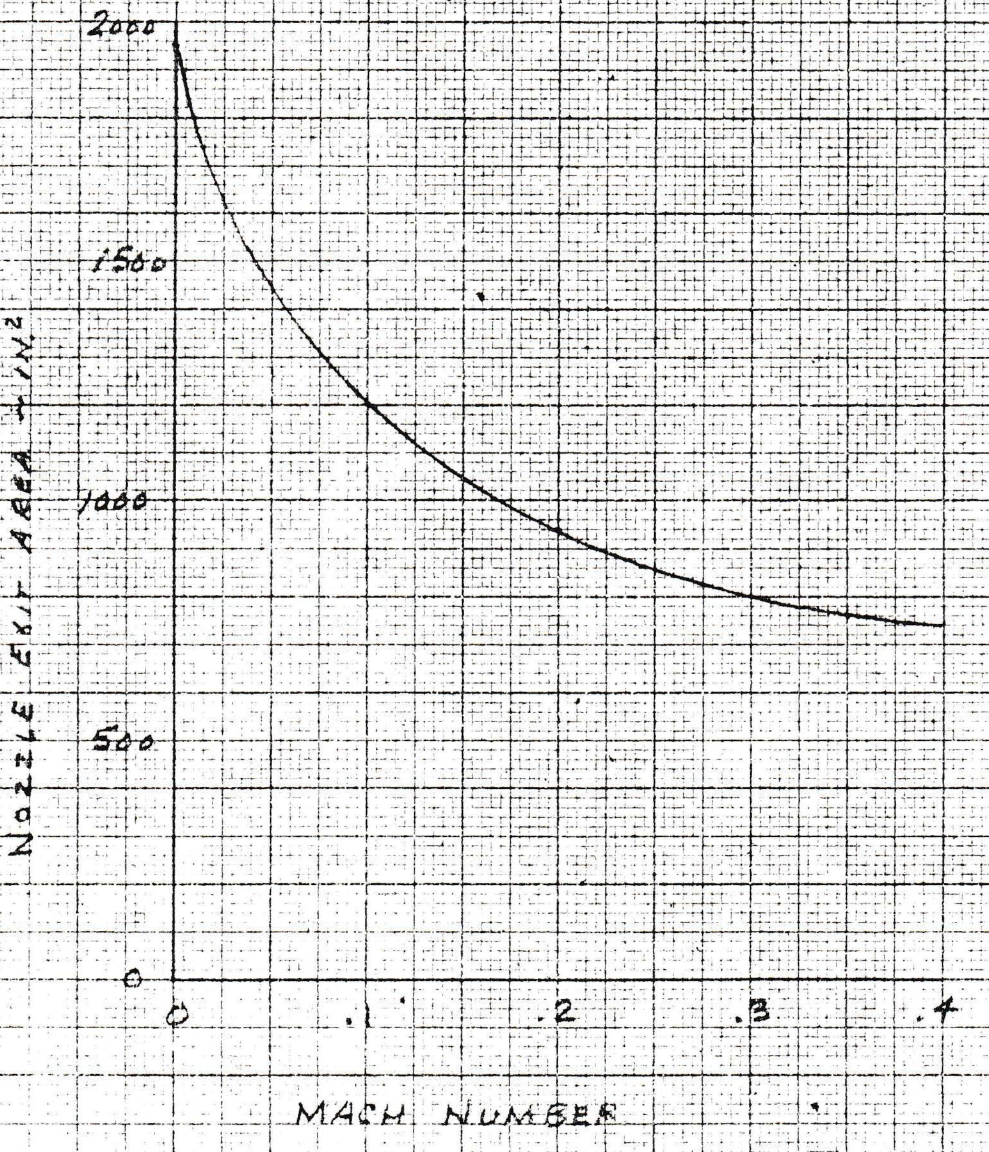

Fig. 37

NET THRUST VS FAN PRESSURE RATIO

SEA LEVEL

2 ASTAZOU II ENGINES
FAN AREA = 2160 IN.²

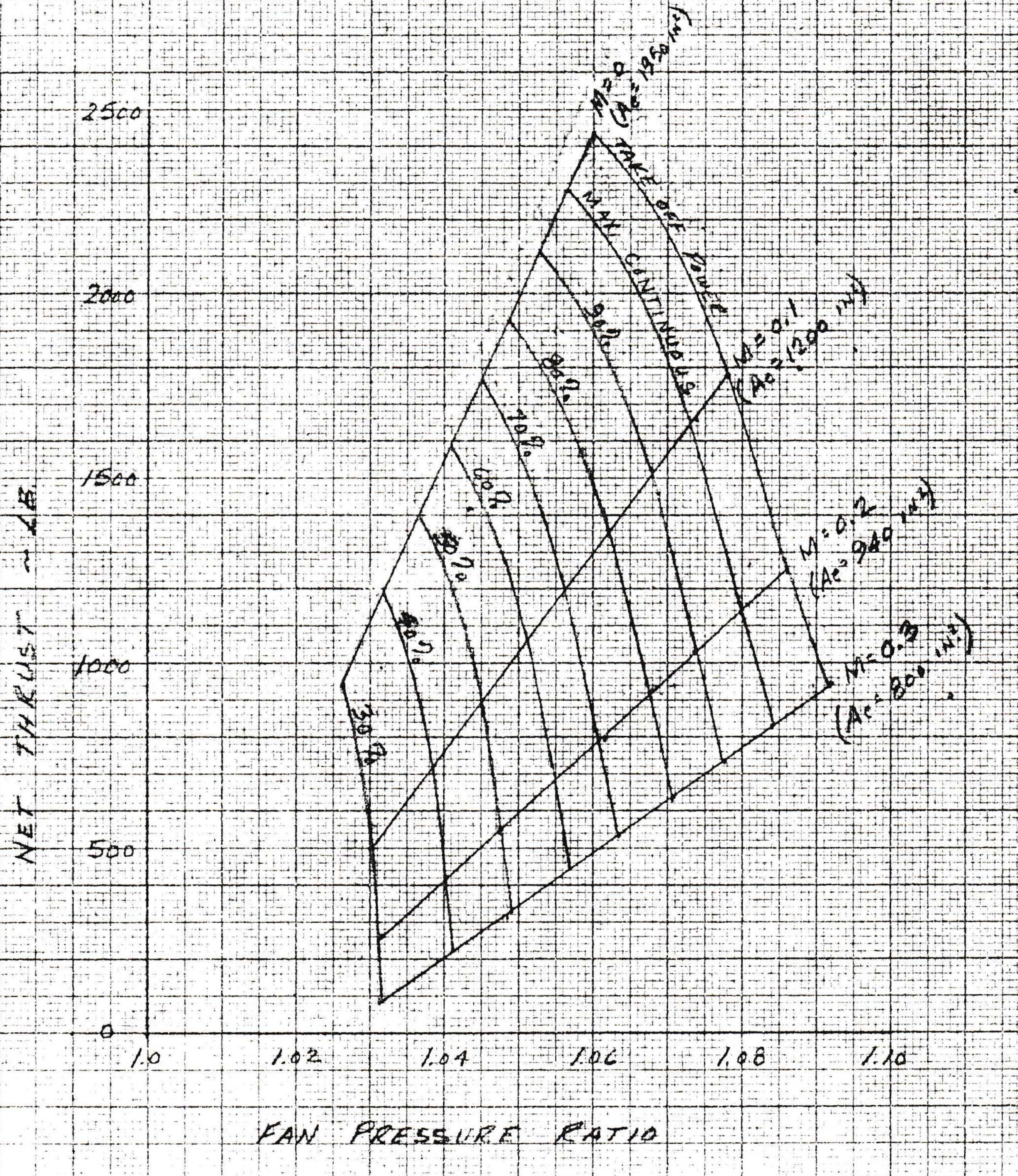

FIG. 3.8

THRUST & DRAG VS MACH NUMBER

SEA LEVEL

TWO ASTAZOU II ENGINES

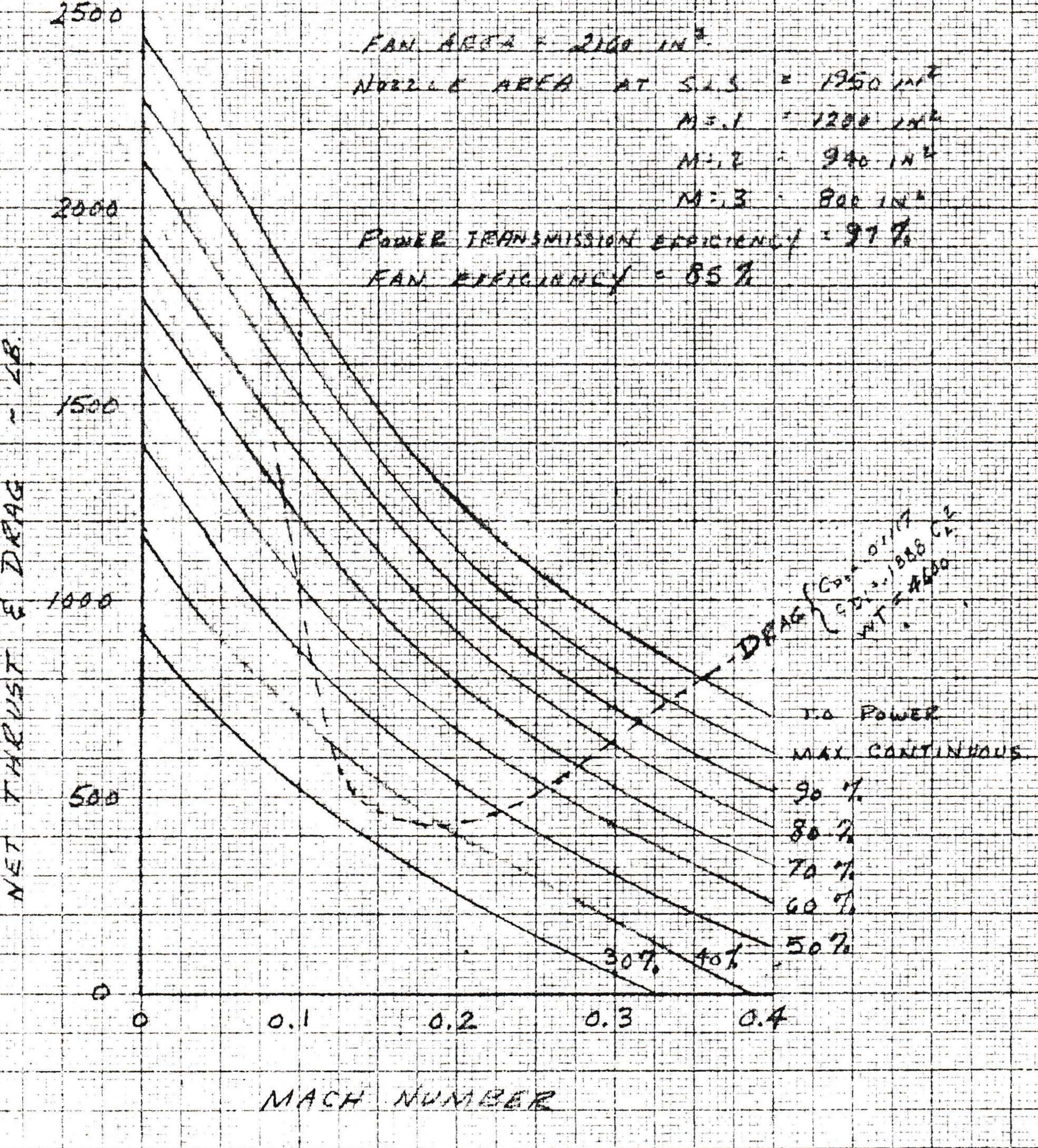

FIG. 3.9

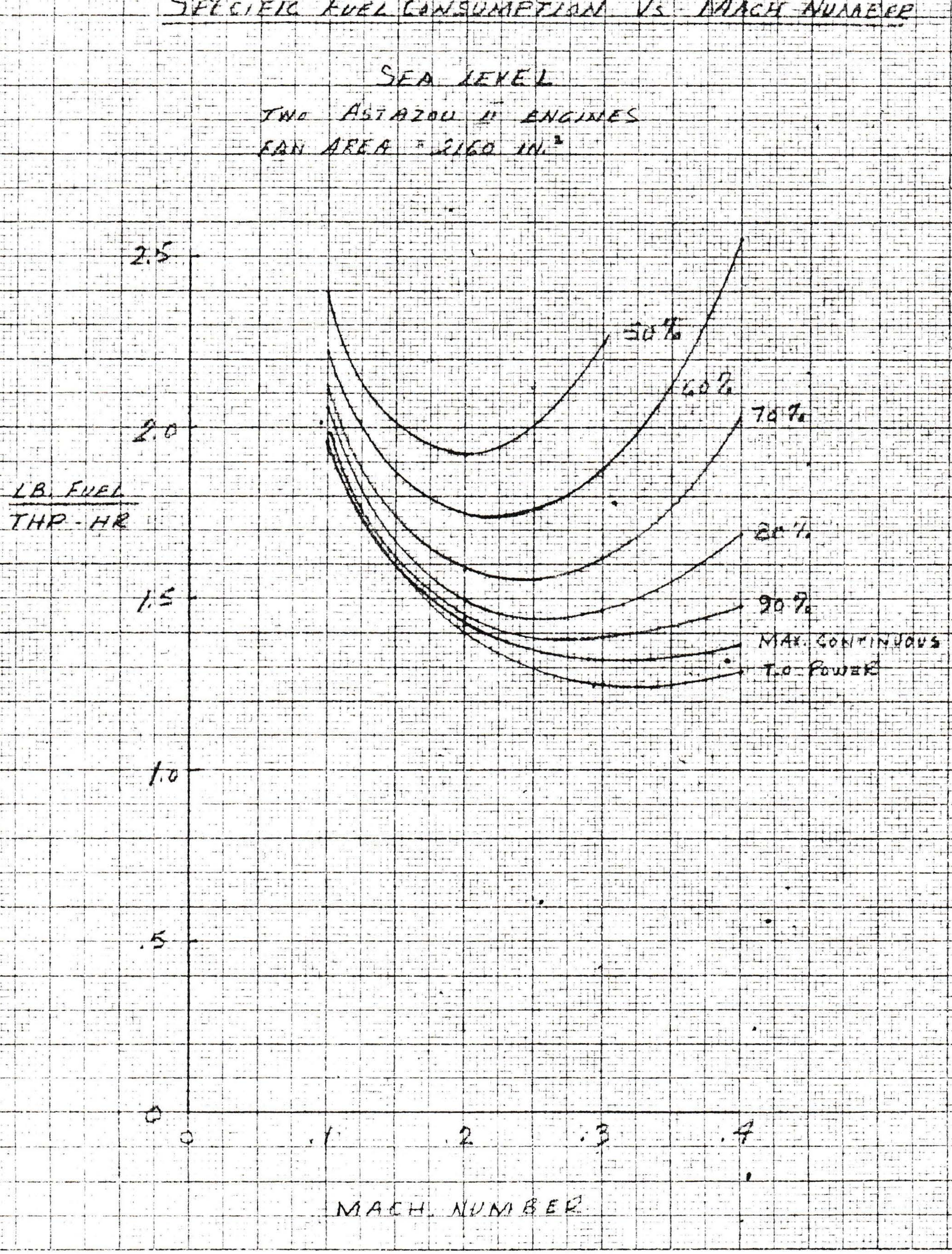
SPECIFIC FUEL CONSUMPTION Vs MACH NUMBER
SEA LEVEL
TWO ASTAZOU II ENGINES
FAN AREA = 2160 IN.²
2.5
2.0
1.5
1.0
.5
0
LB. FUEL
THP - HR
50%
60%
70%
80%
90%
MAX. CONTINUOUS
T.O. POWER
0
.1
.2
.3
.4
MACH NUMBER

FIG. 2.16

NET THRUST VS FAN PRESSURE RATIO

10,000 FT.

TWO ASTAZOU II ENGINES

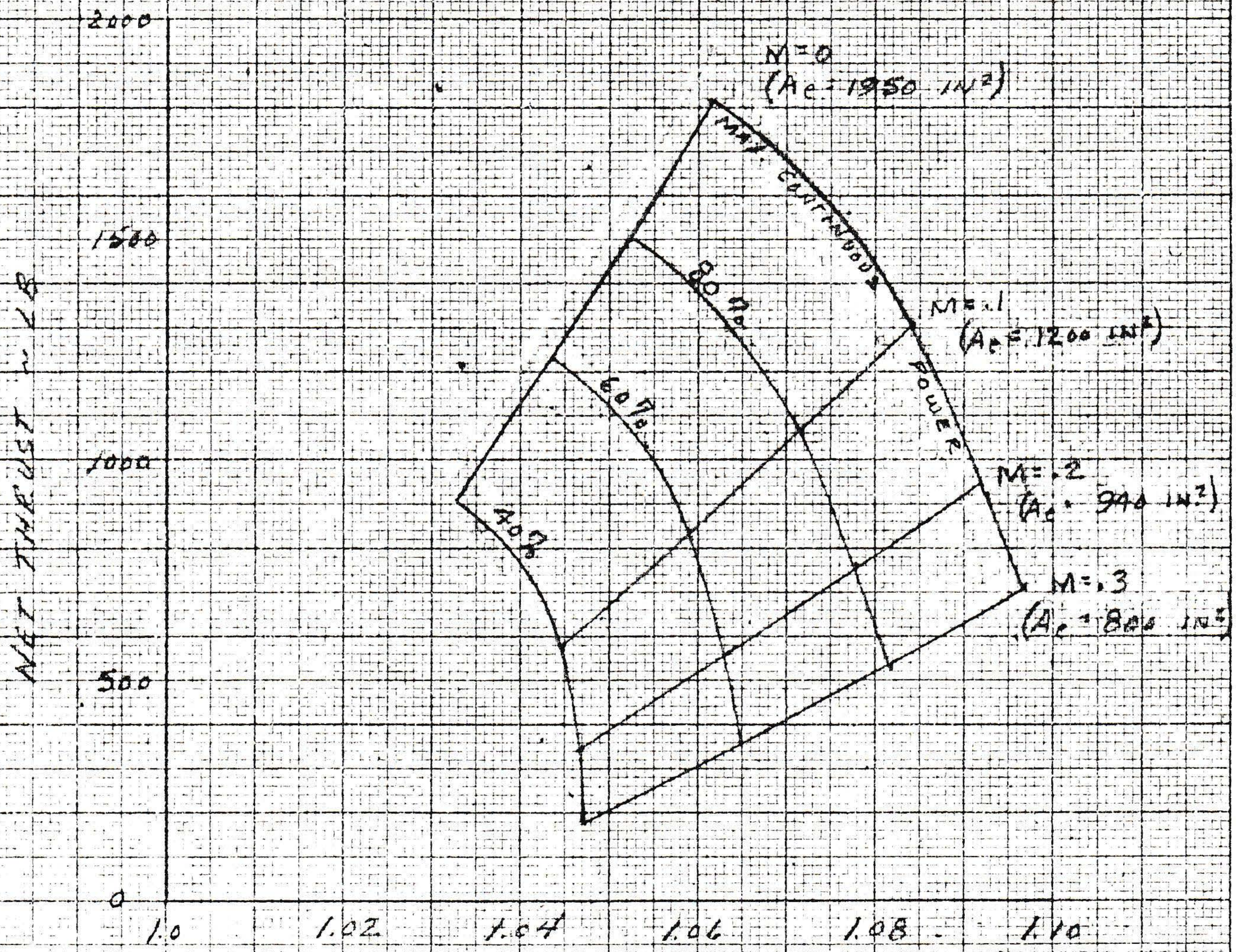

FIG. 3.11

THRUST & DRAG VS MACH NUMBER

10,000 FT.

TWO ASTAZOU II ENGINES

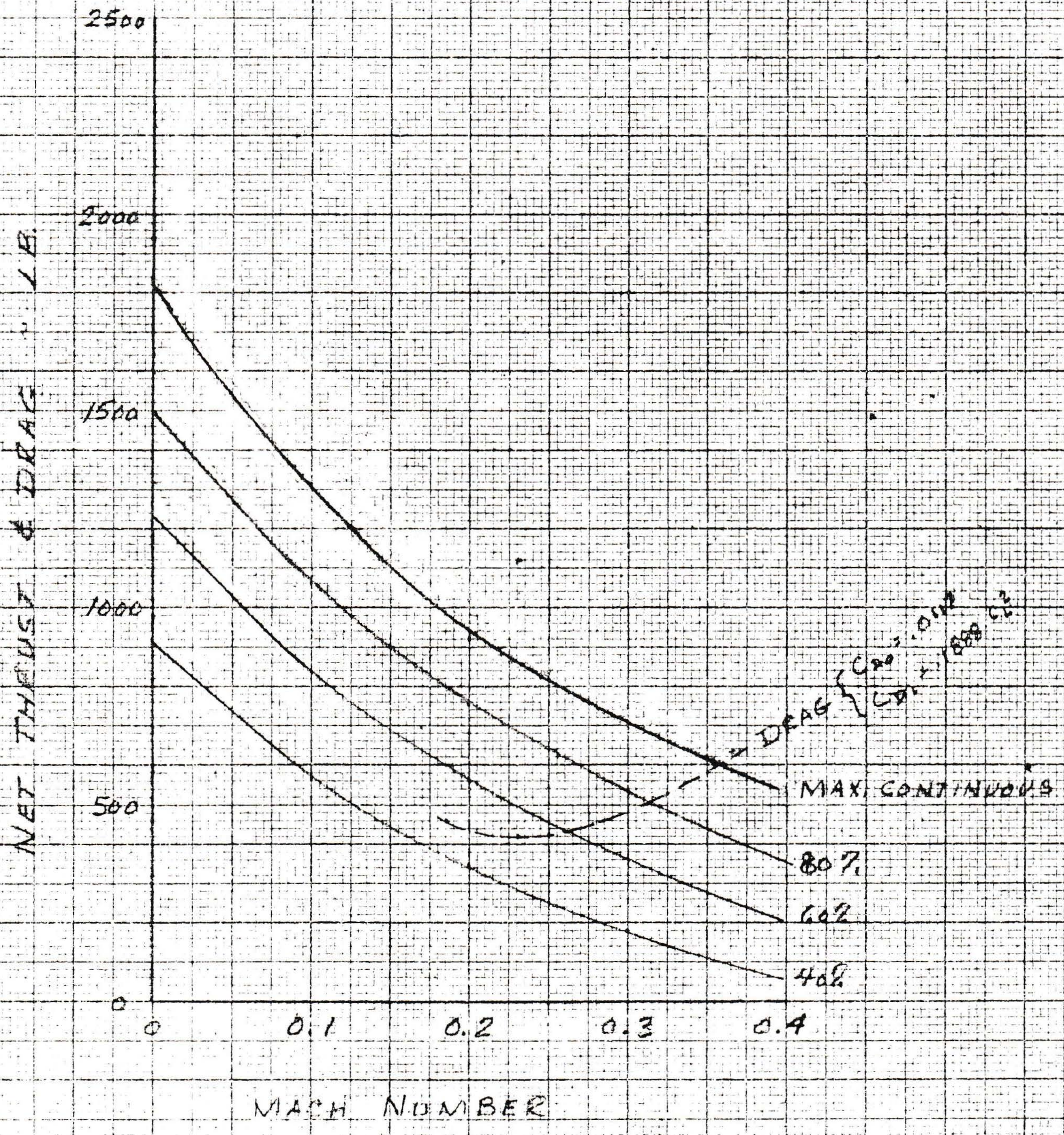

FIG. 3.12

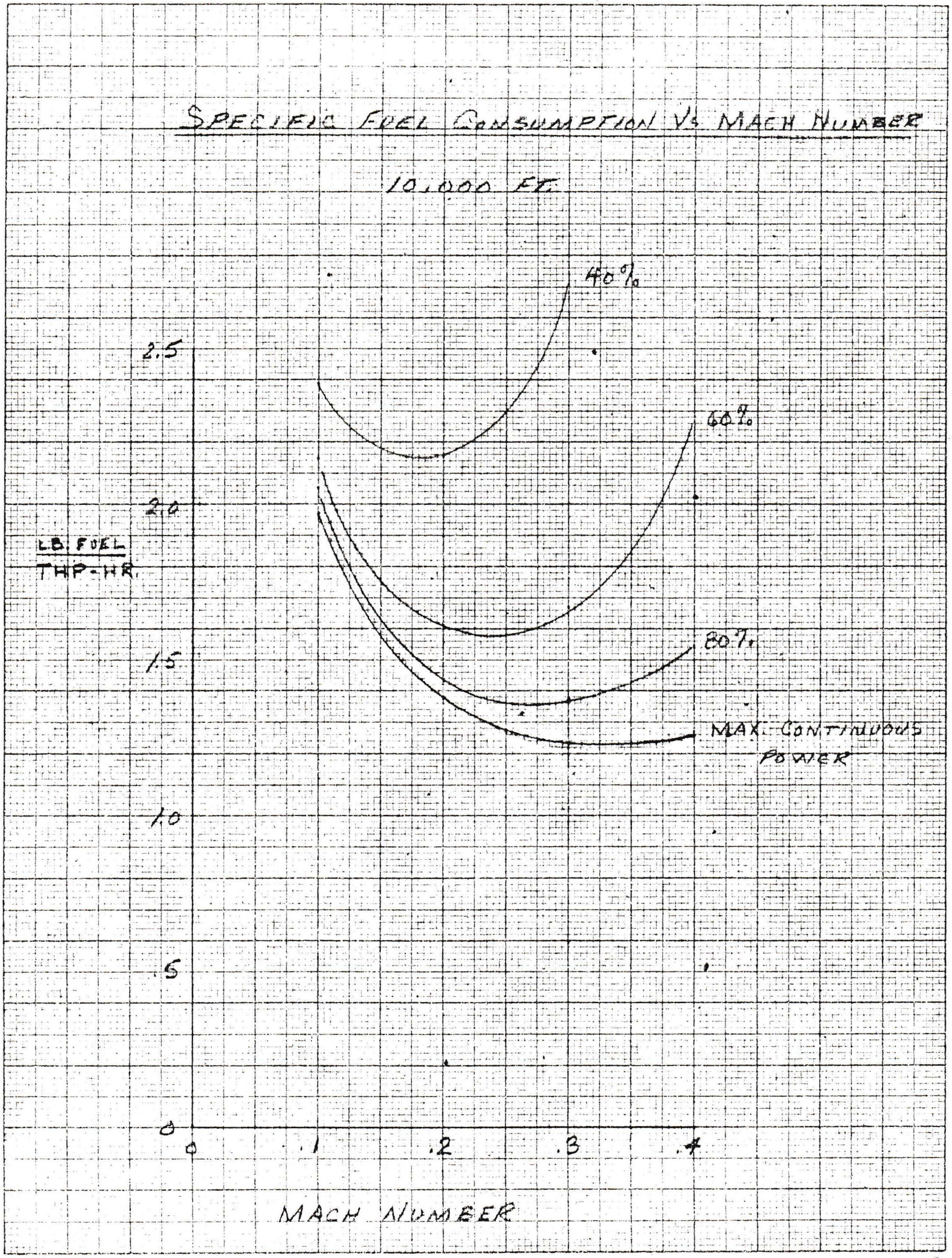
SPECIFIC FUEL CONSUMPTION VS MACH NUMBER
10,000 FT.
40%
60%
80%
MAX. CONTINUOUS POWER
2.5
2.0
1.5
1.0
.5
0
LB. FUEL / THP-HR
0
.1
.2
.3
.4
MACH NUMBER

FIG. 3.13

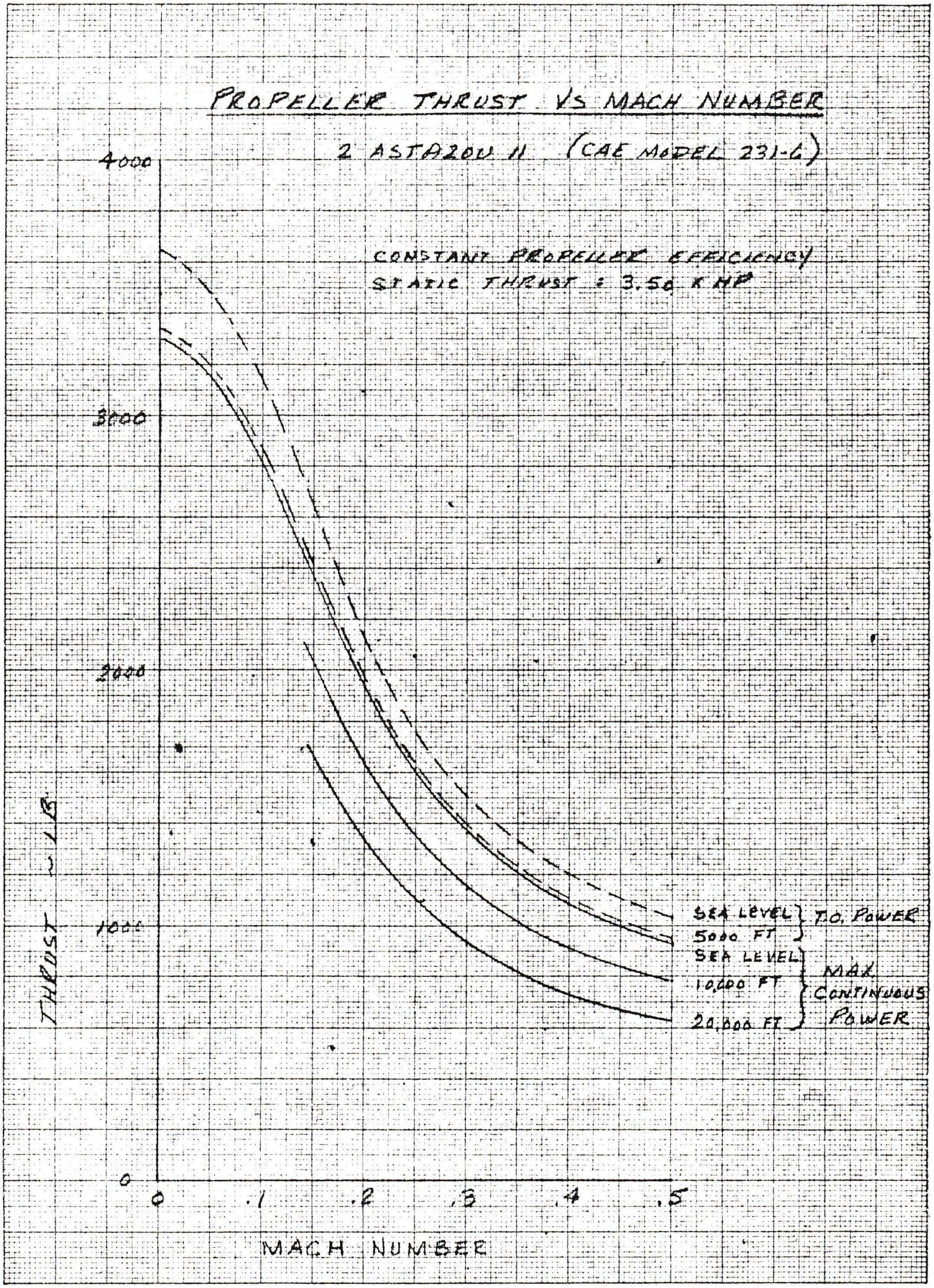
PROPELLER THRUST VS MACH NUMBER
2 ASTAZOU II (CAE MODEL 231-6)
CONSTANT PROPELLER EFFICIENCY
STATIC THRUST = 3.50 x HP
4000
3000
2000
1000
0
THRUST ~ LB
0
.1
.2
.3
.4
.5
MACH NUMBER
SEA LEVEL
5000 FT
T.O. POWER
SEA LEVEL
10,000 FT
20,000 FT
MAX CONTINUOUS POWER

FIG. 3.14

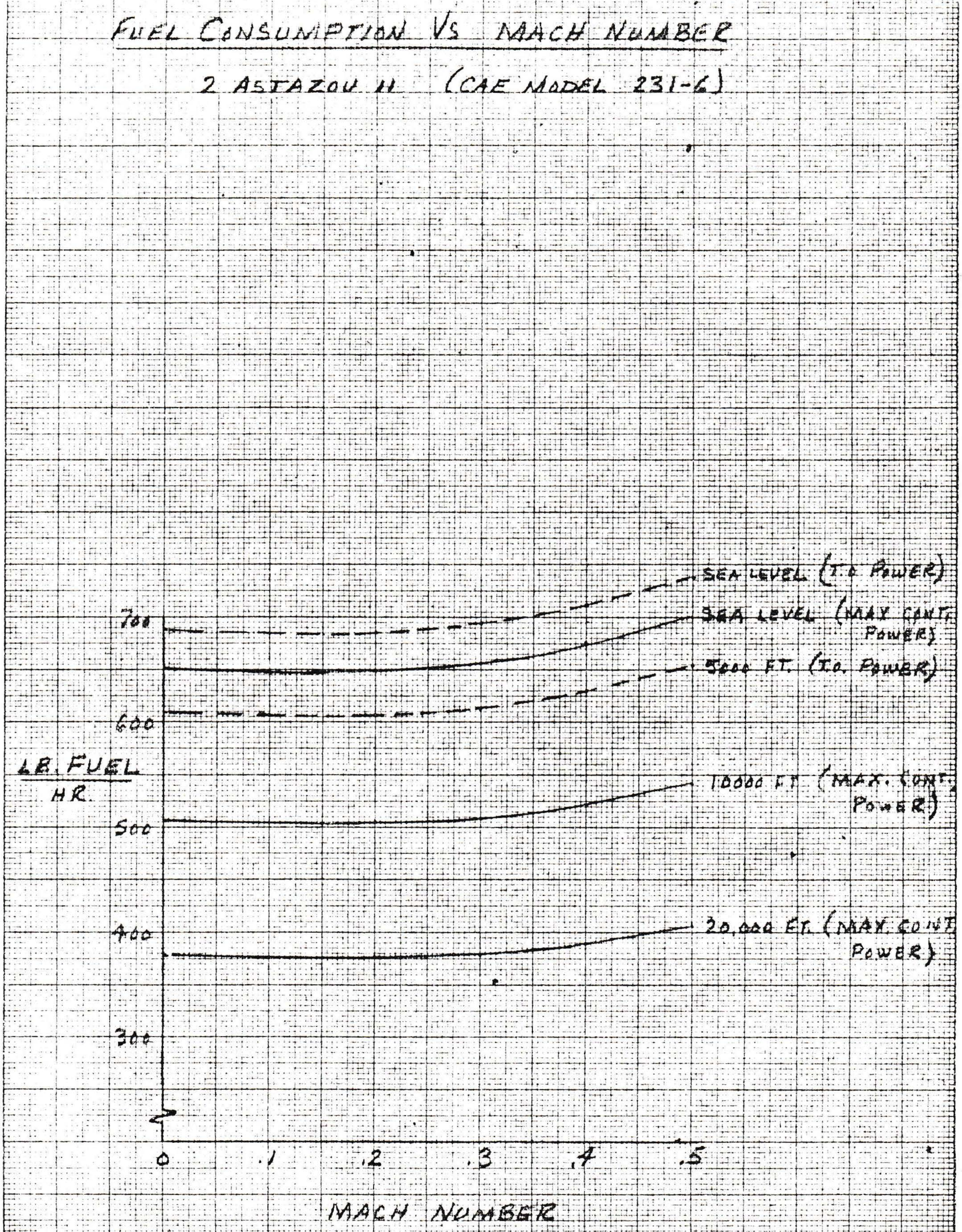
FUEL CONSUMPTION VS MACH NUMBER
2 ASTAZOU II (CAE MODEL 231-6)
LB. FUEL / HR.
700
600
500
400
300
0
.1
.2
.3
.4
.5
MACH NUMBER
SEA LEVEL (T.O. POWER)
SEA LEVEL (MAX CONT. POWER)
5000 FT. (T.O. POWER)
10000 FT (MAX. CONT. POWER)
20,000 FT. (MAX CONT POWER)

FIG. 3.15

2 ASTAZOU II

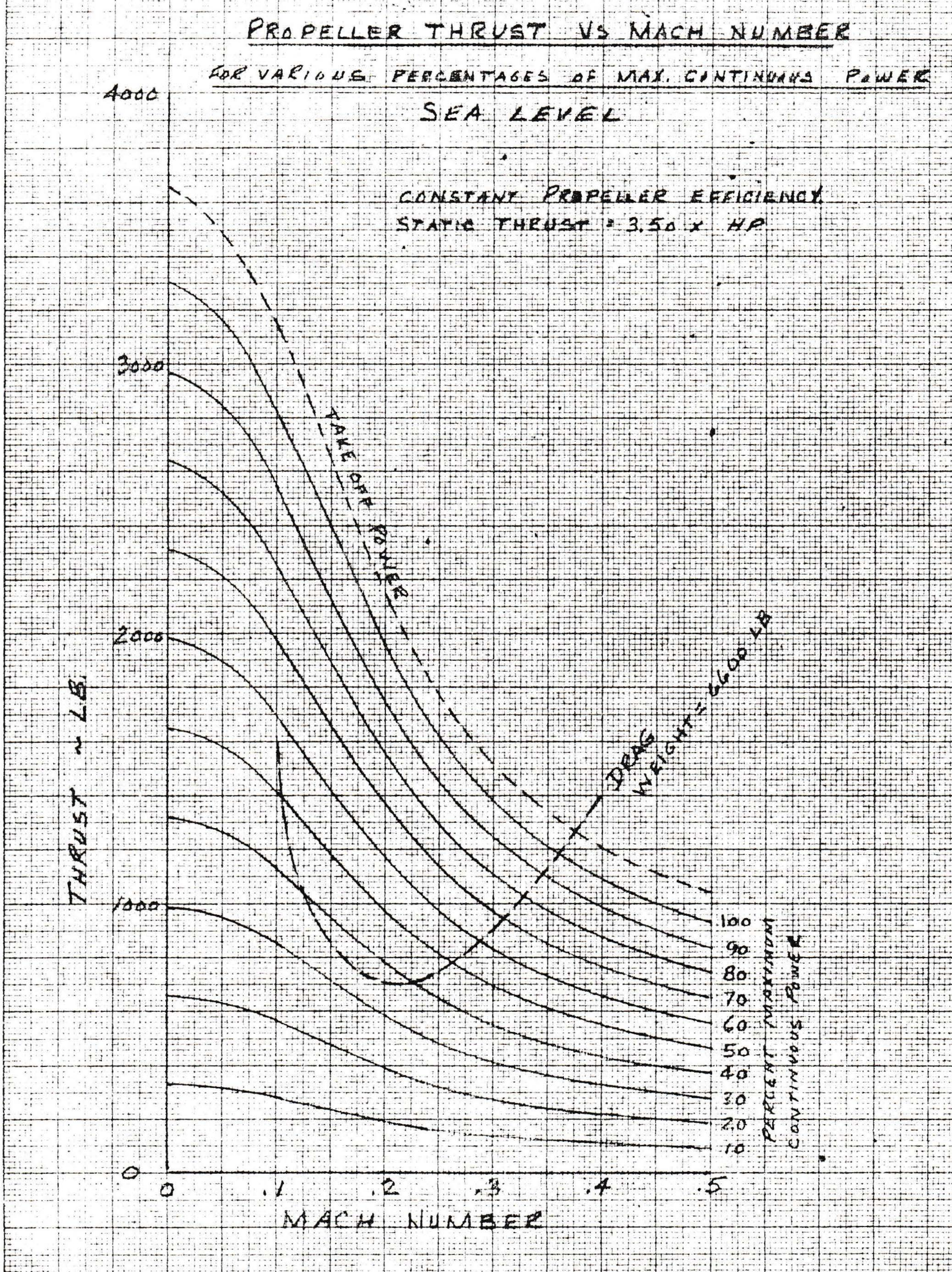

10 X 10 TO THE CM. 359-14 KEUFFEL & ESSER CO. MADE IN U.S.A.

FIG. 3.16

2 ASTAZOU II

PROPELLER THRUST VS MACH NUMBER

FOR VARIOUS PERCENTAGES OF MAX. CONTINUOUS POWER

10,000 FT

CONSTANT PROPELLER EFFICIENCY

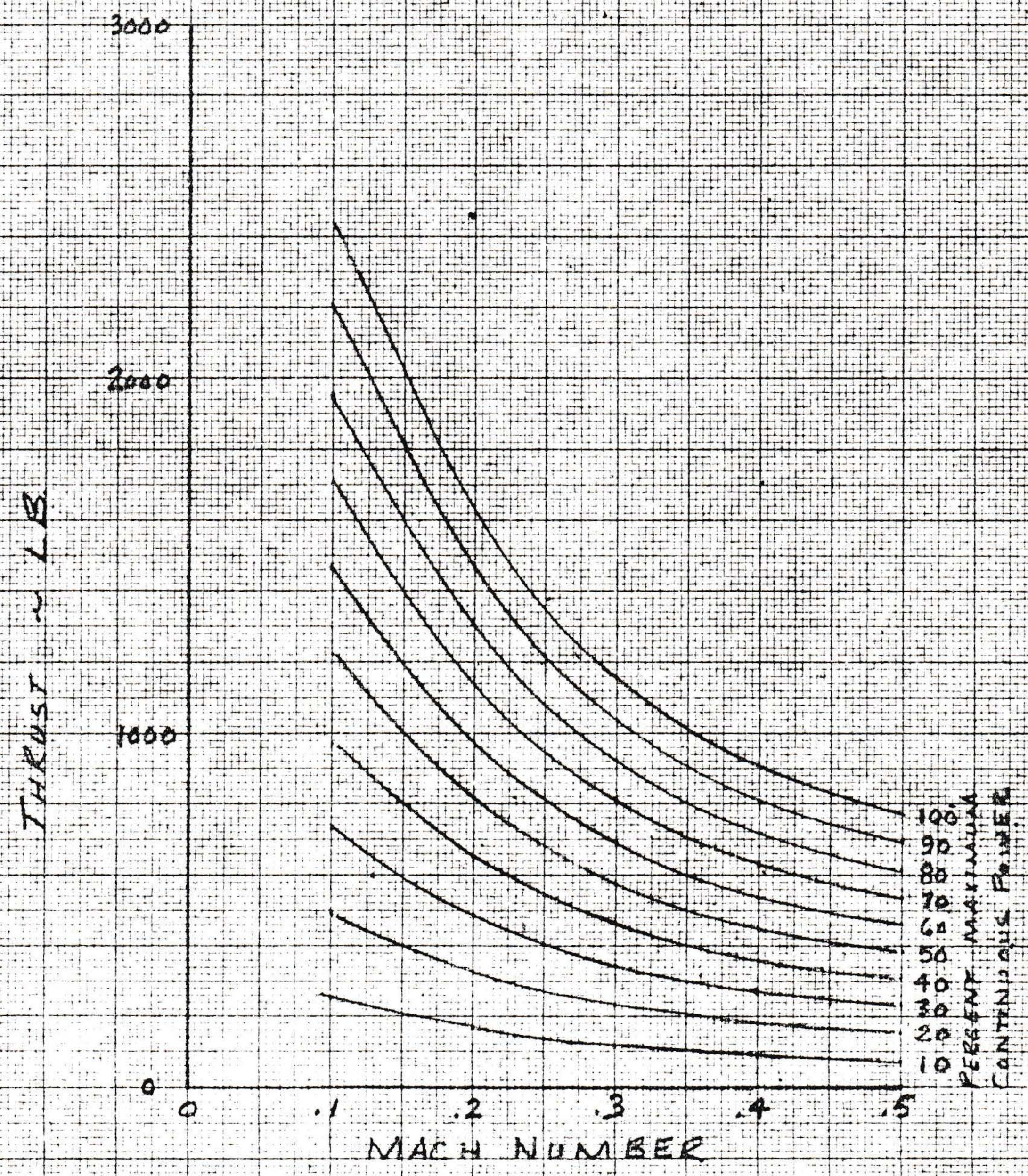

FIG. 3.17

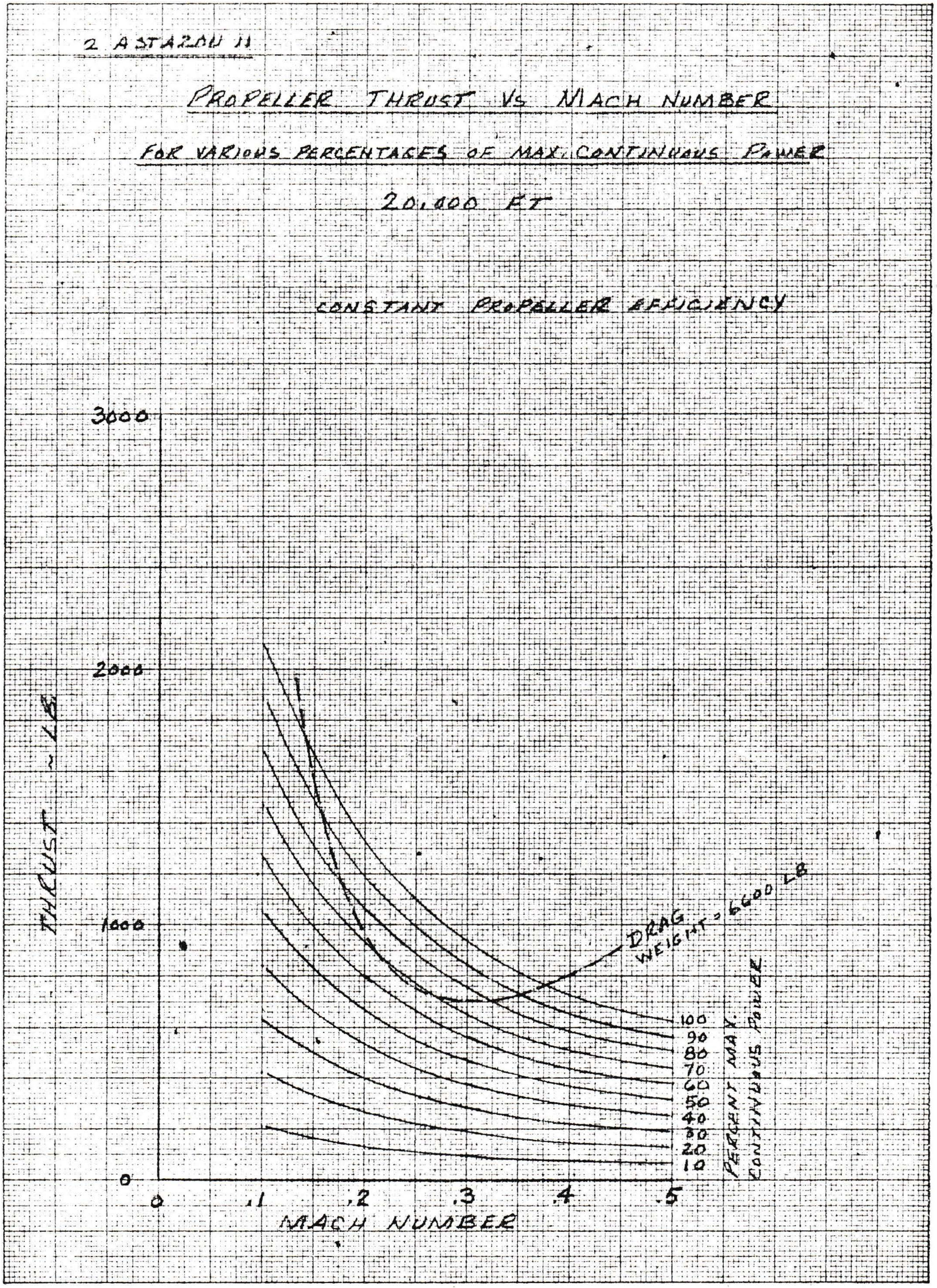

2 ASTAZOU II
PROPELLER THRUST VS MACH NUMBER
FOR VARIOUS PERCENTAGES OF MAX. CONTINUOUS POWER
20,000 FT
CONSTANT PROPELLER EFFICIENCY
THRUST ~ LB
3000
2000
1000
0
0
.1
.2
.3
.4
.5
MACH NUMBER
DRAG
WEIGHT = 6600 LB
100
90
80
70
60
50
40
30
20
10
PERCENT MAX. CONTINUOUS POWER

FIG. 3.18

2 ASTAZOU II

FUEL CONSUMPTION VS ENGINE POWER

BASED ON TWO ENGINES OPERATING AT SOME

% OF MAX. CONTINUOUS POWER

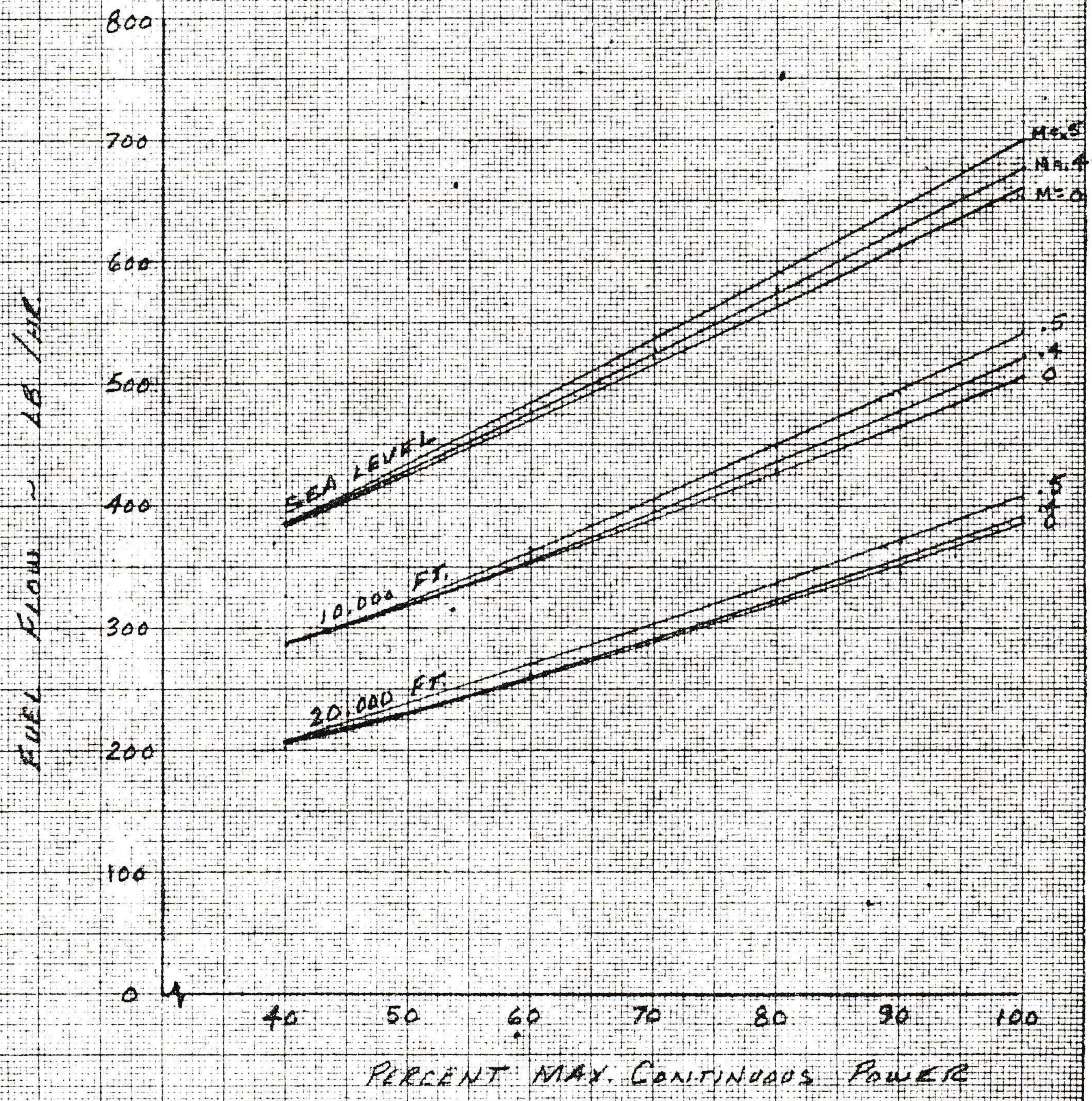

FIG. 3.19

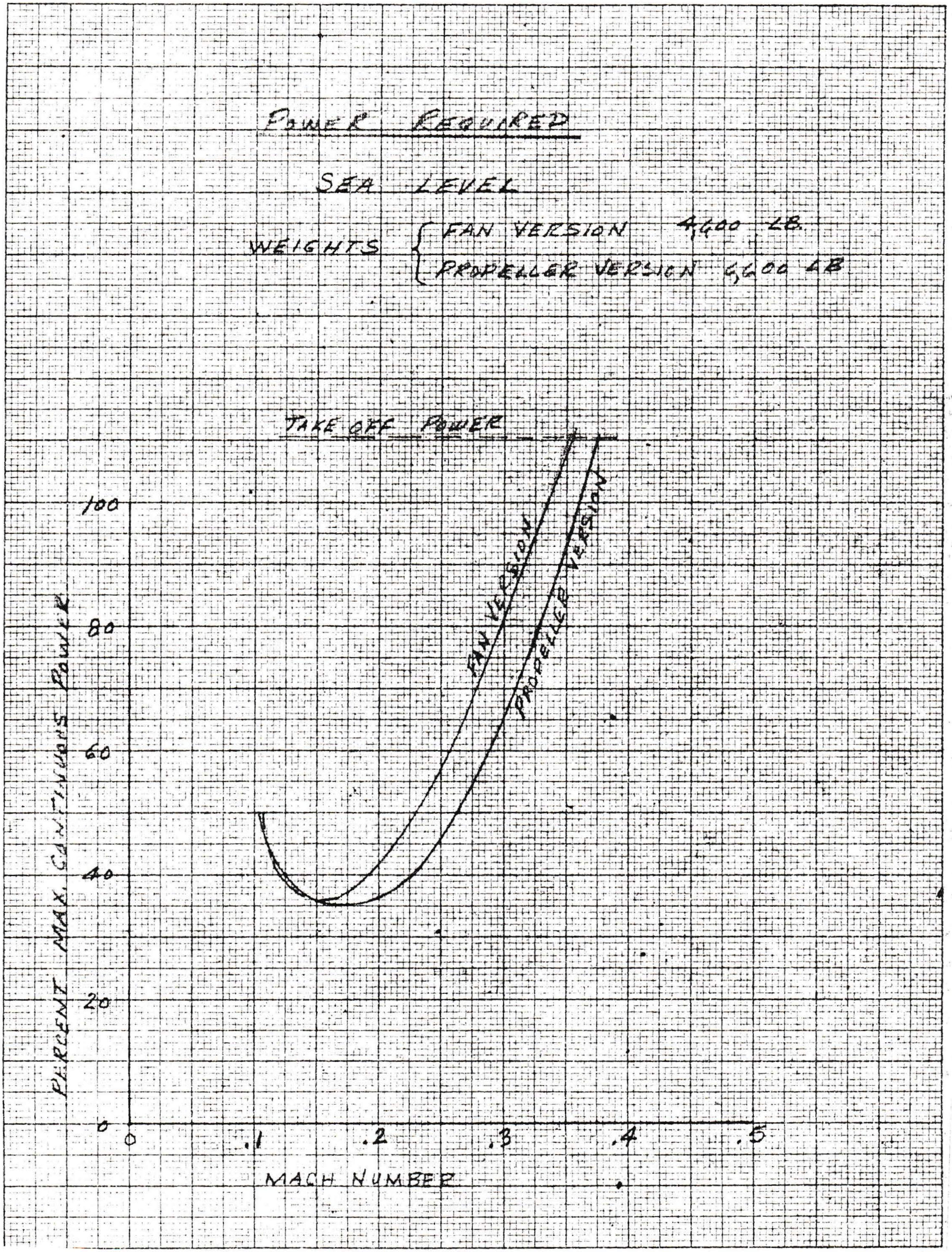
POWER REQUIRED
SEA LEVEL
WEIGHTS
FAN VERSION 4,600 LB.
PROPELLER VERSION 5,600 LB
TAKE OFF POWER
FAN VERSION
PROPELLER VERSION
100
80
60
40
20
0
PERCENT MAX. CONTINUOUS POWER
0
.1
.2
.3
.4
.5
MACH NUMBER

FIG. 3.20

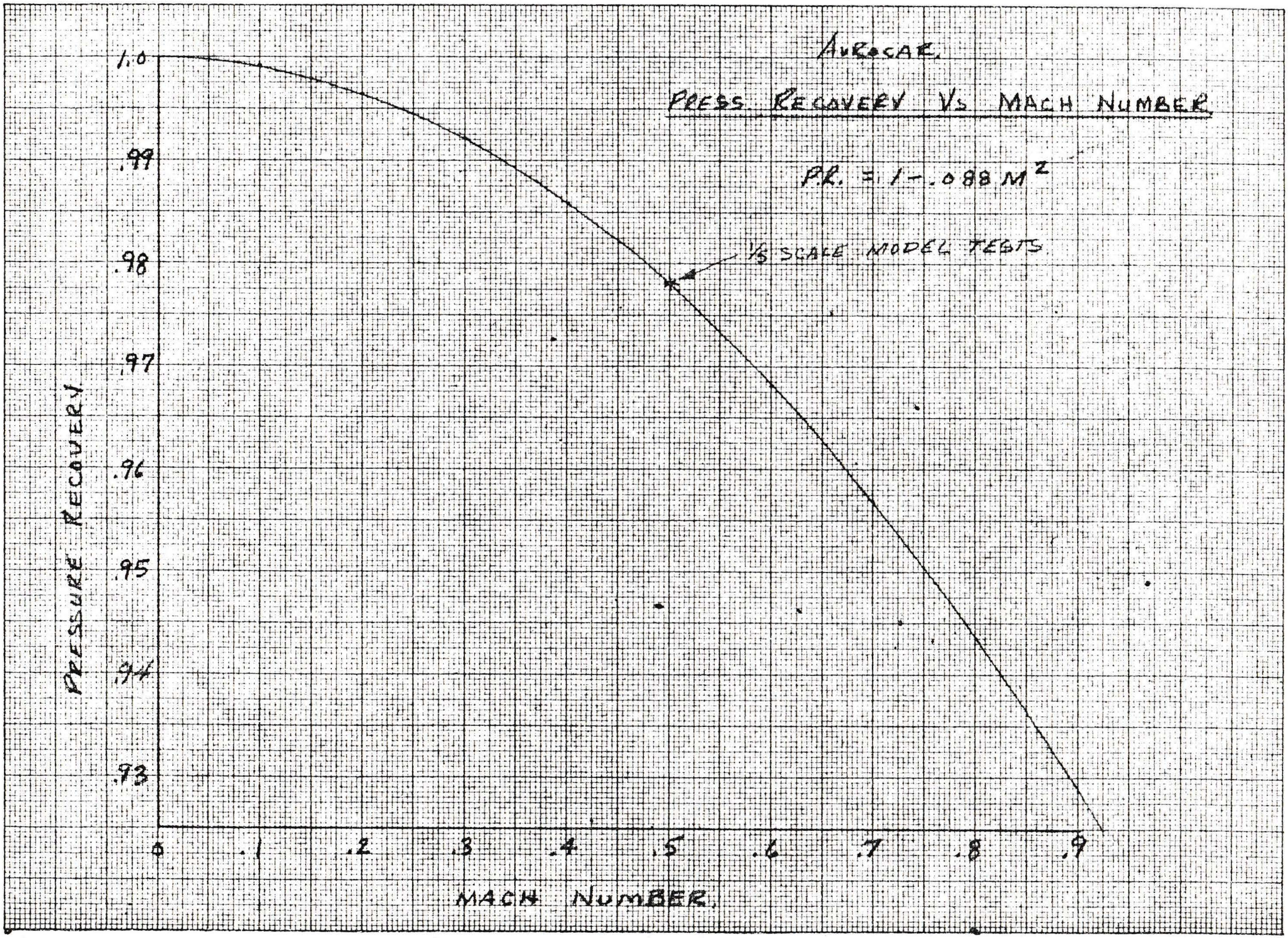
AEROCAR
PRESS. RECOVERY Vs MACH NUMBER
P.R. = 1 - .088 M²
1/5 SCALE MODEL TESTS
PRESSURE RECOVERY
1.0
.99
.98
.97
.96
.95
.94
.93
0
.1
.2
.3
.4
.5
.6
.7
.8
.9
MACH NUMBER

FIG. 4.1

NOZZLE EXIT AREA Vs MACH NUMBER

COMPRESSOR EXIT AREA = 1000 IN.^{2}

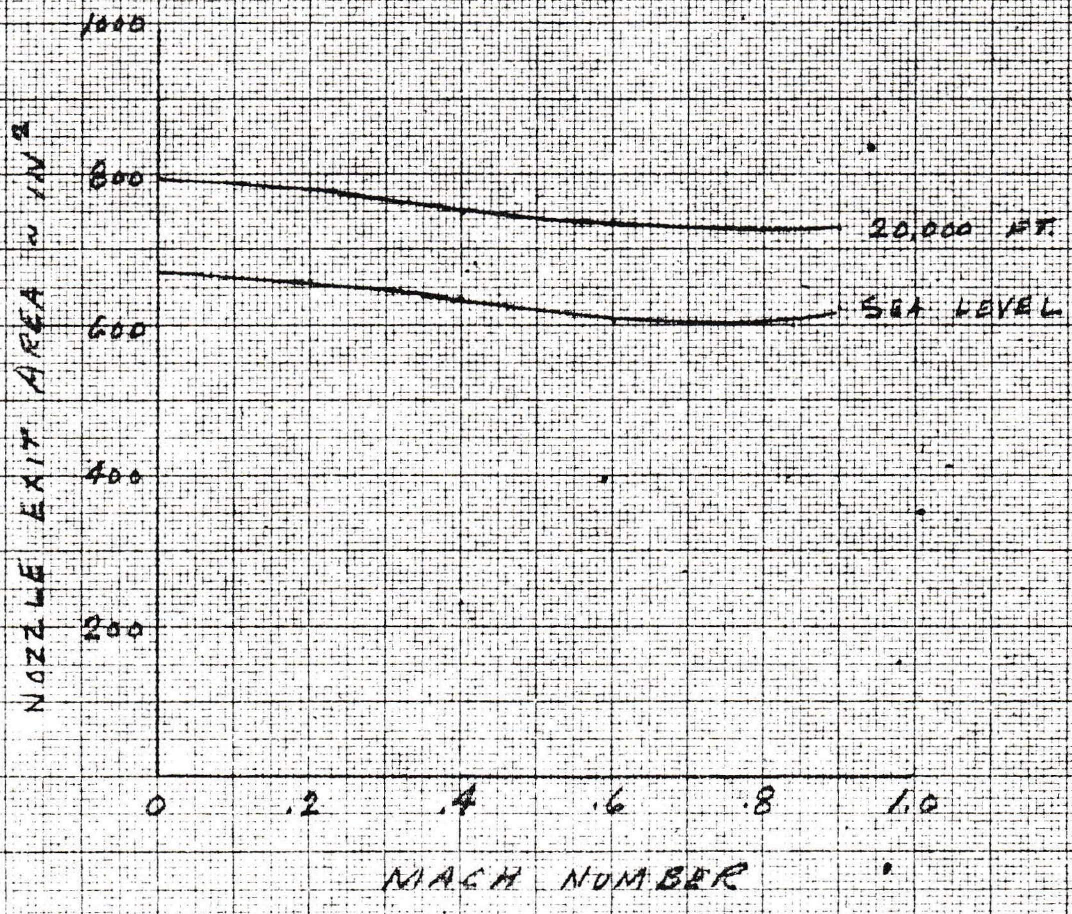

FIG. 4.2.

NET THRUST Vs MACH NUMBER

SEA LEVEL

TWO J-85's MILITARY POWER

CENTRIFUGAL FAN :- PRESSURE RATIO = 1.5:1
FAN EXIT AREA = 1000 IN.^{2}

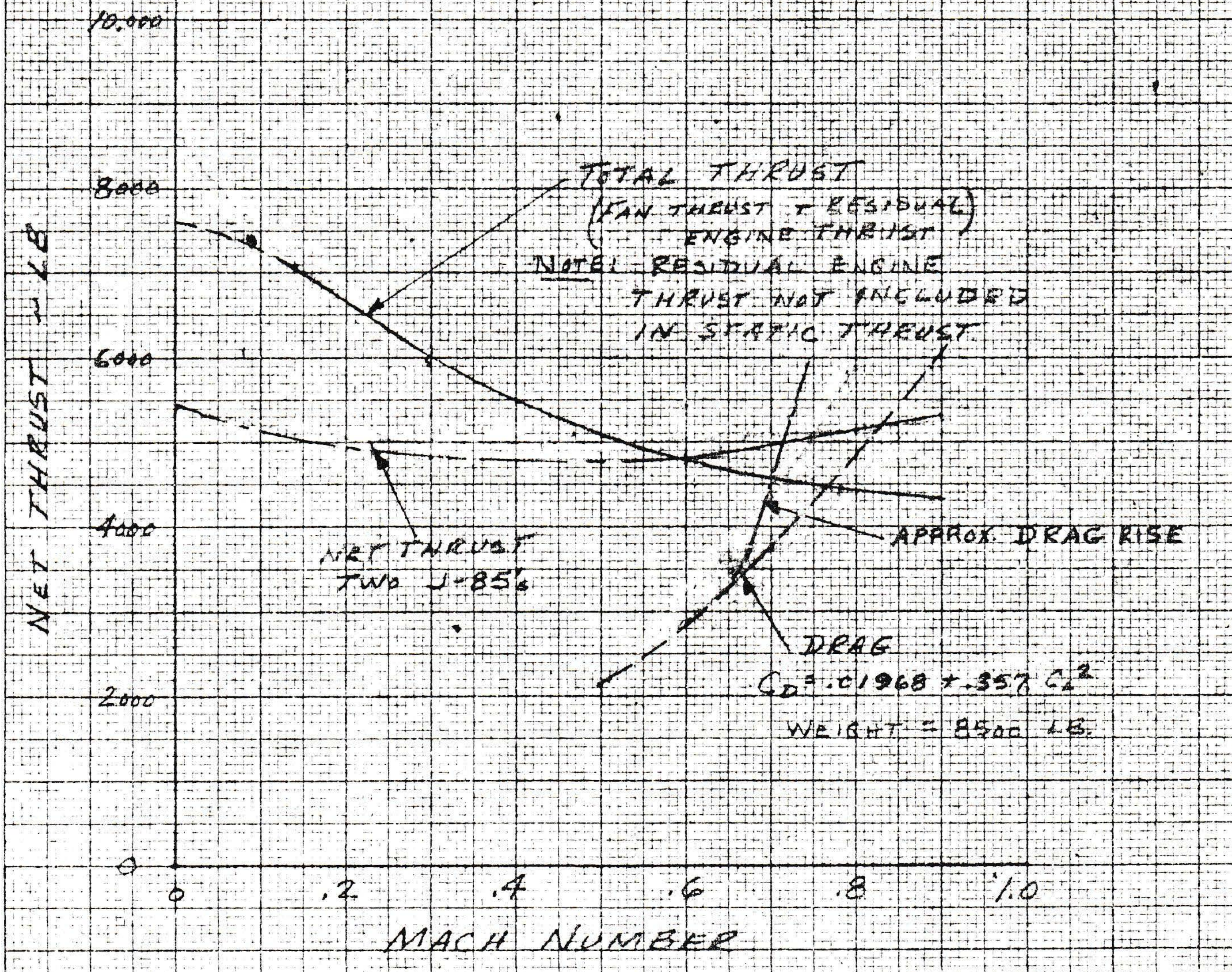

FIG. 4. 3

NET THRUST Vs MACH NUMBER

20,000 FEET

TWO J-85'S - MILITARY POWER

CENTRIFUGAL FAN - PRESSURE RATIO = 1.5:1

FAN EXIT AREA = 1000 IN.²

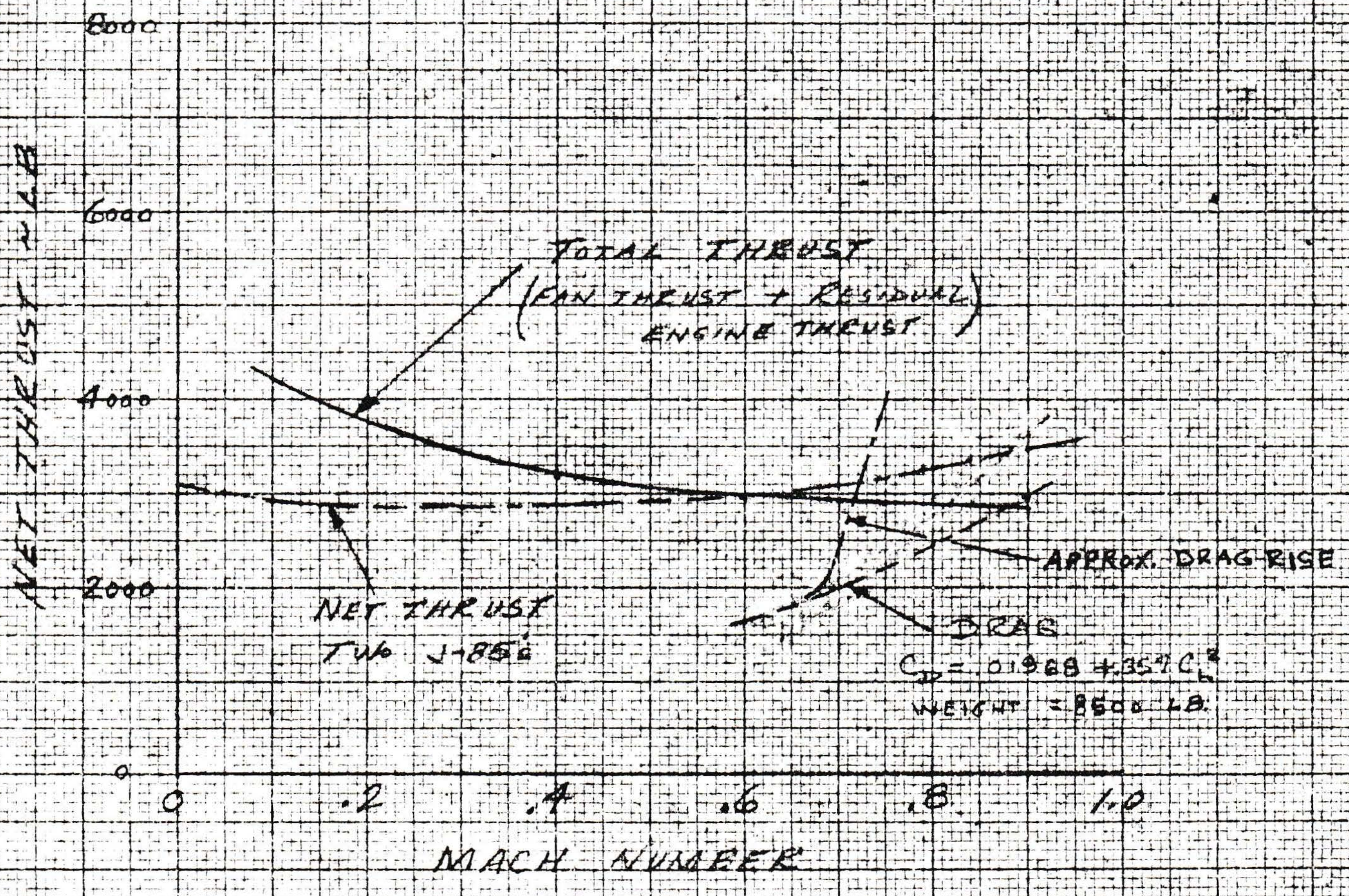

FIG. 4.4

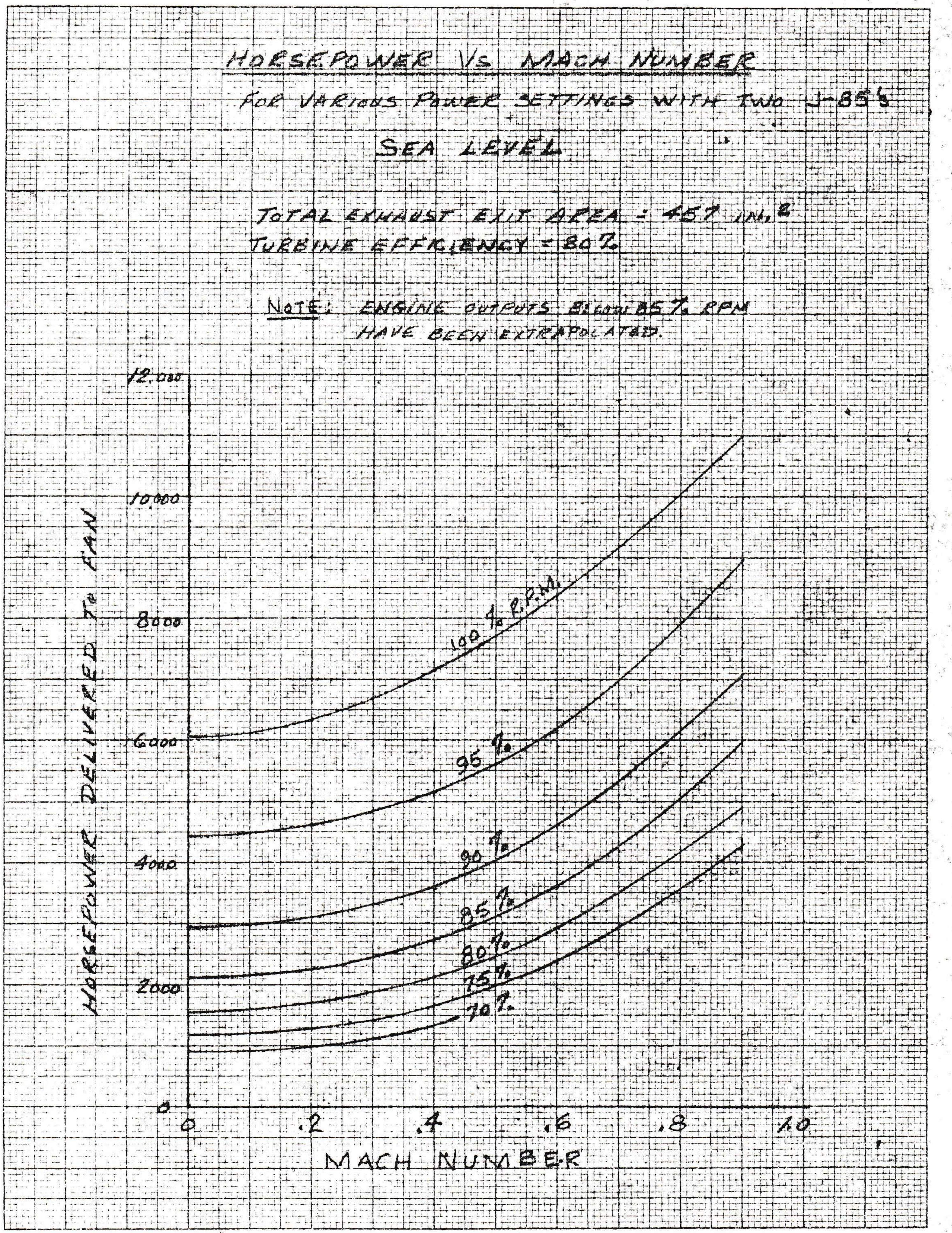
HORSEPOWER VS MACH NUMBER
FOR VARIOUS POWER SETTINGS WITH TWO J-85's
SEA LEVEL
TOTAL EXHAUST EXIT AREA = 457 IN.²
TURBINE EFFICIENCY = 80%
NOTE: ENGINE OUTPUTS BELOW 85% RPM HAVE BEEN EXTRAPOLATED.
HORSEPOWER DELIVERED TO FAN
0
2000
4000
6000
8000
10,000
12,000
MACH NUMBER
0
.2
.4
.6
.8
1.0
100% R.P.M.
95%
90%
85%
80%
75%
70%

FIG. 4.5

HORSEPOWER VS MACH NUMBER

FOR VARIOUS POWER SETTINGS WITH TWO J-85's

20.000 FT.

TOTAL EXHAUST EXIT AREA = 457 IN.^{2}
TURBINE EFFICIENCY = 80%

NOTE: ENGINE OUTPUTS BELOW 85% R.P.M. HAVE BEEN EXTRAPOLATED.

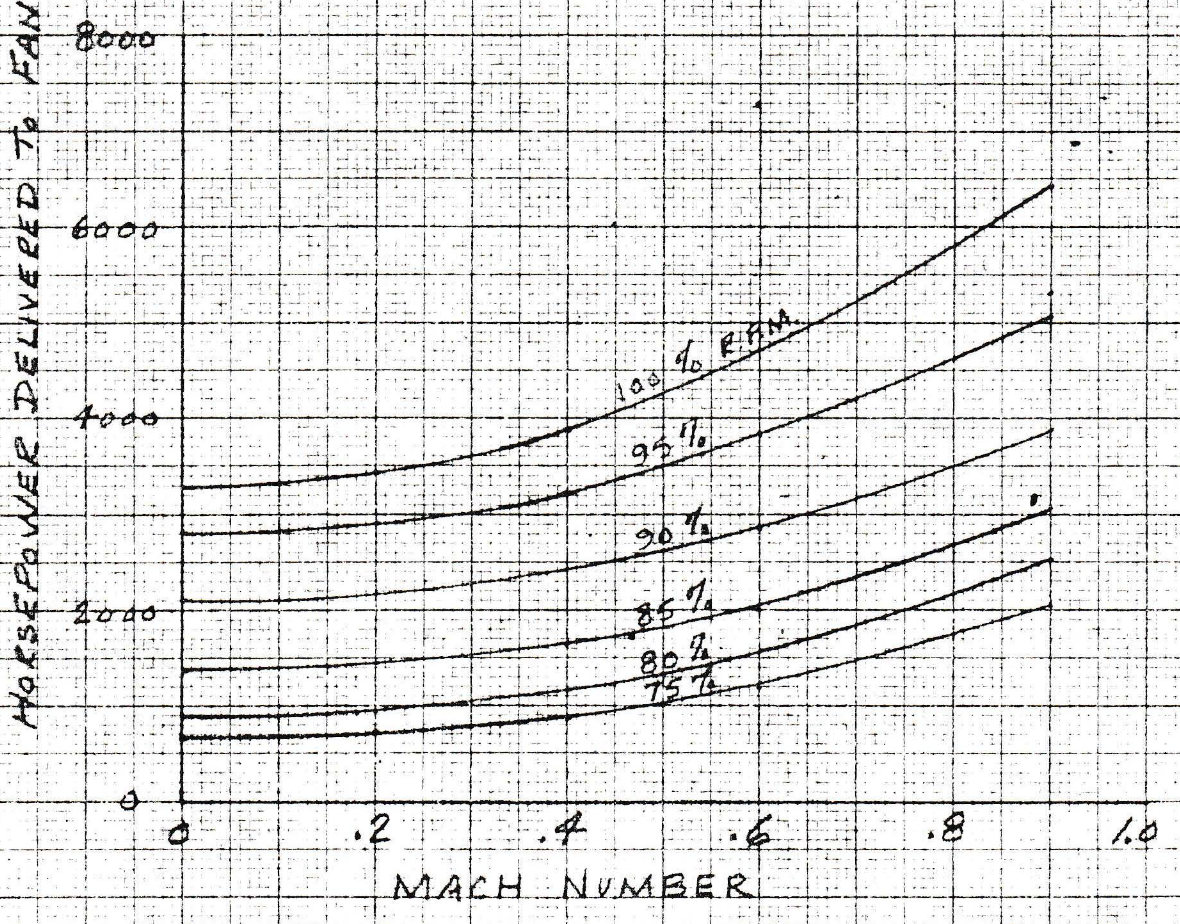

FIG. 4.6

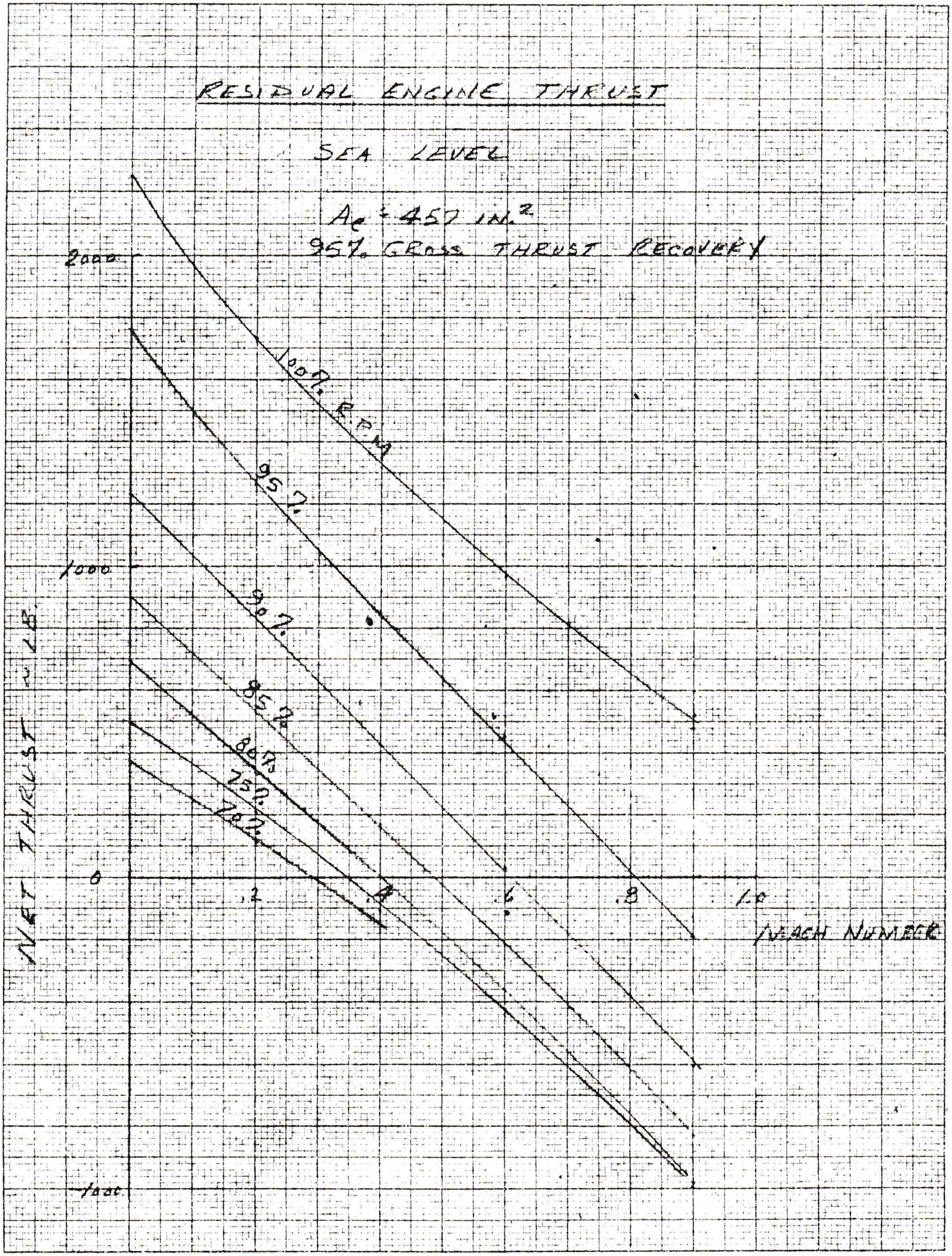

10 X 10 TO THE ½ INCH 359-12
KEUFFEL & ESSER CO. MADE IN U.S.A.

FIG. 4.7

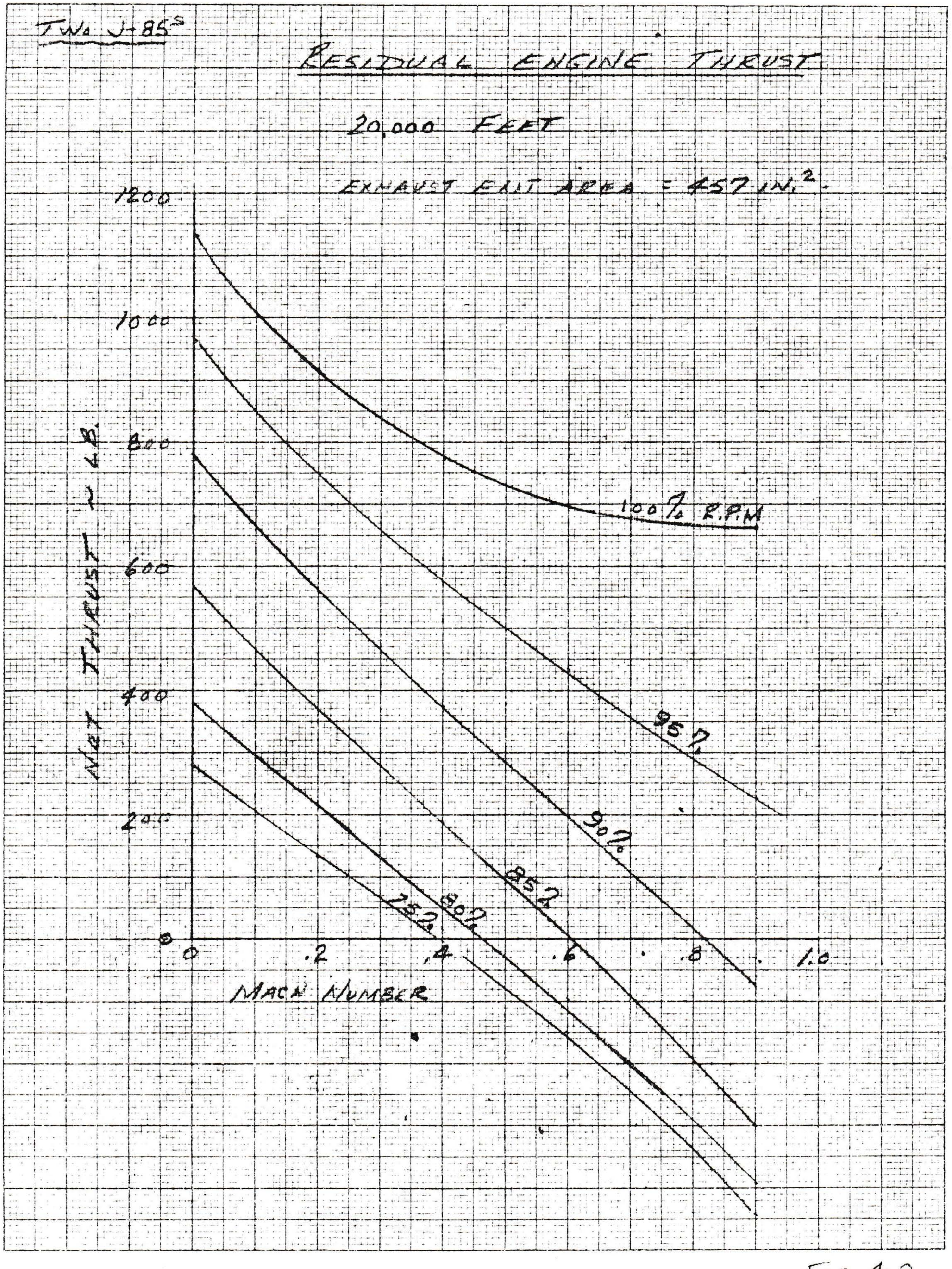
TWO J-85S
RESIDUAL ENGINE THRUST
20,000 FEET
EXHAUST EXIT AREA = 457 IN.²
NET THRUST ~ LB.
1200
1000
800
600
400
200
0
0
.2
.4
.6
.8
1.0
MACH NUMBER
100% R.P.M.
95%
90%
85%
80%
75%

FIG. 4.8

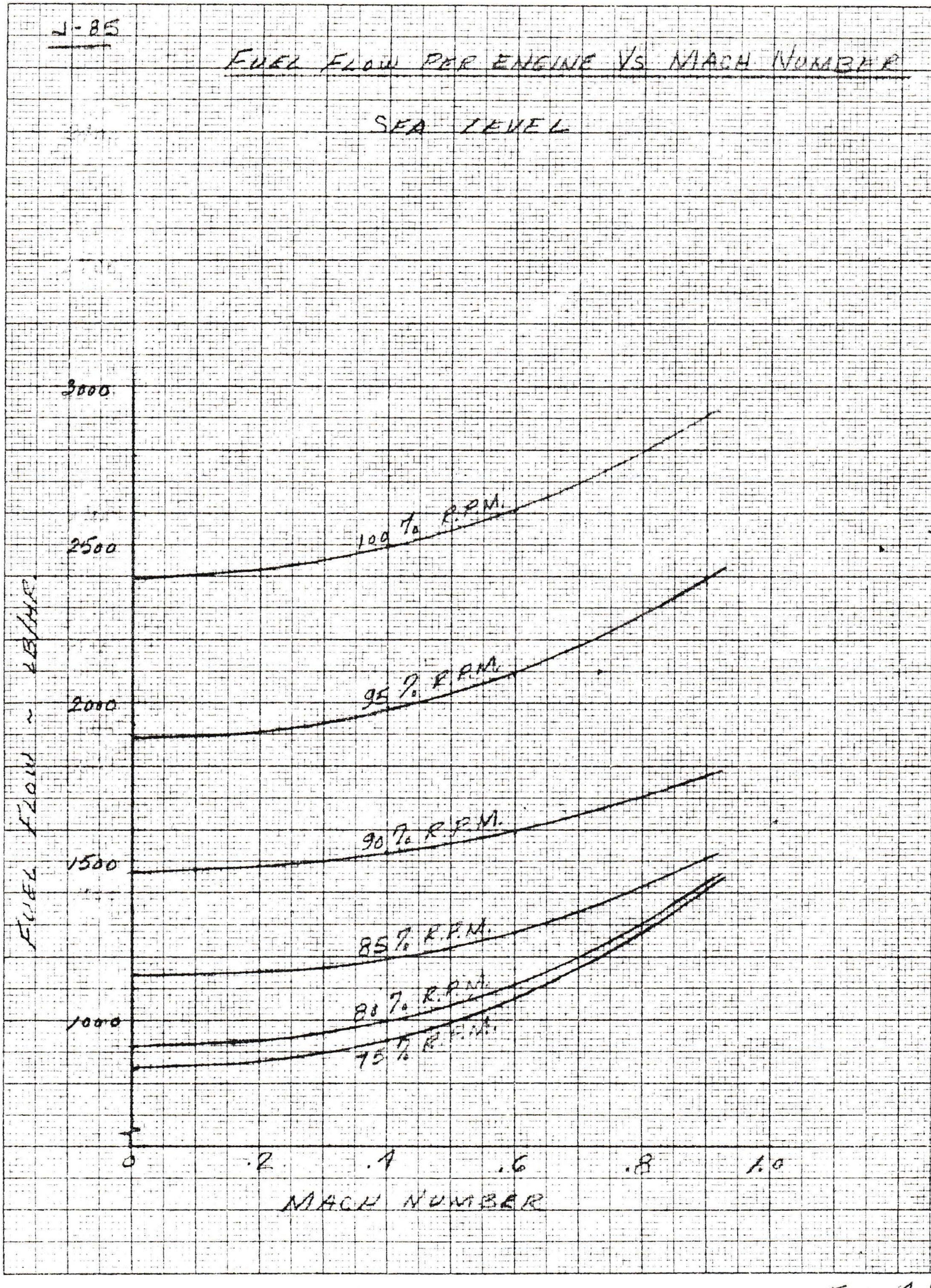

J-85
FUEL FLOW PER ENGINE VS MACH NUMBER
SEA LEVEL
3000
2500
2000
1500
1000
FUEL FLOW ~ LB/HR
100 % R.P.M.
95 % R.P.M.
90 % R.P.M.
85 % R.P.M.
80 % R.P.M.
75 % R.P.M.
0
.2
.4
.6
.8
1.0
MACH NUMBER

FIG. 4.9

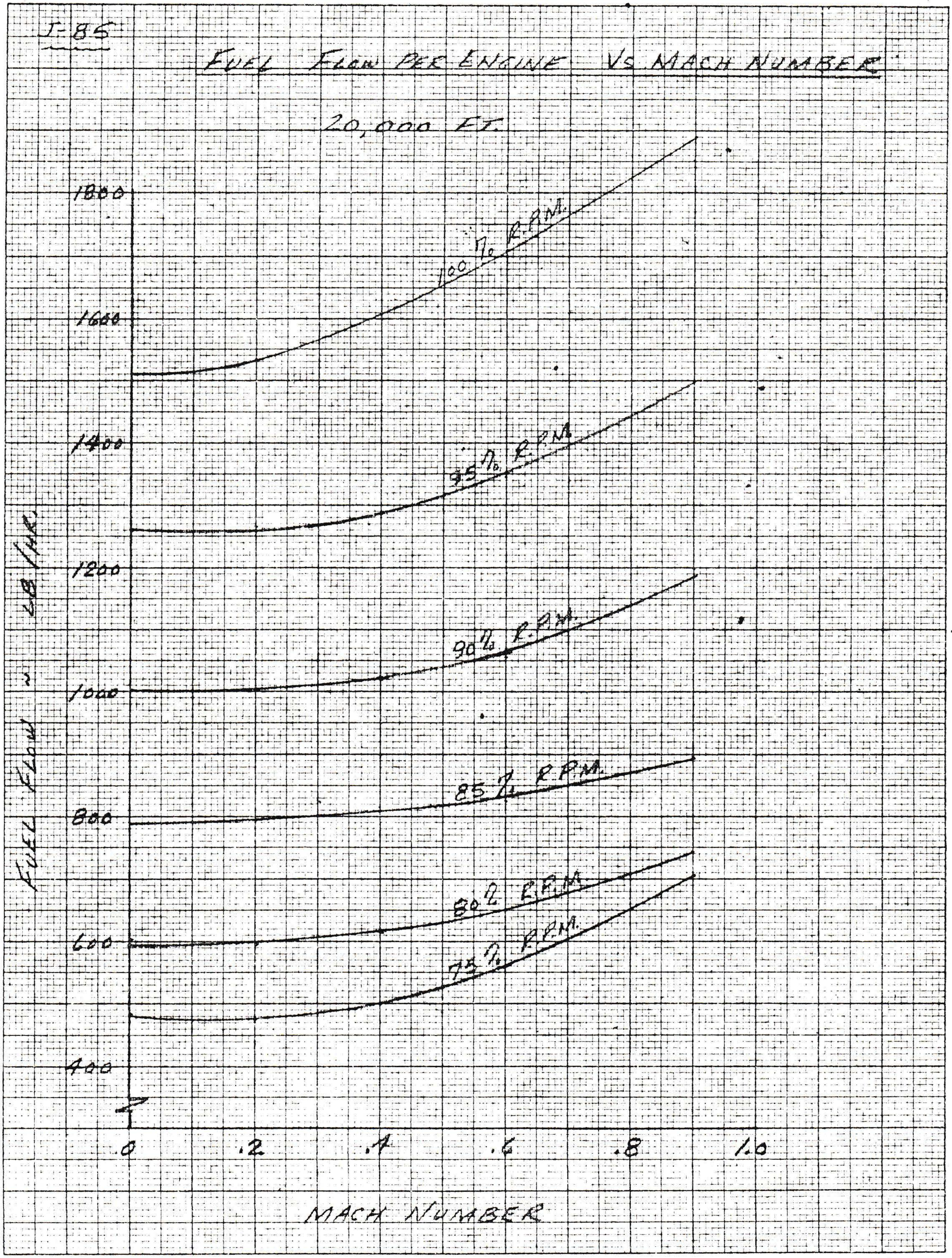

FIG. 4.10

10 X 10 TO THE ½ INCH 359-12 KEUFFEL & ESSER CO. MADE IN U.S.A.

NET THRUST VS FAN PRESSURE RATIO

SEA LEVEL

TWO J-85's - 100 % RPM

CENTRAL JET AREA = 1310 IN.^{2} } FORWARD FLIGHT CONFIG.
95 % GROSS THRUST RECOVERY

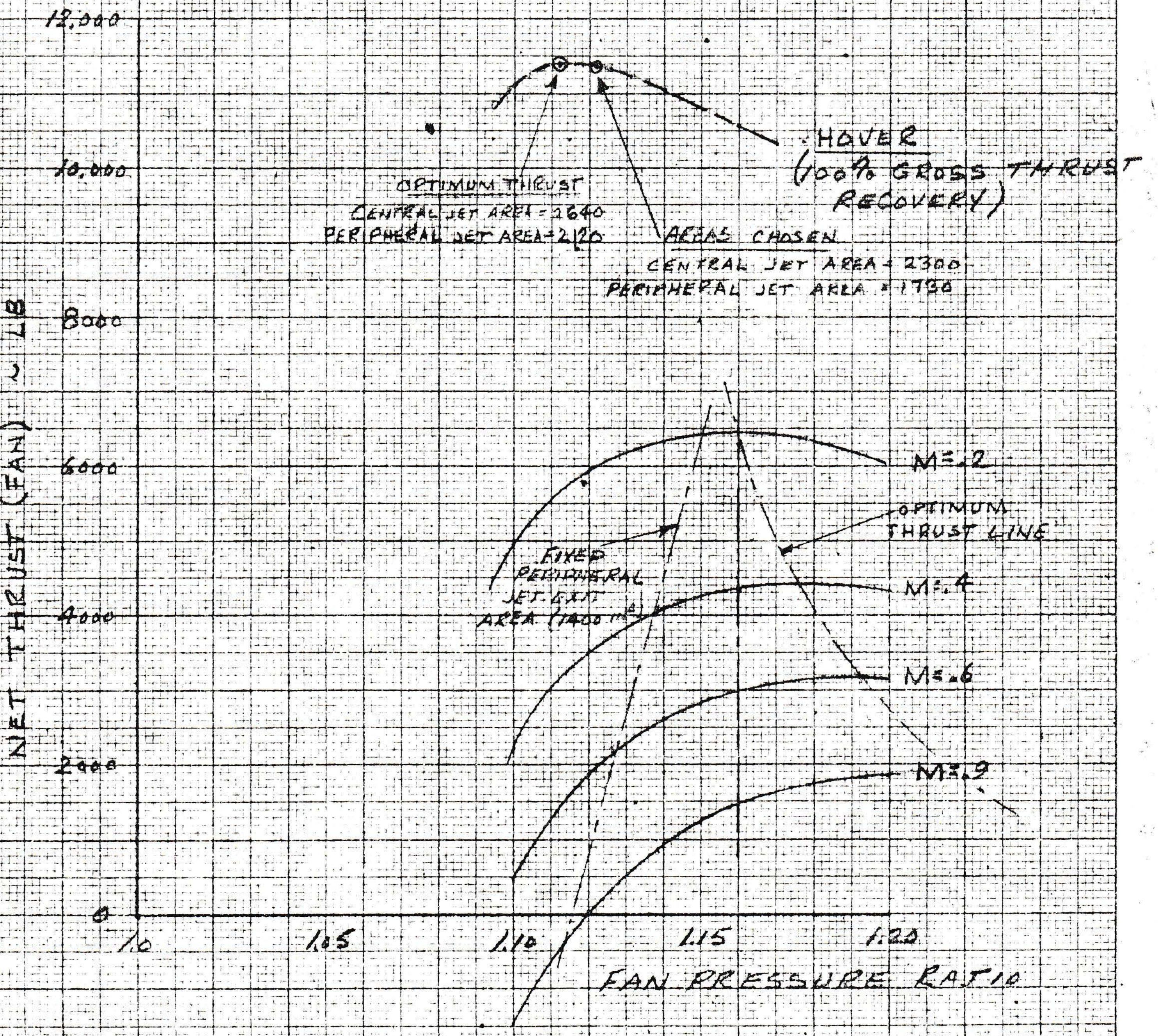

FIG. 4.11

JET EXIT AREA FOR HOVER

TWO J-85's ~ 100% R.P.M.

FAN AREA = 3800 IN.^{2}

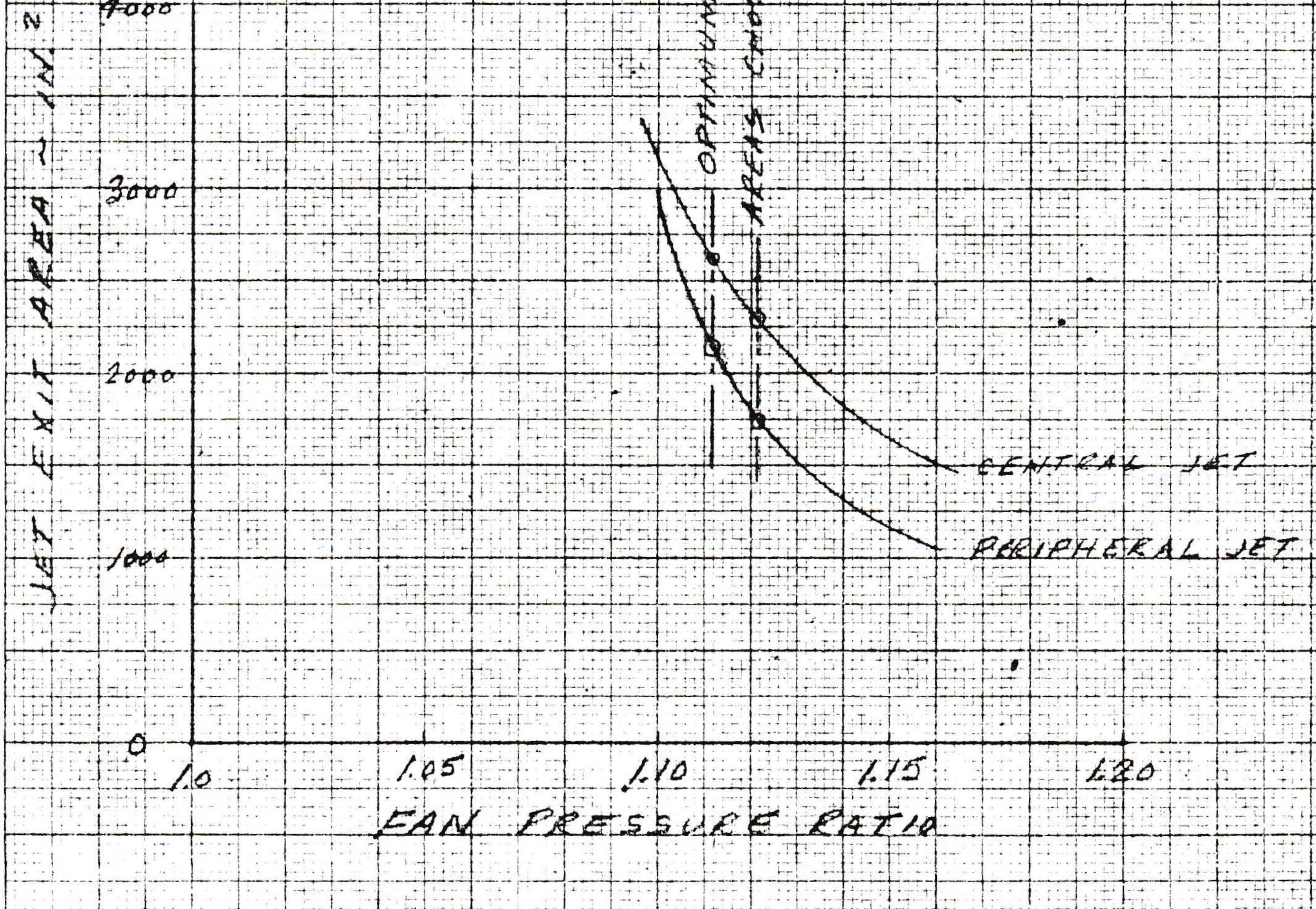

FIG. 4.12

PERIPHERAL JET EXIT AREA VS FAN PRESSURE RATIO

SEA LEVEL ~ FORWARD FLIGHT

TWO J-85's ~ 100% R.P.M.

FWD FLIGHT CENTRAL JET EXIT AREA = 1310 IN.^{2}

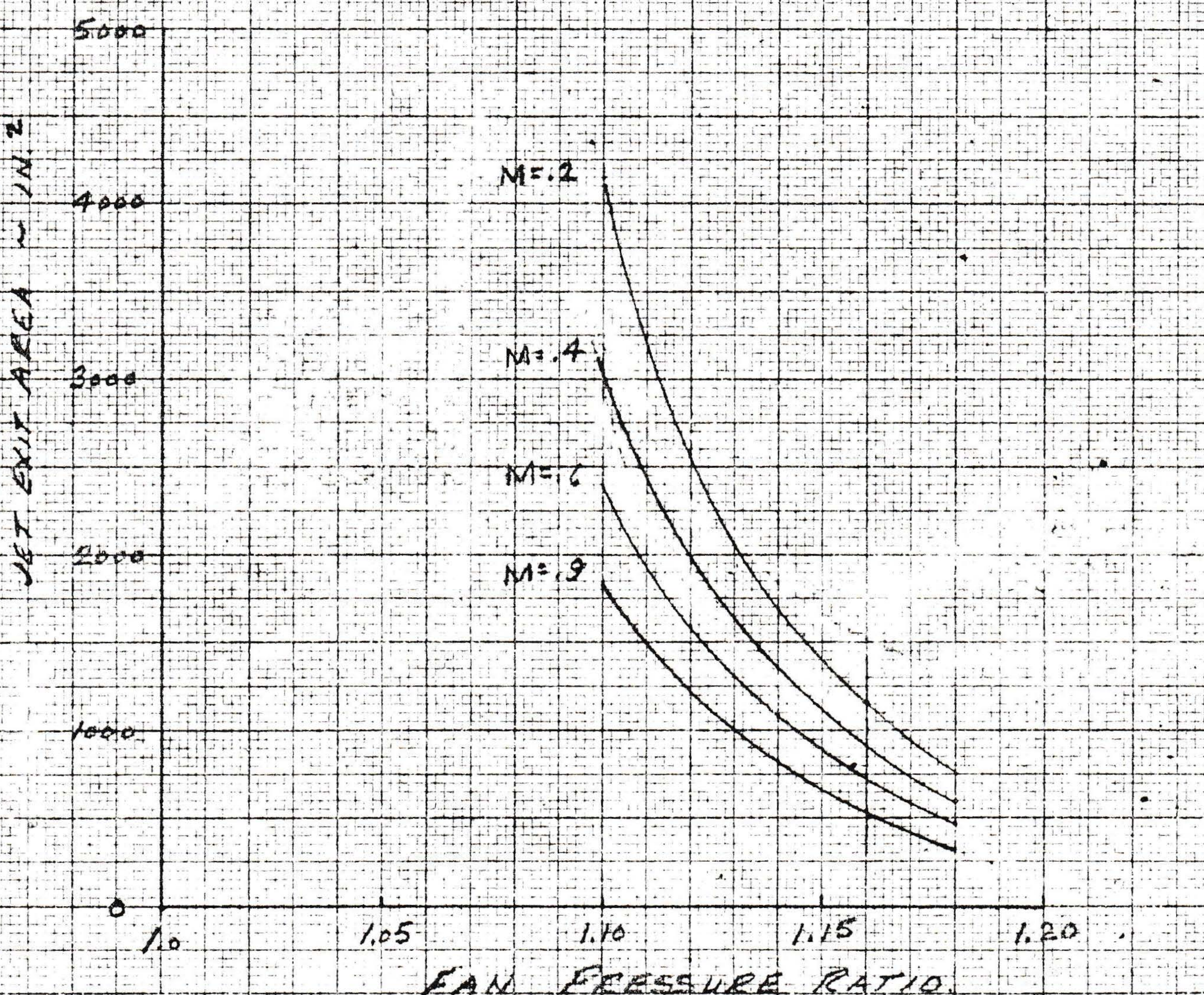

FIG. 4.13

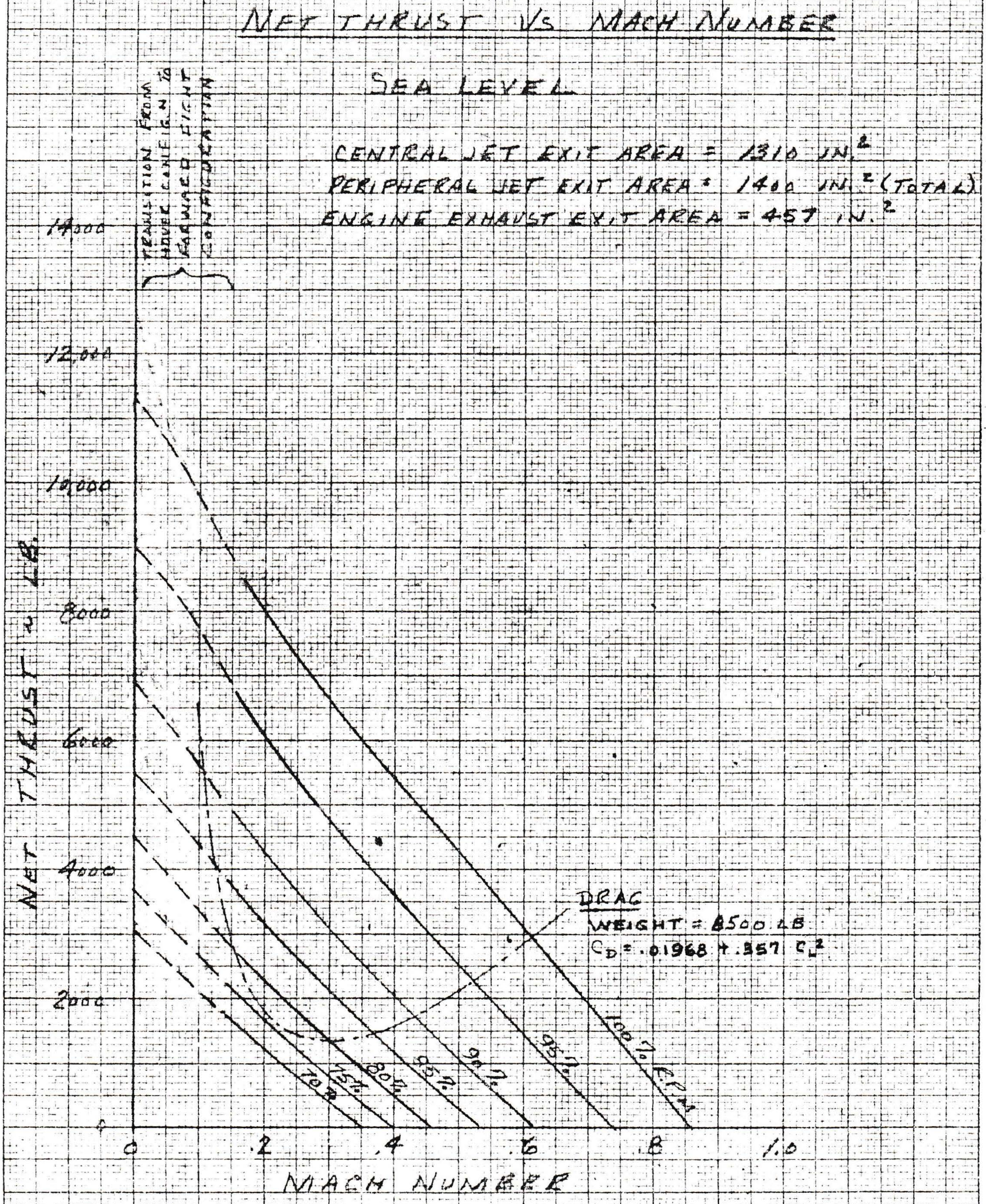
NET THRUST VS MACH NUMBER
SEA LEVEL
CENTRAL JET EXIT AREA = 1310 IN.²
PERIPHERAL JET EXIT AREA = 1400 IN.² (TOTAL)
ENGINE EXHAUST EXIT AREA = 457 IN.²
TRANSITION FROM HOVER CONFIGURATION TO FORWARD FLIGHT CONFIGURATION
NET THRUST ~ LB.
14000
12,000
10,000
8000
6000
4000
2000
0
0
.2
.4
.6
.8
1.0
MACH NUMBER
DRAG
WEIGHT = 8500 LB
CD = .01968 + .357 CL²
100% RPM
98%
90%
85%
80%
75%
70%

FIG. 4.14

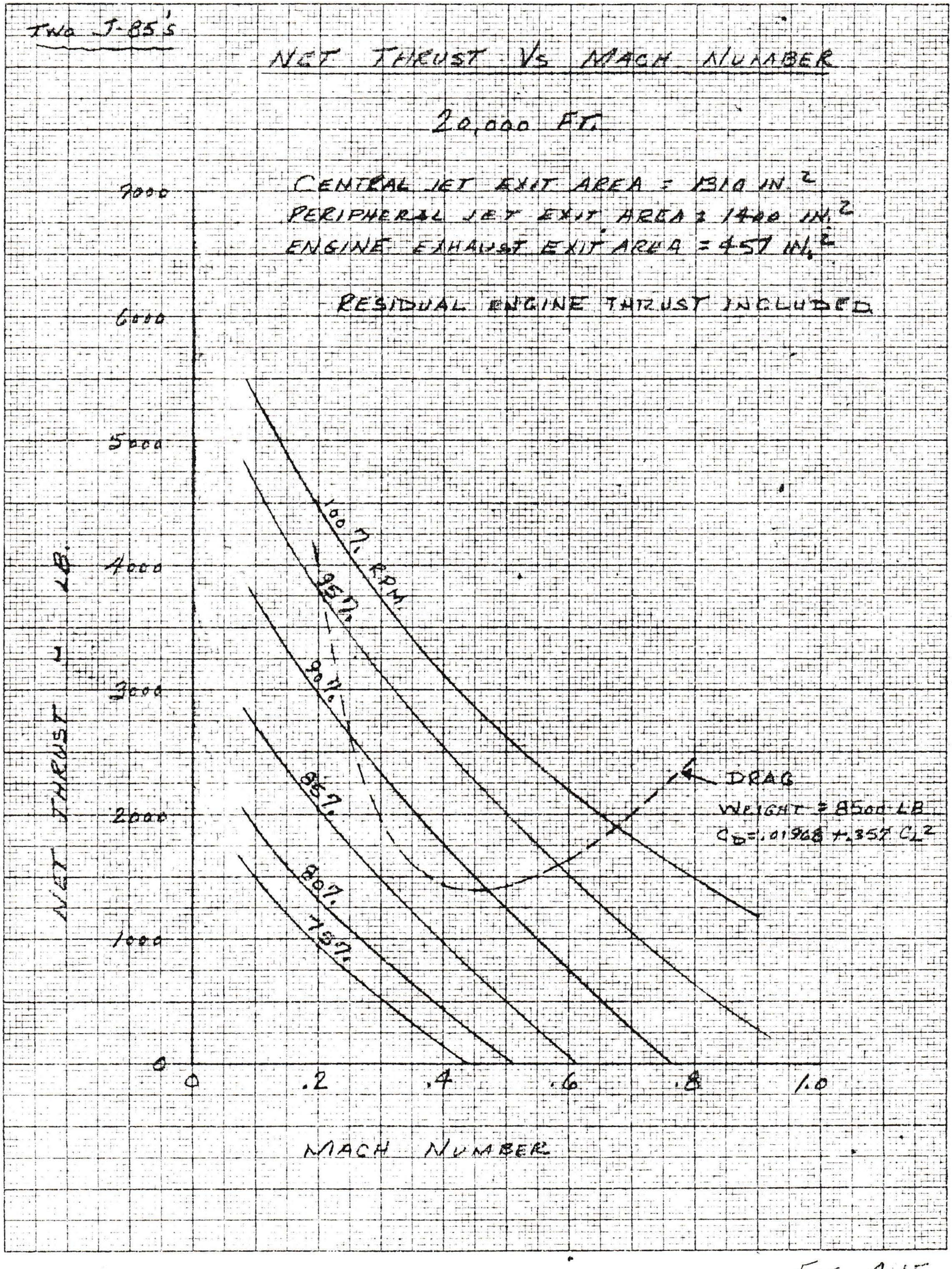

FIG. 4.15

10 X 10 TO THE 1/2 INCH 359-12 KEUFFEL & ESSER CO. MADE IN U.S.A.

PERIPHERAL JET EXIT AREA

VARIATION WITH MACH NUMBER

CENTRAL JET EXIT AREA = 1210 IN.^{2}

PERIPHERAL JET EXIT AREA VARIED TO GIVE A FAN PRESSURE = 1.16 AT SEA LEVEL WITH 100% R.P.M.

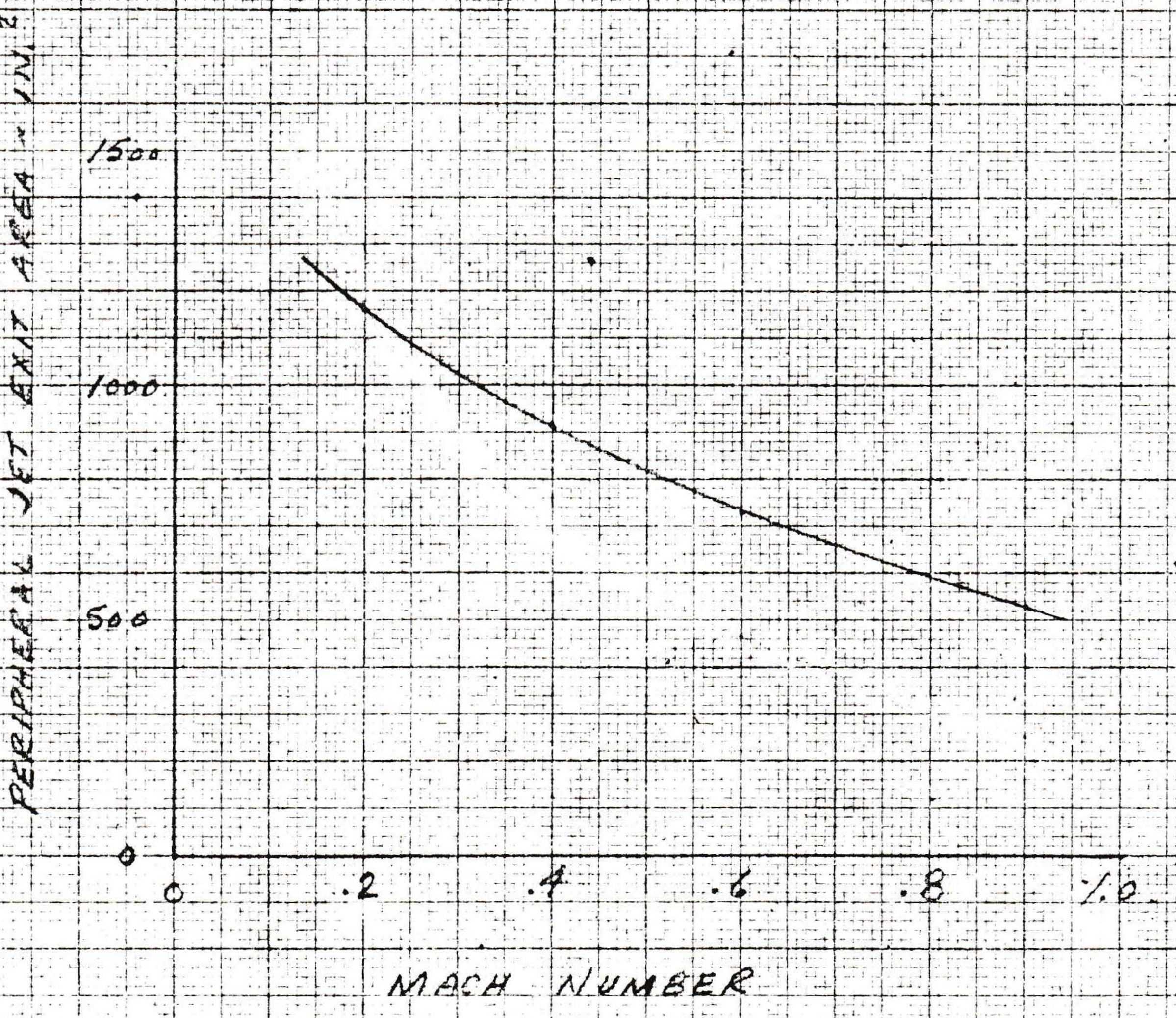

FIG. 4.16

TWO J-85's

NET THRUST VS MACH NUMBER

SEA LEVEL

CENTRAL JET EXIT AREA = 1310 IN.^{2}
ENGINE EXHAUST EXIT AREA = 457 IN.^{2}
95% GROSS THRUST RECOVERY

NOTE: PERIPHERAL JET EXIT AREA SCHEDULED AS SHOWN IN FIG. 4.16

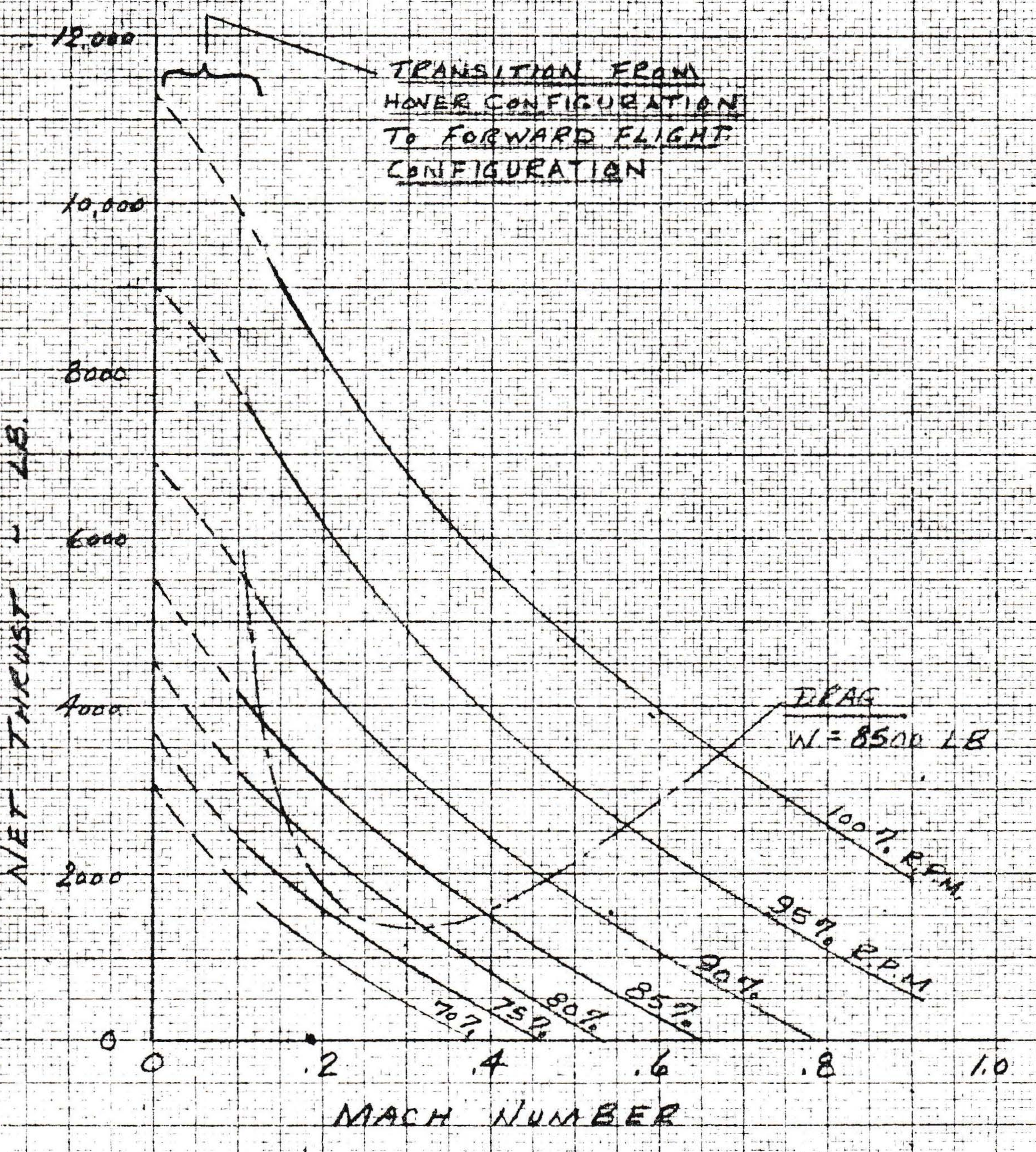

FIG. 4.17

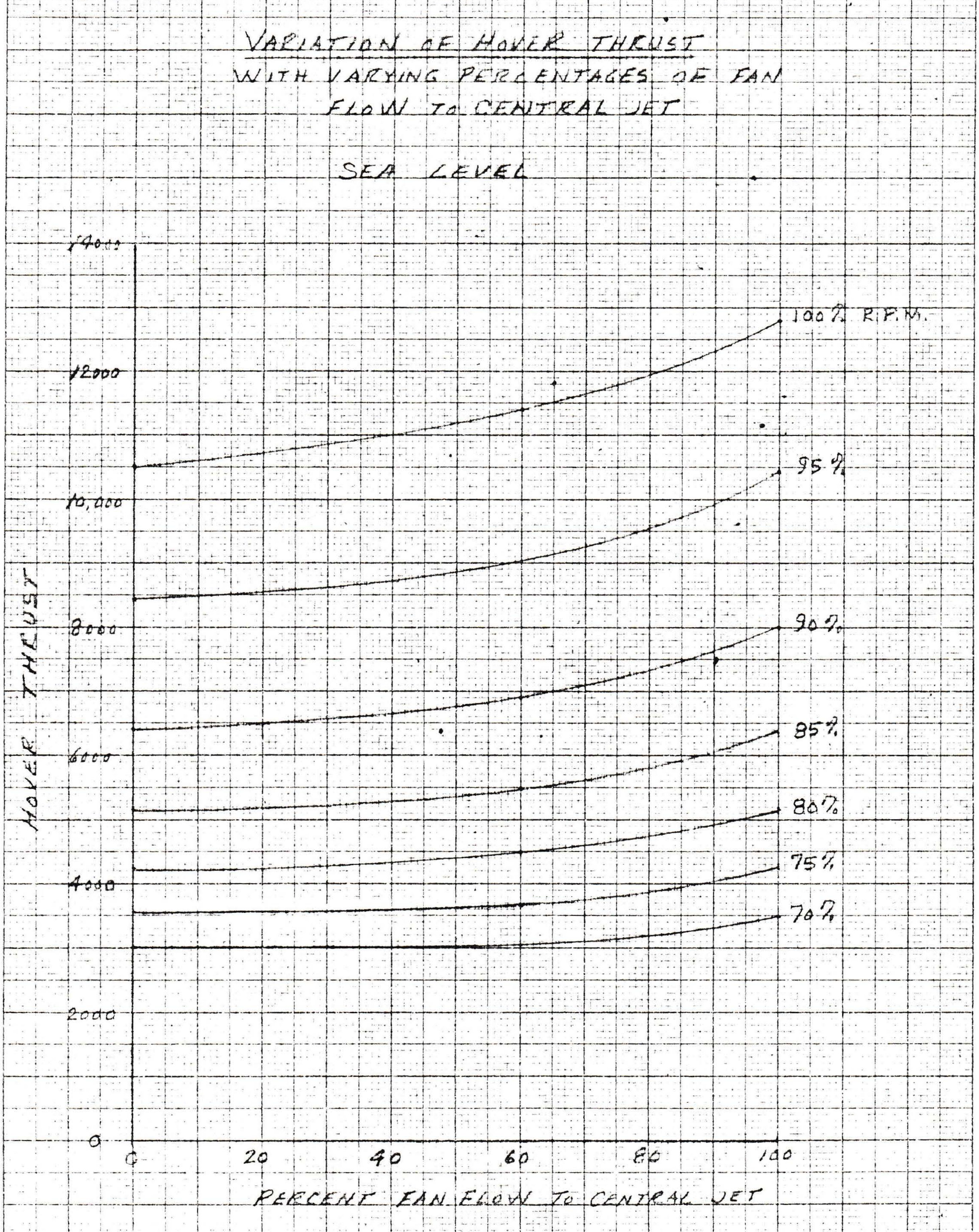
VARIATION OF HOVER THRUST
WITH VARYING PERCENTAGES OF FAN
FLOW TO CENTRAL JET
SEA LEVEL
14000
12000
10,000
8000
6000
4000
2000
0
HOVER THRUST
100% R.P.M.
95%
90%
85%
80%
75%
70%
0
20
40
60
80
100
PERCENT FAN FLOW TO CENTRAL JET

FIG 4.18

VARIATION OF CENTRAL JET AND PERIPHERAL JET
EXIT AREA

FOR VARIOUS PERCENTAGES OF FAN FLOW
TO CENTRAL JET

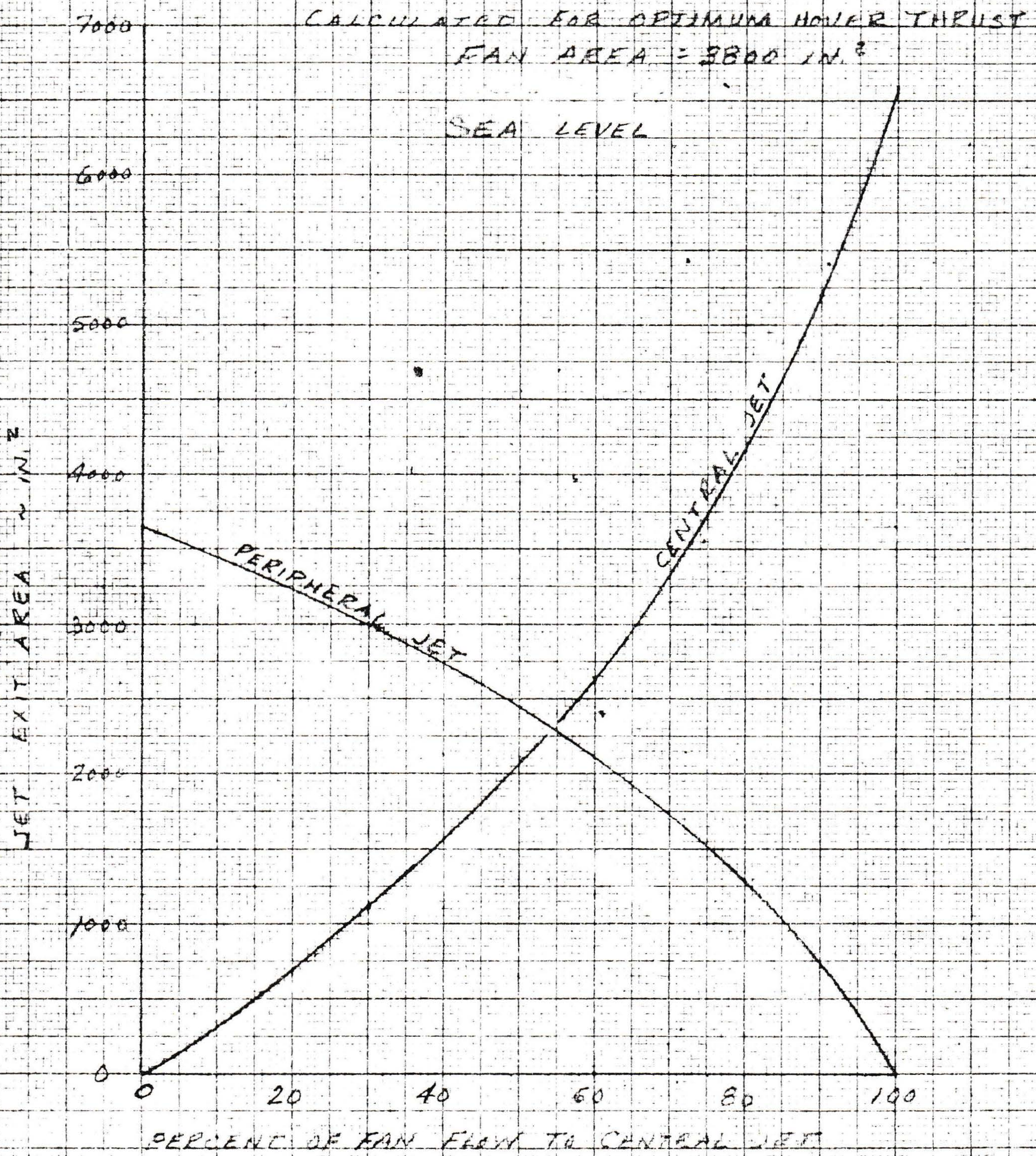

FIG. 4.19

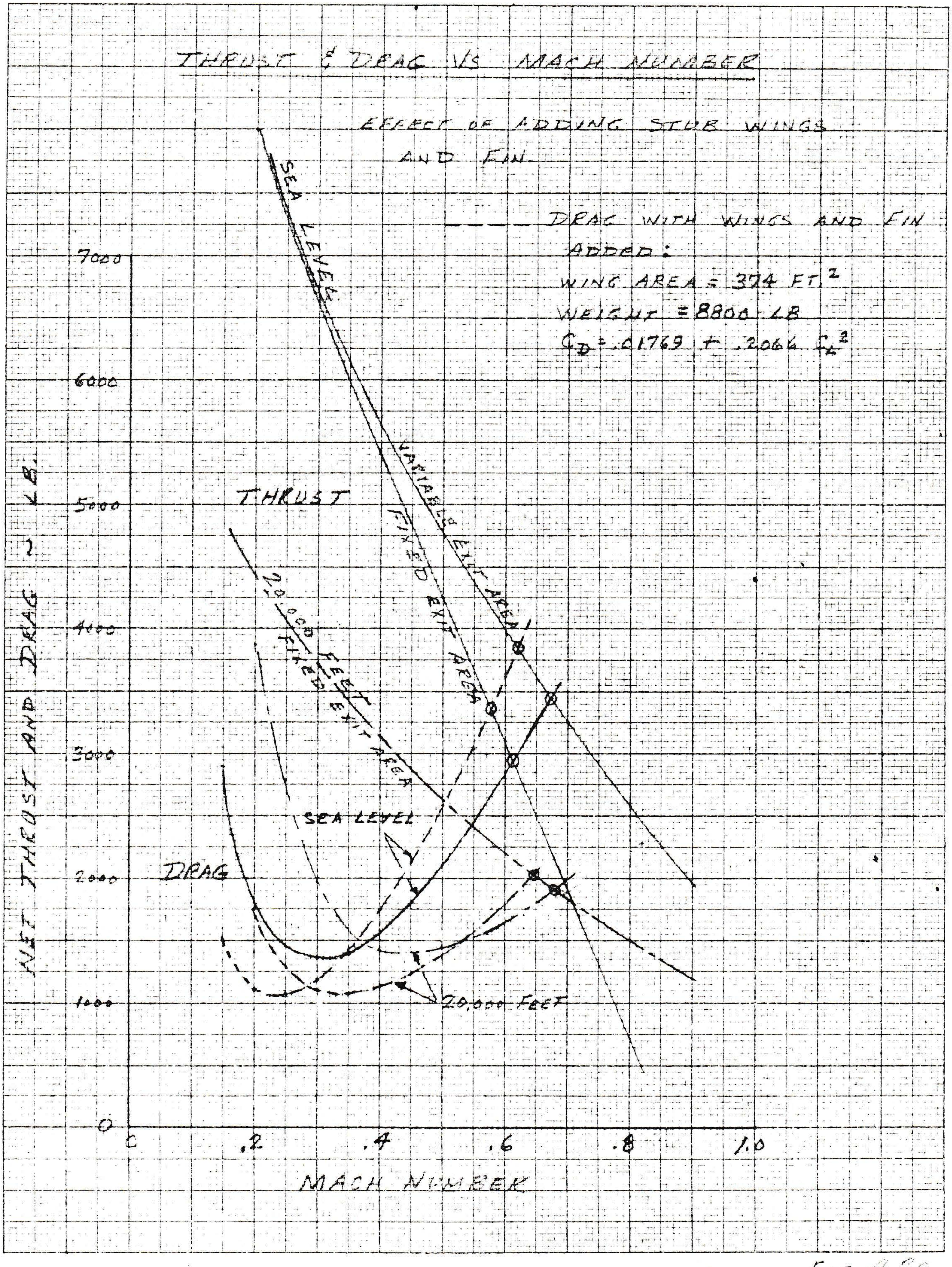
THRUST & DRAG VS MACH NUMBER
EFFECT OF ADDING STUB WINGS AND FIN.
DRAG WITH WINGS AND FIN ADDED:
WING AREA = 374 FT²
WEIGHT = 8800 LB
$C_D = .01769 + .2066\ C_L^2$
SEA LEVEL
VARIABLE EXIT AREA
FIXED EXIT AREA
THRUST
20,000 FEET
FIXED EXIT AREA
SEA LEVEL
DRAG
20,000 FEET
NET THRUST AND DRAG ~ LB
7000
6000
5000
4000
3000
2000
1000
0
0
.2
.4
.6
.8
1.0
MACH NUMBER

FIG 4.20

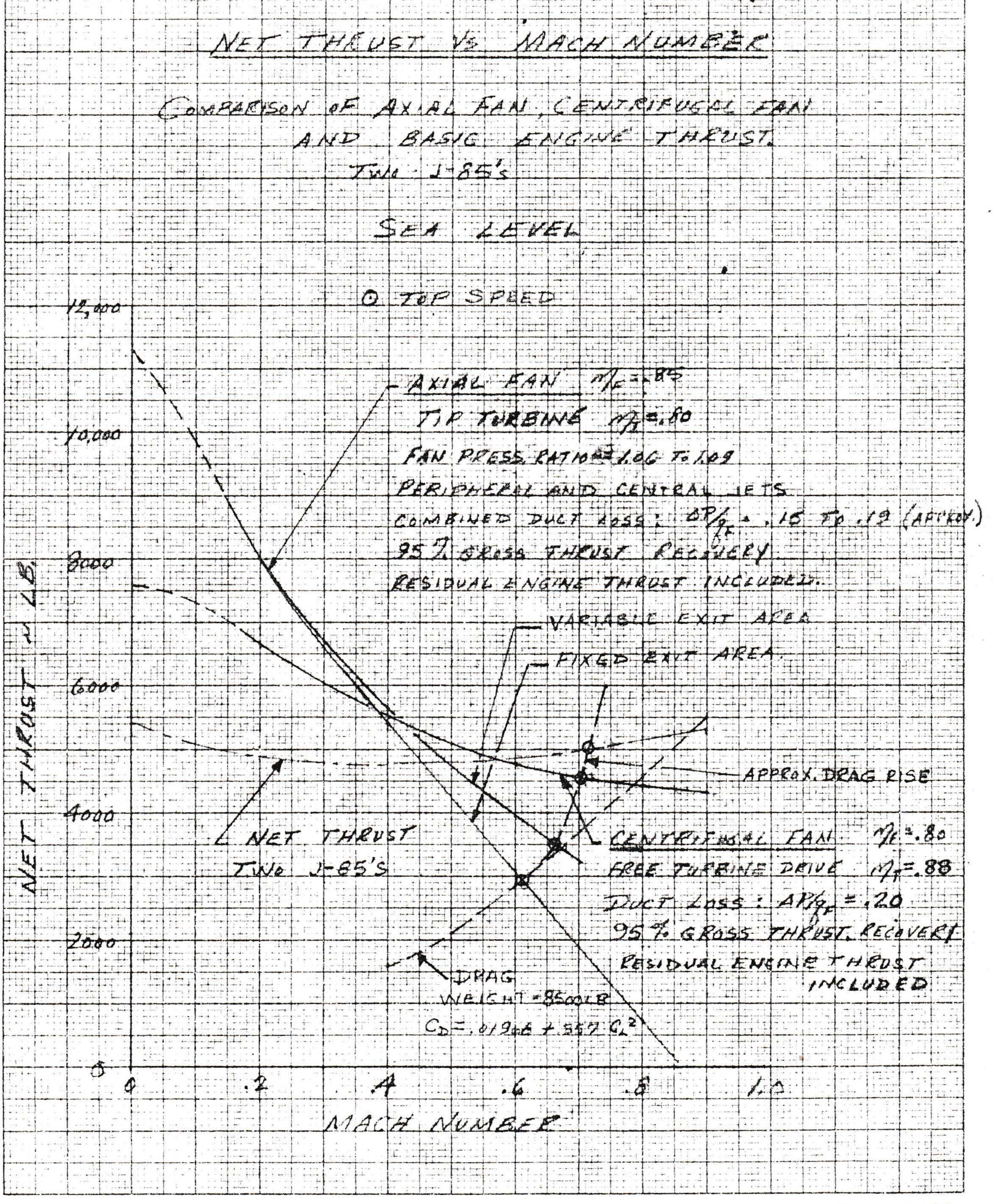
NET THRUST VS MACH NUMBER
COMPARISON OF AXIAL FAN, CENTRIFUGAL FAN AND BASIC ENGINE THRUST.
TWO J-85's
SEA LEVEL
⊙ TOP SPEED
AXIAL FAN η_F = .85
TIP TURBINE η_T = .80
FAN PRESS. RATIO = 1.06 TO 1.09
PERIPHERAL AND CENTRAL JETS
COMBINED DUCT LOSS: $\Delta P/q_F$ = .15 TO .19 (APPROX.)
95% GROSS THRUST RECOVERY
RESIDUAL ENGINE THRUST INCLUDED.
VARIABLE EXIT AREA
FIXED EXIT AREA
APPROX. DRAG RISE
NET THRUST TWO J-85'S
CENTRIFUGAL FAN η_F = .80
FREE TURBINE DRIVE η_T = .88
DUCT LOSS: $\Delta P/q_F$ = .20
95% GROSS THRUST RECOVERY
RESIDUAL ENGINE THRUST INCLUDED
DRAG
WEIGHT = 8500 LB
$C_D = .0196 + .557 C_L^2$
NET THRUST ~ LB.
12,000
10,000
8000
6000
4000
2000
0
0
.2
.4
.6
.8
1.0
MACH NUMBER

FIG. 4.21

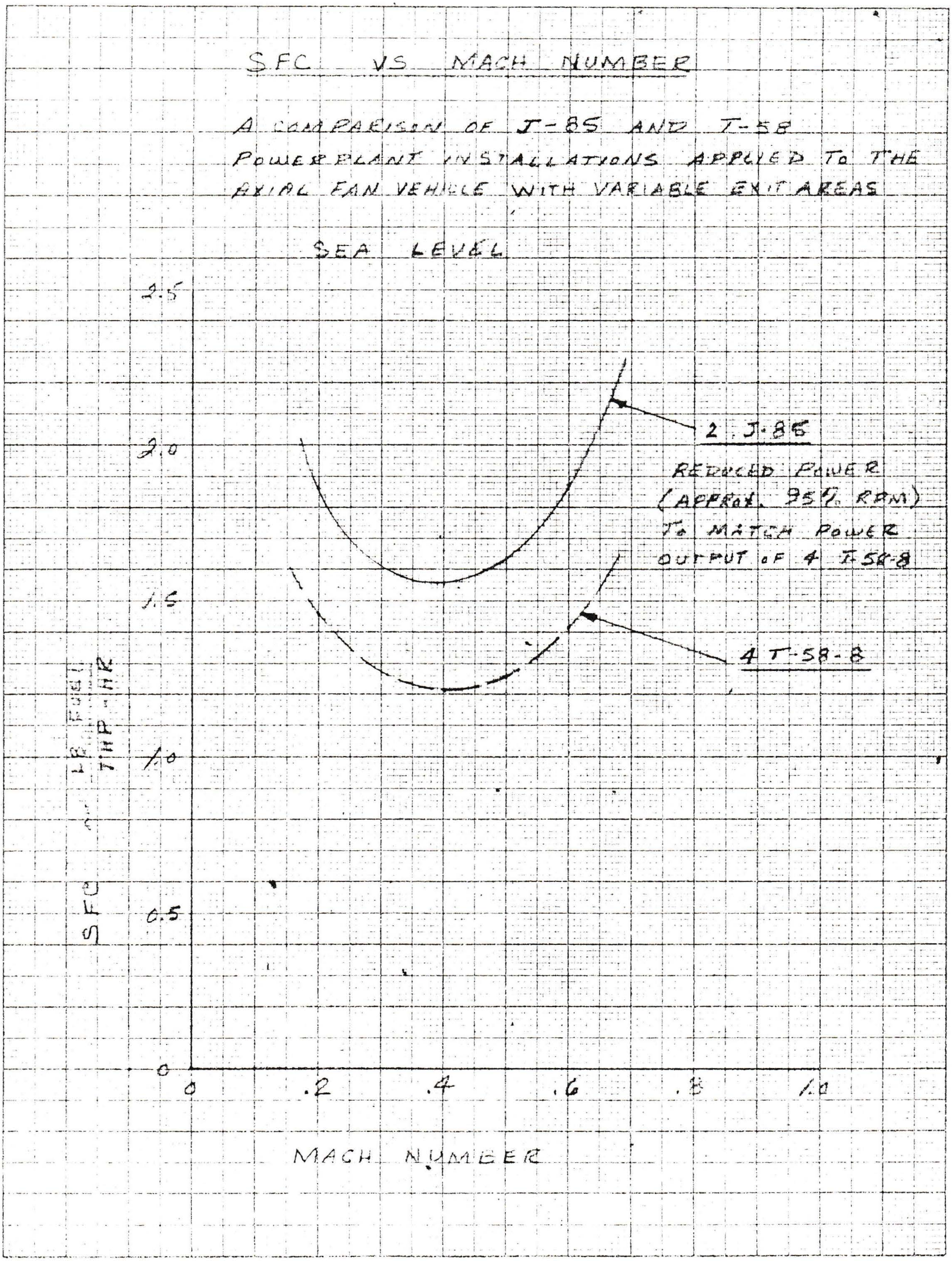
SFC VS MACH NUMBER
A COMPARISON OF J-85 AND T-58
POWERPLANT INSTALLATIONS APPLIED TO THE
AXIAL FAN VEHICLE WITH VARIABLE EXIT AREAS
SEA LEVEL
2.5
2.0
1.5
1.0
0.5
0
0
.2
.4
.6
.8
1.0
SFC ~ LB FUEL / THP - HR
MACH NUMBER
2 J-85
REDUCED POWER
(APPROX. 95% RPM)
TO MATCH POWER
OUTPUT OF 4 T-58-8
4 T-58-8

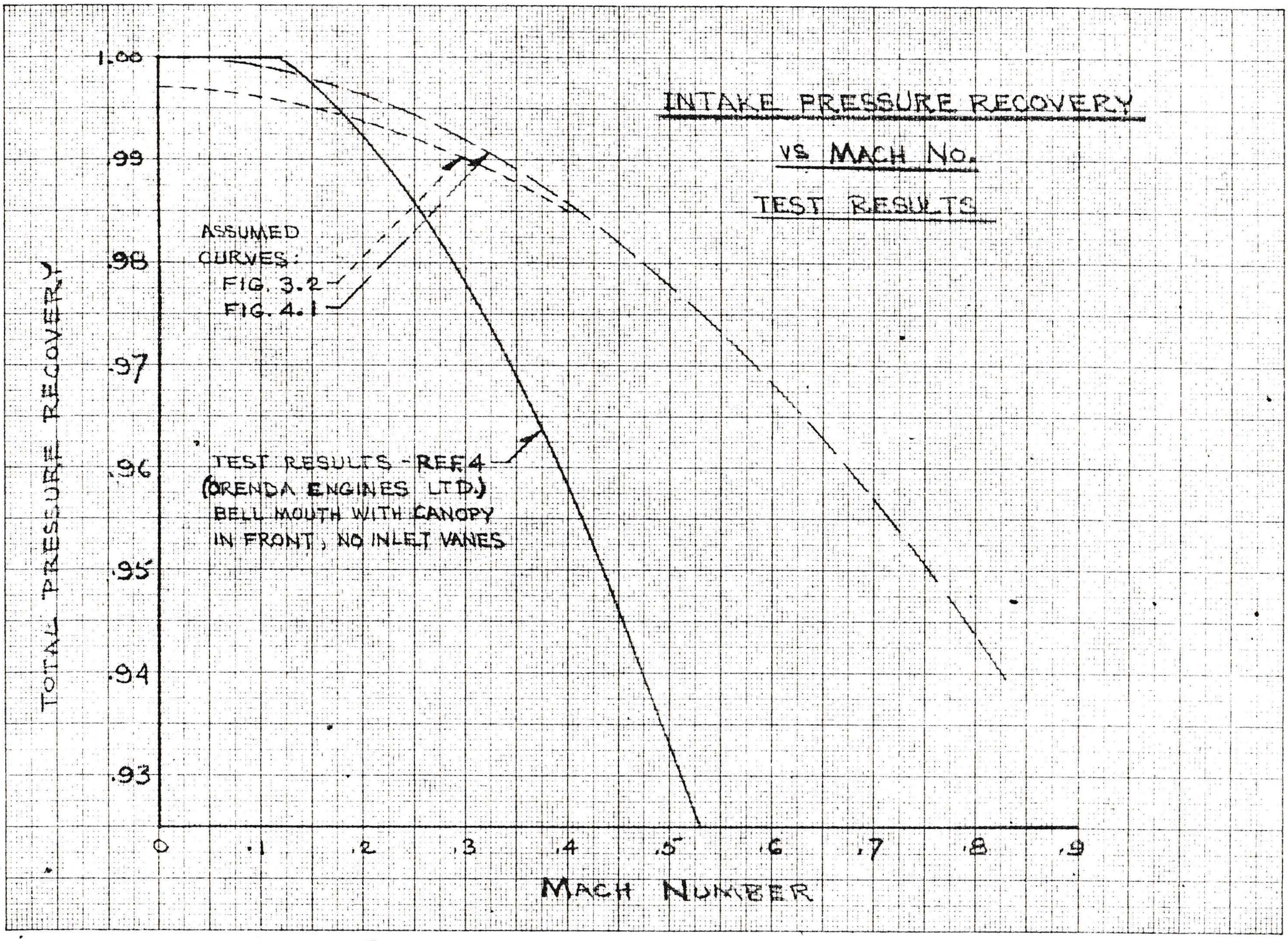
INTAKE PRESSURE RECOVERY
VS MACH No.
TEST RESULTS
ASSUMED CURVES:
FIG. 3.2
FIG. 4.1
TEST RESULTS - REF 4
(ORENDA ENGINES LTD.)
BELL MOUTH WITH CANOPY
IN FRONT, NO INLET VANES
TOTAL PRESSURE RECOVERY
1.00
.99
.98
.97
.96
.95
.94
.93
0
.1
.2
.3
.4
.5
.6
.7
.8
.9
MACH NUMBER

FIG 4.23

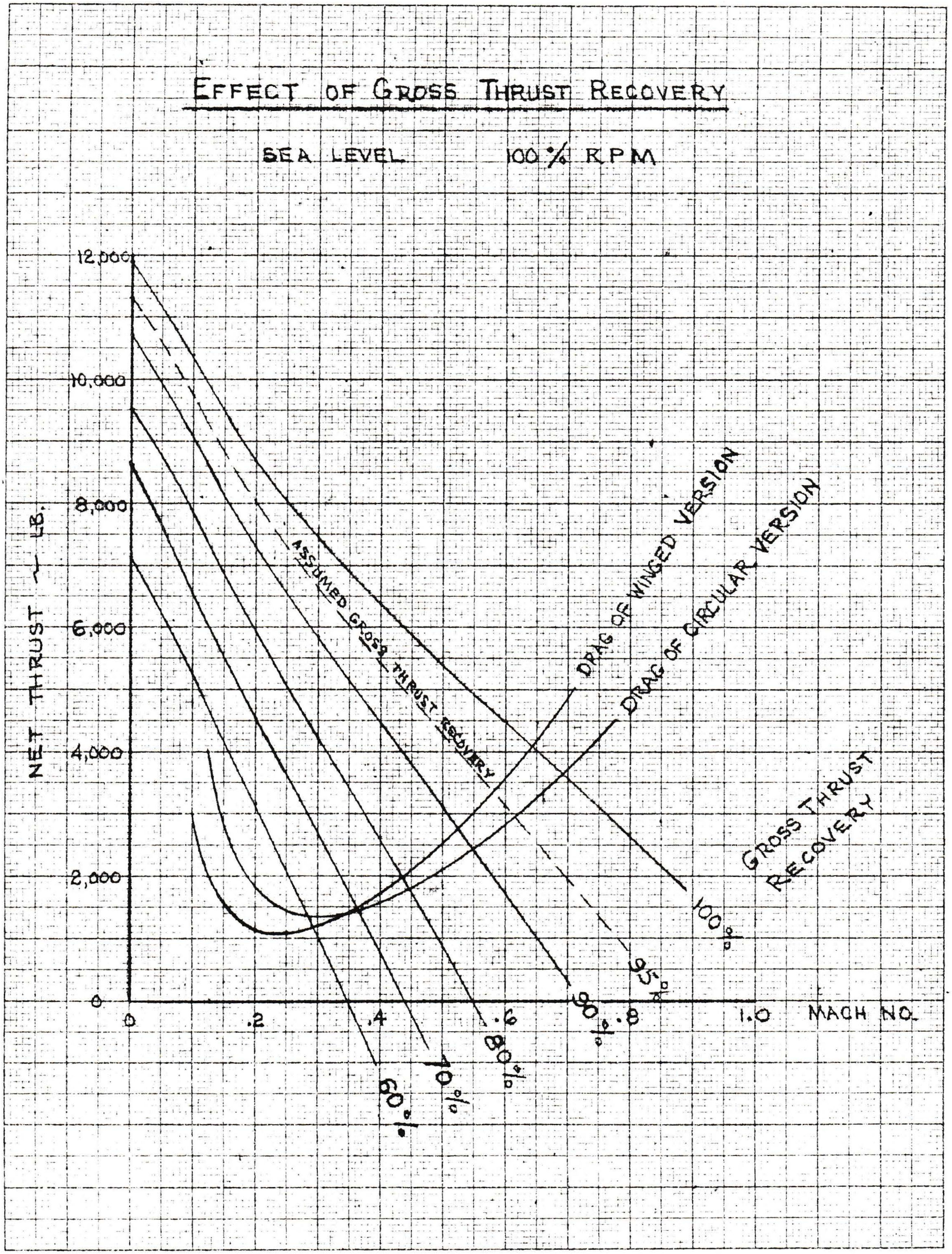

EFFECT OF GROSS THRUST RECOVERY
SEA LEVEL 100% RPM
NET THRUST ~ LB.
12,000
10,000
8,000
6,000
4,000
2,000
0
0
.2
.4
.6
.8
1.0
MACH NO.
ASSUMED GROSS THRUST RECOVERY
DRAG OF WINGED VERSION
DRAG OF CIRCULAR VERSION
GROSS THRUST RECOVERY
100%
95%
90%
80%
70%
60%

10 X 10 TO THE 1/2 INCH 359-12
KEUFFEL & ESSER CO.

FIG 4.24

APPENDIX 'A'

List of Illustrations

APPENDIX 'A'

LIFTING FAN THEORY

A.1 **Introduction**

A method is outlined for the analysis of lifting fan vehicles and takes into account such variables as horsepower, fan pressure ratio, fan area, nozzle exit area, and duct loss factor. The method is then applied to sea level static conditions to show the variation of thrust/HP considering all these variables.

A typical vehicle is analyzed next, which extends the previous work to include specific fuel consumption and the effects of forward speed and altitude.

Operation in the ground cushion is not considered.

A.2 **Theory**

The horsepower delivered to the fan can be found once the drive efficiency is known. Then with the introduction of fan pressure ratio and fan efficiency, the temperature rise through the fan is determined. Finally, the duct loss will establish the nozzle exit pressure and thrust.

For an adiabatic process the work done on a unit mass is given by the expression:

$$\text{work} = w\, C_p J \Delta T$$

$$\text{or HP} = \frac{w\, C_p J \Delta T}{550}$$

Therefore, airflow $w = \dfrac{1.637 \times HP}{\Delta T}$ lb/sec.

where ΔT is the temperature rise through the fan and is equal to

$$T_3 - T_2 = \frac{T_2}{\eta_F}\left[\left(\frac{P_3}{P_2}\right)^{\frac{\gamma-1}{\gamma}} - 1\right]$$

where T_2 = fan entrance temperature

T_3 = fan exit temperature

P_3/P_2 = fan pressure ratio = $\dfrac{\text{fan exit pressure}}{\text{fan entrance pressure}}$

η_F = fan efficiency

Theory (cont'd)

The shape of the exhaust passage determines the pressure losses incurred and by relating the total loss in the exhaust system to the dynamic pressure at the fan exit (q_F) the duct loss coefficient is produced.

$$K = \frac{\Delta P_{loss}}{q_F}$$

The nozzle exit total pressure

$$P_e = P_3 - \Delta P_{loss} = P_3 - Kq_F$$

when the fan area equals the nozzle exit area then:

$$q_F = q_e = P_e - p_a$$

where p_a = atmospheric pressure

Therefore, $P_e = P_3 - K\ (P_e - p_a) = \dfrac{P_3 + Kpa}{1 + K}$

However, if the fan area (A_f) is not equal to the nozzle exit area (A_e) then:

$$\Delta P_{loss} = \Delta P_f - \Delta P_e = K\left(\frac{A_e}{A_f}\right)^2 q_e$$

and $\Delta P_e = \dfrac{\Delta P_f}{\left[1 + K\left(\dfrac{A_e}{A_f}\right)^2\right]}$

Therefore, $P_e = \Delta P_e + p_a = \dfrac{\Delta P_f}{\left[1 + K\left(\dfrac{A_e}{A_f}\right)^2\right]} + p_a$

The pressure ratio (p_a/P_e) may now be found. Then neglecting ground effect, the gross thrust

$$F_g = \rho A_e V_j{}^3$$

$$\text{or} \quad F_g = \left(\frac{V}{\sqrt{T}}\right)\left(\frac{W\sqrt{T}}{g}\right) = \left[\frac{2JC_p}{g}\left(1 - \frac{1}{\left(\frac{P_e}{P_a}\right)^{\frac{\gamma-1}{\gamma}}}\right)\right]^{1/2} W\sqrt{T}$$

$$= 4.569\ (W\sqrt{T})\left[1 - \frac{1}{\left(P_e/_{pa}\right)^{.286}}\right]^{1/2}$$

A.2 Theory (cont'd)

Knowing the pressure ratio p_a/p_e, the values $\frac{V}{\sqrt{T}}$ and $\frac{W\sqrt{T}}{AP}$ may be read directly from air tables. The terms, $W, \sqrt{T}$ and P are known values.

Hence, gross thrust and nozzle exit area may be calculated. The fan area may also be determined from A_e/A_f.

In most cases not all of the gross thrust will be recoverable due to the direction of the thrust force. For example, a peripheral jet vehicle while hovering would probably have about 95% of the thrust force acting in a vertical direction. In addition, momentum drag may cause serious losses with forward flight. In forward flight the net thrust

$$T = F_g \text{ (gross thrust recovery factor) } - MV$$

where MV = momentum drag = mass airflow x flight speed in ft/sec.

A.3 Thrust per Horsepower - Sea Level Static

Considering the thrust equation in Section A.2, the nozzle exit total pressure depends on the fan pressure ratio, duct loss factor and the ratio A_e/A_f. Also, the temperature is a function of fan pressure ratio, fan efficiency and inlet temperature. The thrust equation is then completed by introducing airflow which is a function of HP from which thrust may be represented by T/HP. Also, since A_e and A_f are functions of airflow they may be written as A_e/HP and A_f/HP.

Graphs can then be plotted to show T/HP versus fan pressure ratio for various values of A_e/HP, A_f/HP as shown in Figs. A.1, A.2, A.3, and A.4 for

K = 0.1, 0.2, 0.3, and 0.4, respectively.

In Fig. A.5, net thrust per horsepower is plotted against fan pressure ratio for various Mach numbers at sea level with $A_e = A_f$. 100% gross thrust recovery is used.

Fig. A.6 shows a similar plot with 95% gross thrust recovery.

For all calculations, a fan adiabatic efficiency of 85% has been assumed.

A.4 Application of Theory to a Typical Vehicle

The vehicle chosen for this analysis was powered by two General Electric T58-GE-8 engines (1258 SHP each) which were driving an 85% efficient fan through a 95% efficient drive system. Fan pressure ratios ranging from 1.05 to 1.50 were considered:

The three following cases were studied:

(a)	Sea Level	M = 0 to M = .7
(b)	10,000 ft.	M = 0 to M = .7
(c)	20,000 ft.	M = 0 to M = .7

The basic results are plotted in the form of cruise thrust versus sea level static thrust (Figs. A.7 to A.9) and specific fuel consumption versus fan pressure ratio (Figs. A.12 to A.14).

Calculations were based on $A_e/A_f = 1.0$ which gives near optimum thrust for the type of duct systems used on peripheral jet vehicles.

A.4.1 Thrust

With $A_e = A_f$ it is seen from Figs. A.7 to A.9 that for any altitude, thrust optimization is obtained with pressure ratios below 1.05 for speeds up to M = 0.2. With increasing speed the fan pressure ratio required for thrust optimization increases, with a higher fan pressure ratio required for the higher loss system.

Figs. A.10 and A.11 show thrust versus fan pressure ratio for $A_e/A_f = 1.0$.

In Fig. A.10 a fan area of 3000 in.^{2} is used and the thrust shown for various duct loss factors. In Fig. A.11 thrust is shown for various fan areas with a duct loss factor of 0.3.

A.4.2 Specific Fuel Consumption

Specific fuel consumption is given in terms of lb. of fuel/THP hr.* As shown in Figs. A.12 to A.14, for optimum SFC the fan pressure ratio increases as forward speed increases, with the higher loss system optimum at a higher fan pressure ratio than the lower loss system. However, at the higher speeds the gain in SFC is negligible compared with increase in fan pressure ratio beyond the optimum. Altitude produces a slight decrease in SFC but the optimum fan pressure ratio remains nearly constant.

A.4.2 Specific Fuel Consumption (cont'd)

As would be expected, reducing ram pressure recovery and gross thrust recovery has its greatest effect at the higher Mach. numbers. This difference is shown in Fig. A.15. With a constant of 1.2 fan pressure ratio and duct loss factor of .3, the combined effect of 80% ram pressure recovery and 95% gross thrust recovery reduces the SFC by about 5% while moving the minimum value of SFC from M = .32 to M = .4.

In Fig. A.16, various combinations of ram pressure recovery and gross thrust recovery have been assumed with a fan pressure ratio of 1.2 and duct loss factor of 0.3. These SFC curves are compared to those for typical T58 and Tyne turboprop installations. A similar comparison using 1.5 fan pressure ratio is shown in Fig. A.17.

Fig. A.18 compares the SFC of a typical T58 turboprop installation with the SFC of loss free T58 powered fan vehicles, with various fan pressure ratios.

A.5 Central Jets

Most of the lifting fan designs have had peripheral jets but some also make use of a central jet. This is an advantage, as far as internal aerodynamics go, because it usually means that that portion of the fan air passing out the central jet has suffered less duct loss. It follows then that with a central jet a vehicle can be expected to produce more thrust per horsepower.

Central jets are particularly useful during hovering and low speed operation. The additional exit area and the low loss passage leading to it encourages the fan to pass a large mass flow of air at a low pressure ratio. This produces maximum gross thrust.

In cruising flight a higher fan pressure ratio is desirable and this can be achieved by restricting the nozzle area. If the peripheral nozzles were restricted the duct losses in the system could be further reduced but this would be mechanically awkward and only useful if the central jet was aft facing. It might also reduce the power of the pilot's controls. A simple solution is to close off the central jet, or reduce its area while deflecting it rearward.

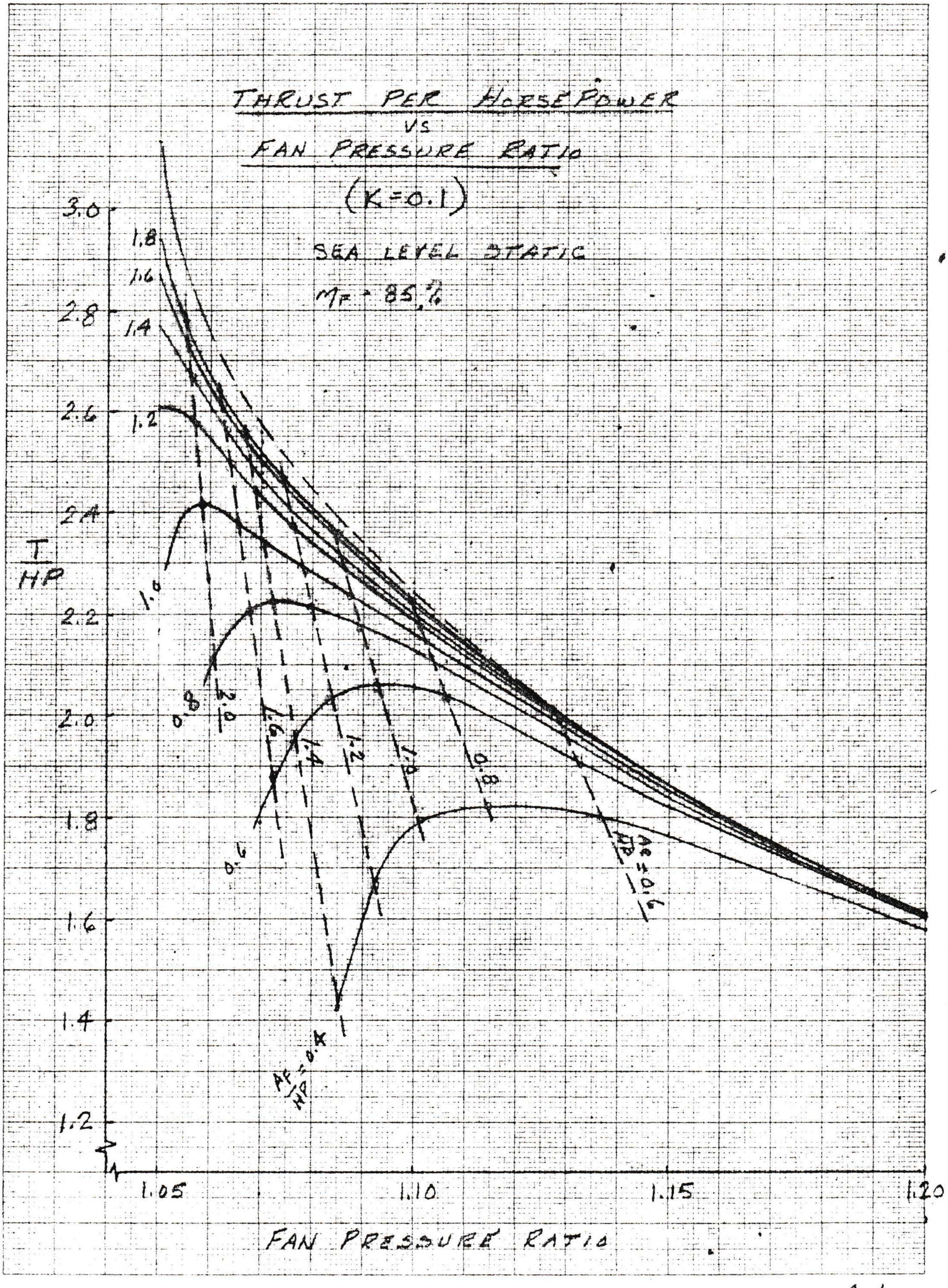
THRUST PER HORSEPOWER
VS
FAN PRESSURE RATIO
(K=0.1)
SEA LEVEL STATIC
η_F = 85%
T/HP
FAN PRESSURE RATIO
3.0
2.8
2.6
2.4
2.2
2.0
1.8
1.6
1.4
1.2
1.05
1.10
1.15
1.20
1.8
1.6
1.4
1.2
1.0
0.8
0.6
2.0
1.6
1.4
1.2
1.0
0.8
AF/HP = 0.6
AF/HP = 0.4

FIG A.1

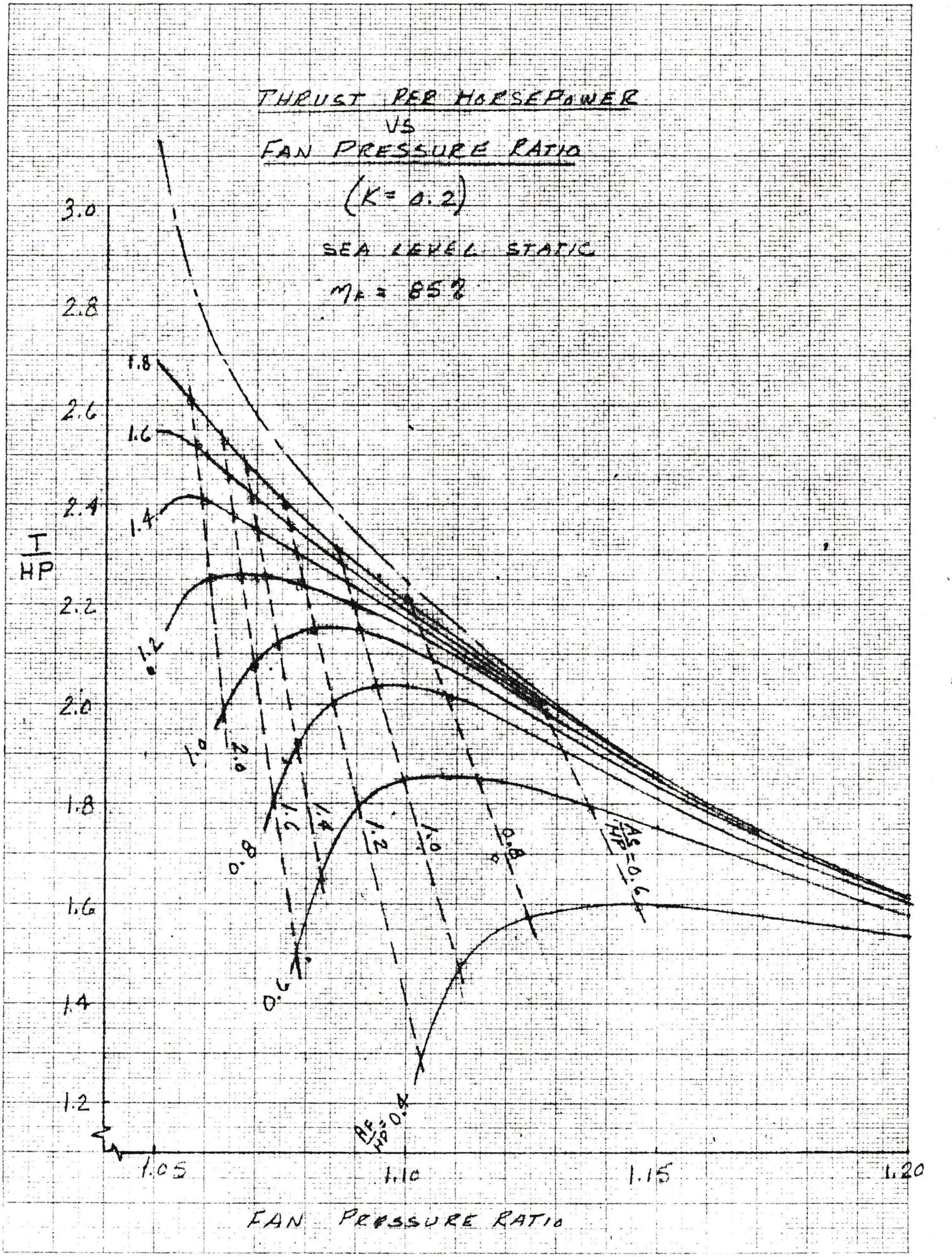
THRUST PER HORSEPOWER
VS
FAN PRESSURE RATIO
(K = 0.2)
SEA LEVEL STATIC
η_F = 85%
T/HP
3.0
2.8
2.6
2.4
2.2
2.0
1.8
1.6
1.4
1.2
1.05
1.10
1.15
1.20
FAN PRESSURE RATIO
$\frac{A_F}{HP}$ = 0.4
$\frac{A_S}{HP}$ = 0.6
10 X 10 TO THE CM. 359-14
KEUFFEL & ESSER CO.

FIG. A.2

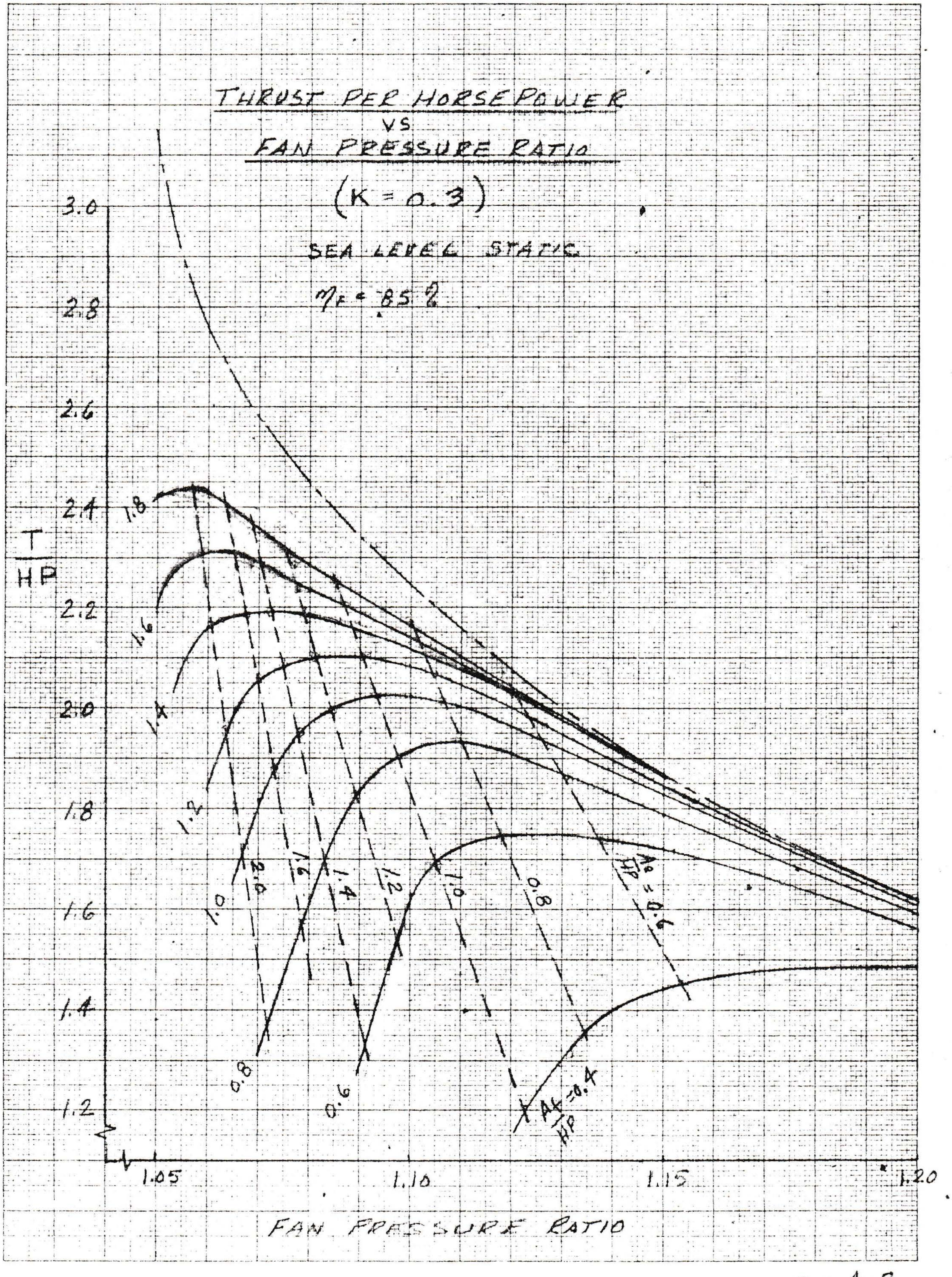
THRUST PER HORSEPOWER
VS
FAN PRESSURE RATIO
(K = 0.3)
SEA LEVEL STATIC
η_F = .85 %
T / HP
3.0
2.8
2.6
2.4
2.2
2.0
1.8
1.6
1.4
1.2
1.8
1.6
1.4
1.2
1.0
0.8
0.6
A_e/HP = 0.6
0.8
1.0
1.2
1.4
1.6
2.0
A_e/HP = 0.4
1.05
1.10
1.15
1.20
FAN PRESSURE RATIO

FIG. A-3

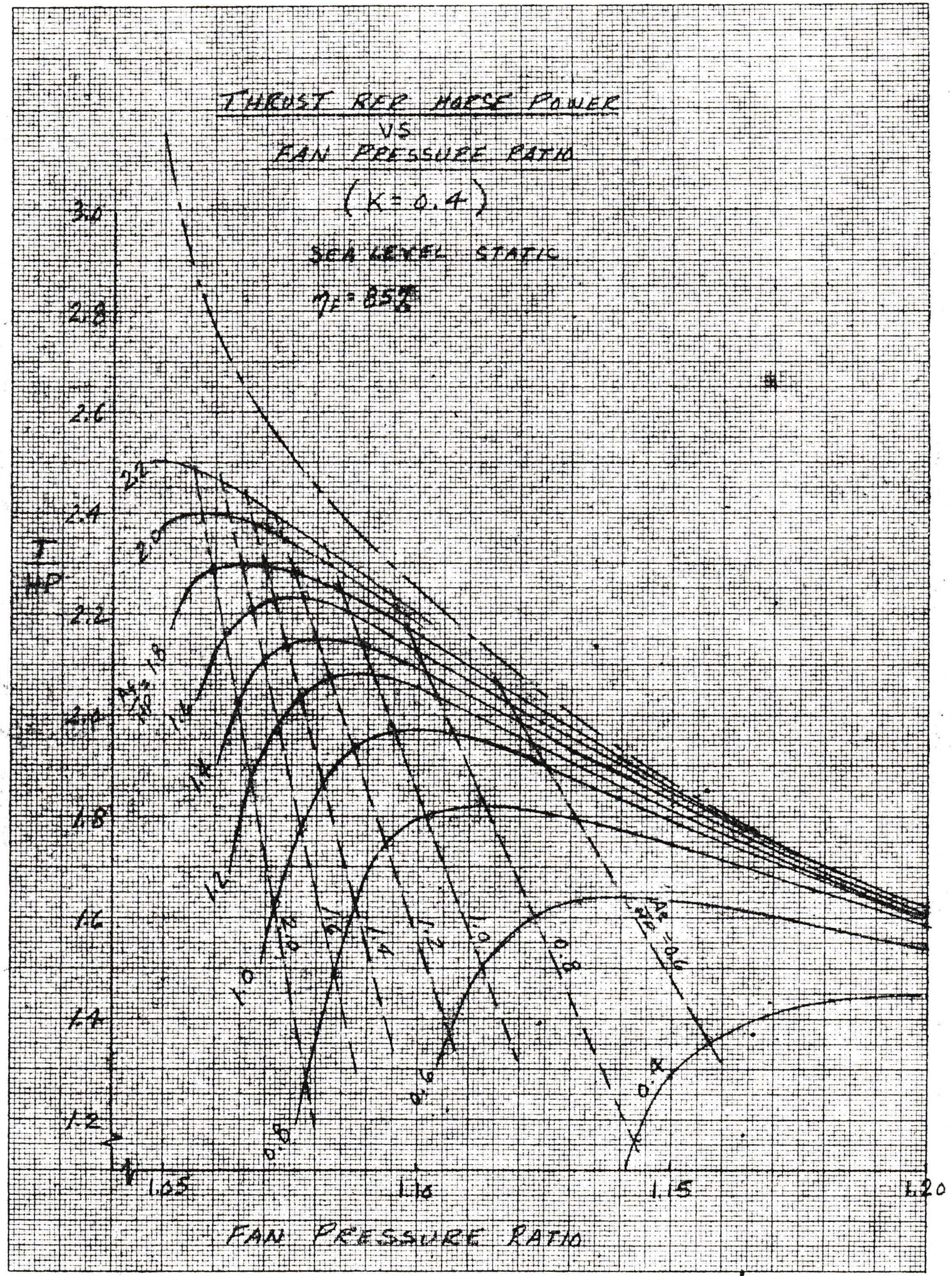

THRUST PER HORSE POWER
VS
FAN PRESSURE RATIO
(K = 0.4)
SEA LEVEL STATIC
T/HP
FAN PRESSURE RATIO
1.05
1.10
1.15
1.20

FIG. A.4

NET THRUST PER HORSEPOWER
VS
FAN PRESSURE RATIO

SEA LEVEL

100% GROSS THRUST RECOVERY
DUCT LOSS FACTOR K = 0.3
FAN AREA = NOZZLE EXIT AREA
η_F = 85%
NOTE: RESIDUAL ENGINE THRUST
NOT INCLUDED.

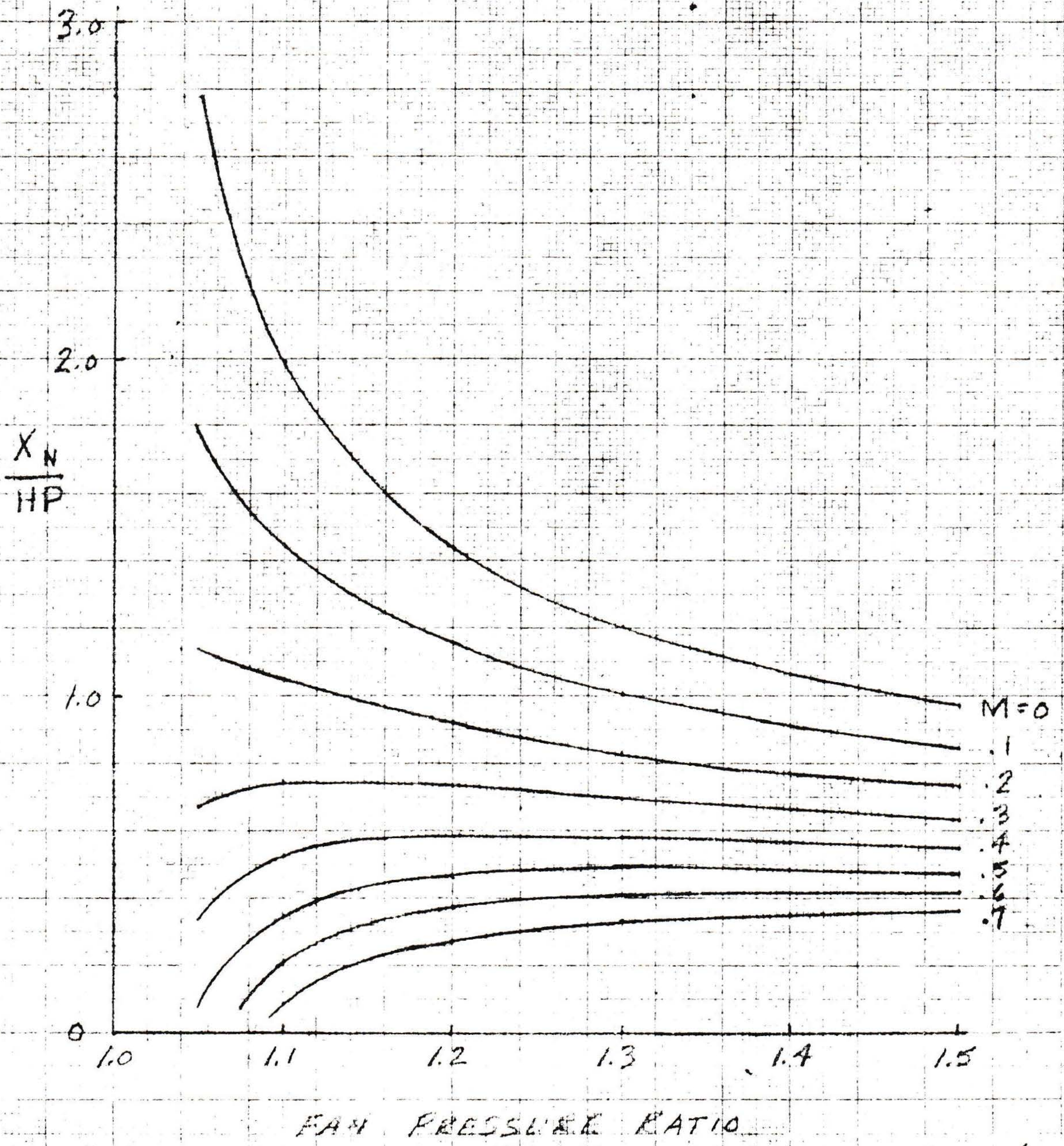

FIG. A.5

LB NET THRUST PER HORSEPOWER
VS
FAN PRESSURE RATIO

SEA LEVEL

95% GROSS THRUST RECOVERY
DUCT LOSS FACTOR K = 0.3
FAN AREA = NOZZLE EXIT AREA
η_F = 85%
NOTE: RESIDUAL ENGINE THRUST
NOT INCLUDED

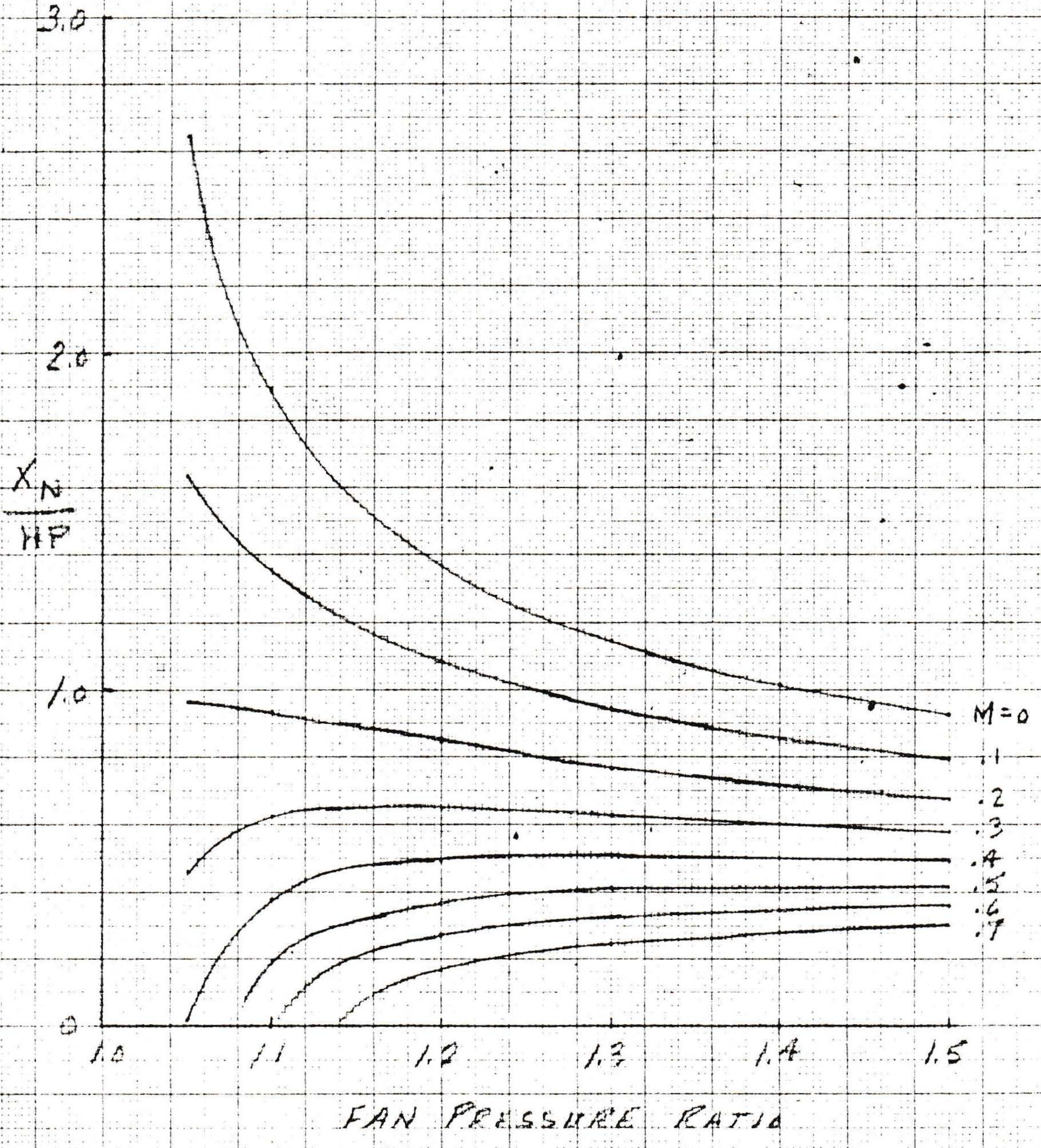

FIG. A.6

SEA LEVEL CRUISE THRUST VS SEA LEVEL STATIC THRUST

FOR VARIOUS MACH NUMBERS, DUCT LOSS FACTORS AND FAN PRESSURE RATIOS

TWO TSR-GE-8 ENGINES

NO LOSSES AT FAN INTAKE OR AT FINAL NOZZLE

MECHANICAL EFFICIENCY = 95%
FAN EFFICIENCY = 85%

FAN AREA = NOZZLE AREA

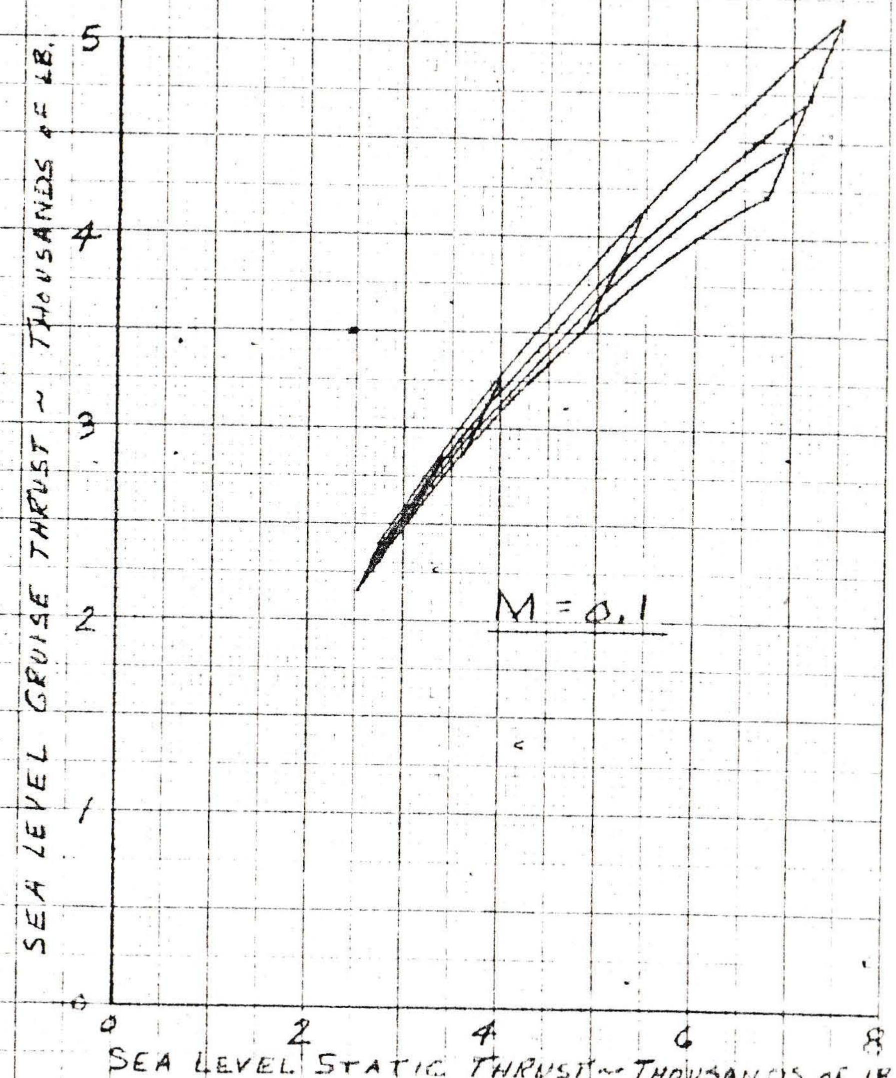

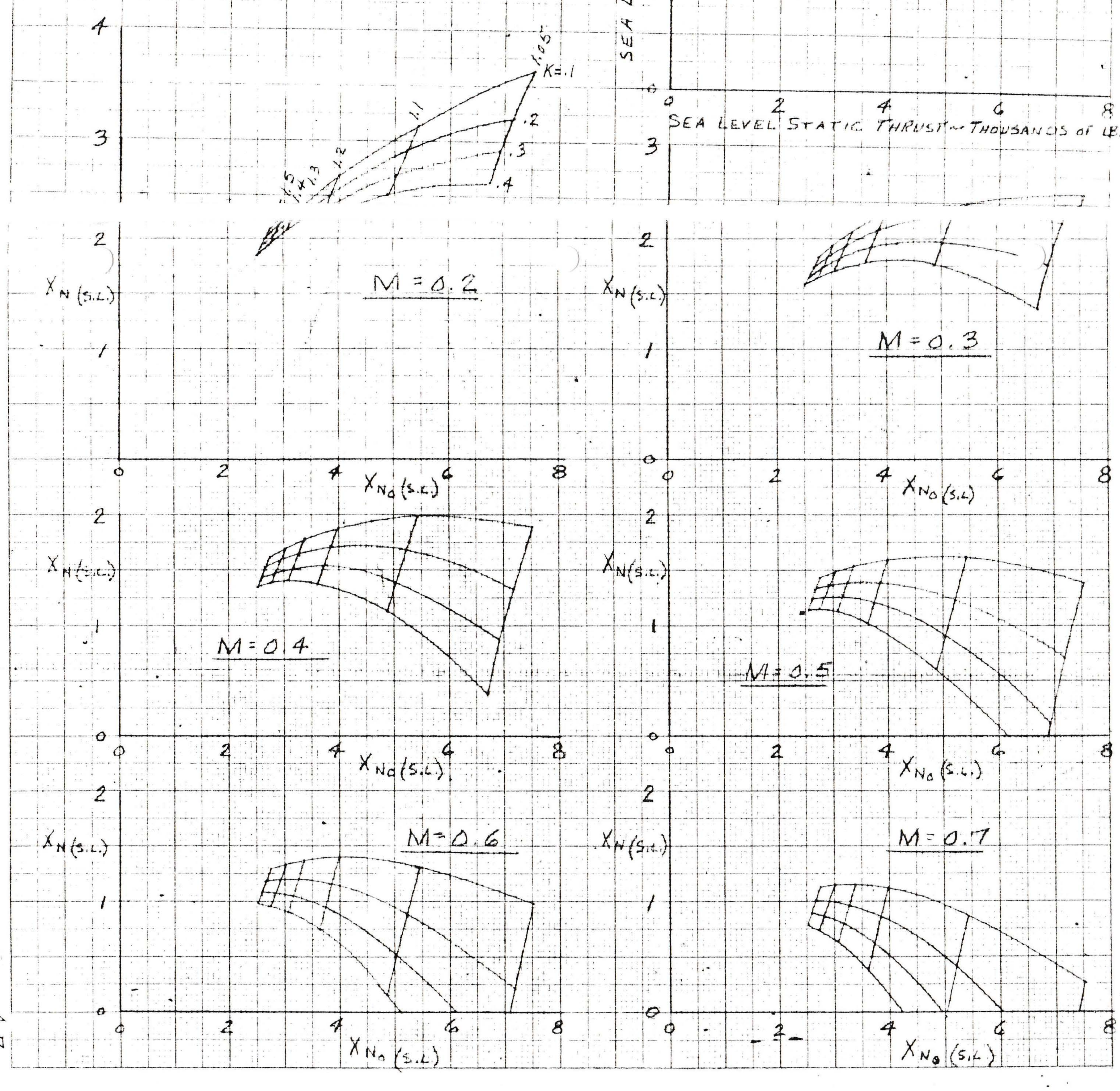

CRUISE THRUST AT 10000 FT. VS SEA LEVEL (STATIC) THRUST

FOR VARIOUS MACH NUMBERS, DUCT LOSS FACTORS & FAN PRESSURE RATIOS.

TWO T-58-GE-8 ENGINES
NO LOSSES AT FAN INTAKE OR AT FINAL NOZZLE.

MECHANICAL EFFICIENCY = 95%
FAN EFFICIENCY = 85%
FAN AREA = NOZZLE AREA

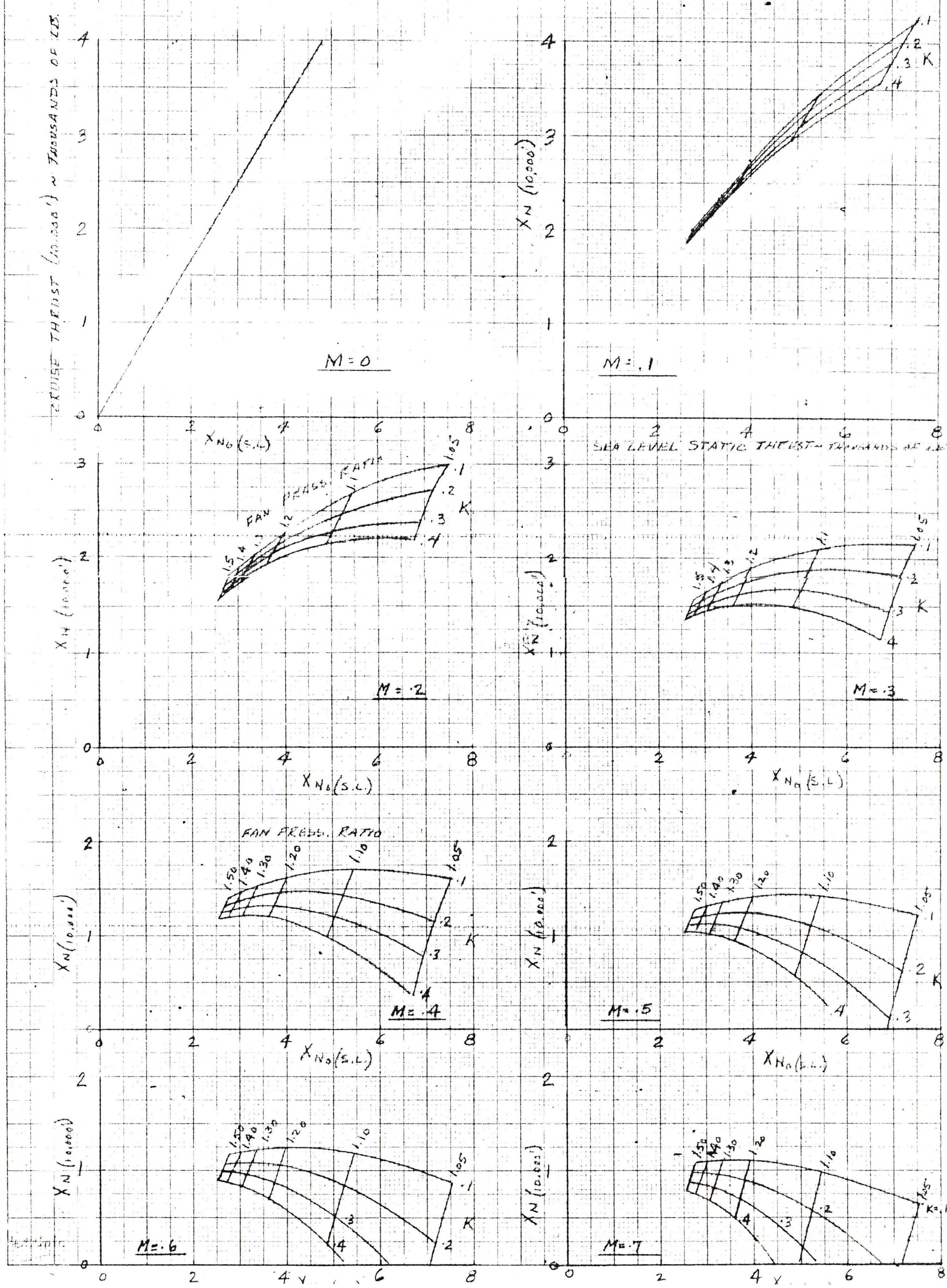

CRUISE THRUST AT 20,000 FT. VS SEA LEVEL STATIC THRUST

FOR VARIOUS MACH NUMBERS, DUCT LOSS FACTORS AND FAN PRESSURE RATIOS

TWO T58-GE-8 ENGINES
NO LOSSES AT FAN INTAKE OR AT FINAL NOZZLE
MECHANICAL EFFICIENCY = 95%
FAN EFFICIENCY = 85%
FAN AREA = NOZZLE AREA

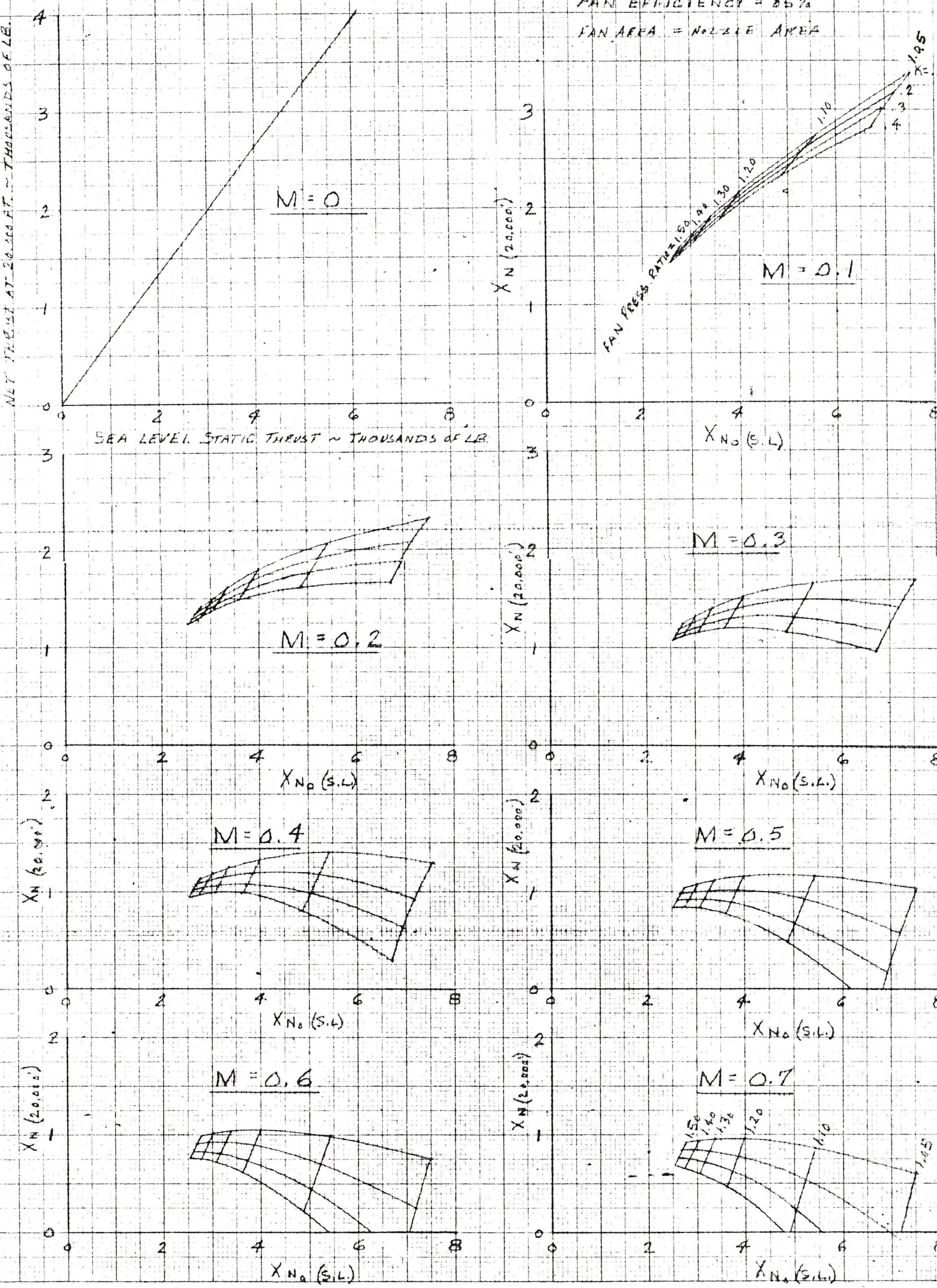

FIG. A.9

THRUST VS FAN PRESSURE RATIO

SEA LEVEL STATIC

FAN AREA = 3000 IN^2

TWO T-58-GE-8 ENGINES

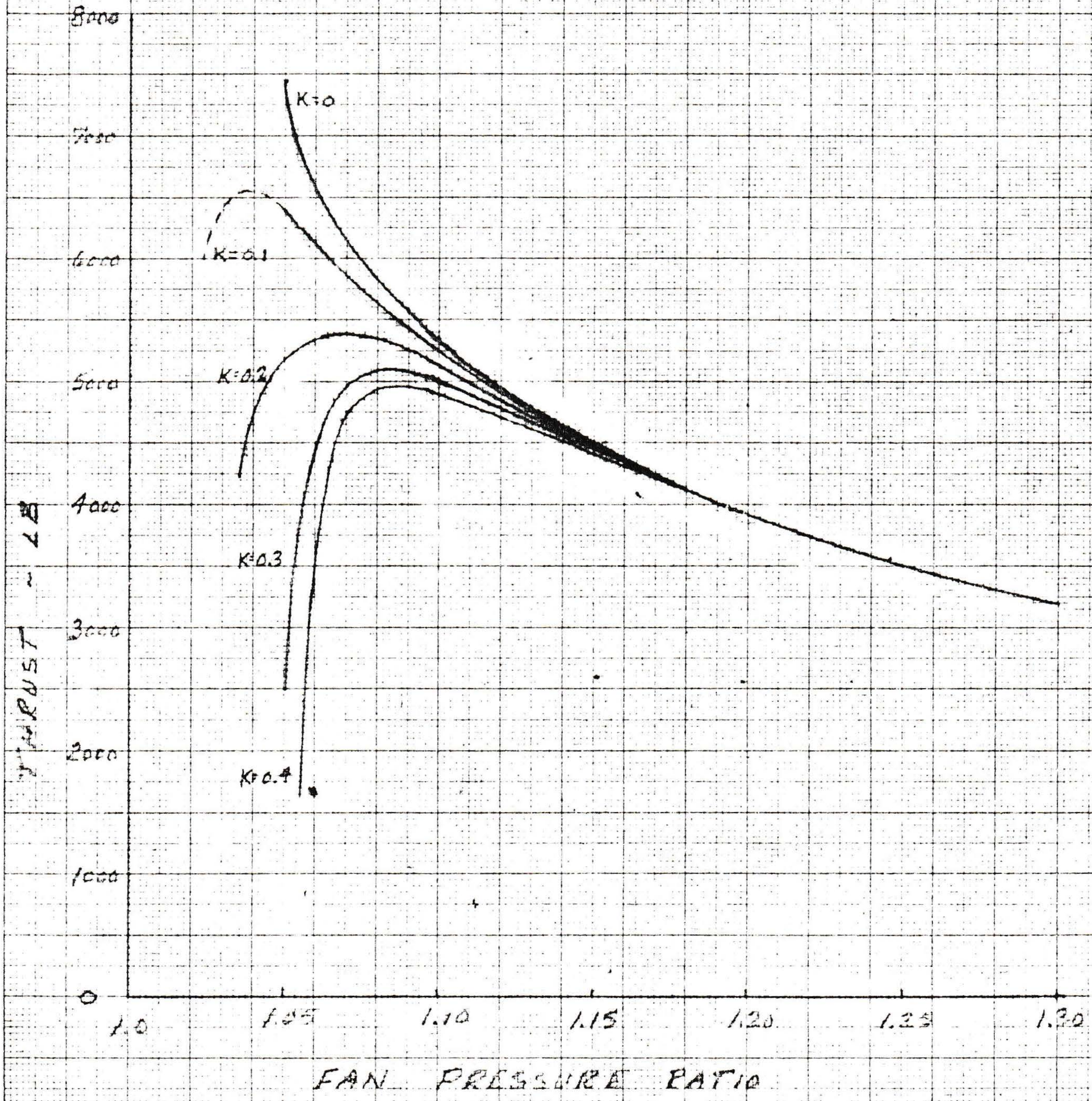

FIG. A.10

THRUST VS FAN PRESSURE RATIO

FOR VARIOUS FAN & NOZZLE EXIT AREAS

SEA LEVEL STATIC

DUCT LOSS FACTOR K = 0.3

TWO T-58-GE-8 ENGINE
MECHANICAL EFFICIENCY = 95%
FAN EFFICIENCY = 85%
NO LOSS AT INTAKE OR
AT FINAL NOZZLE

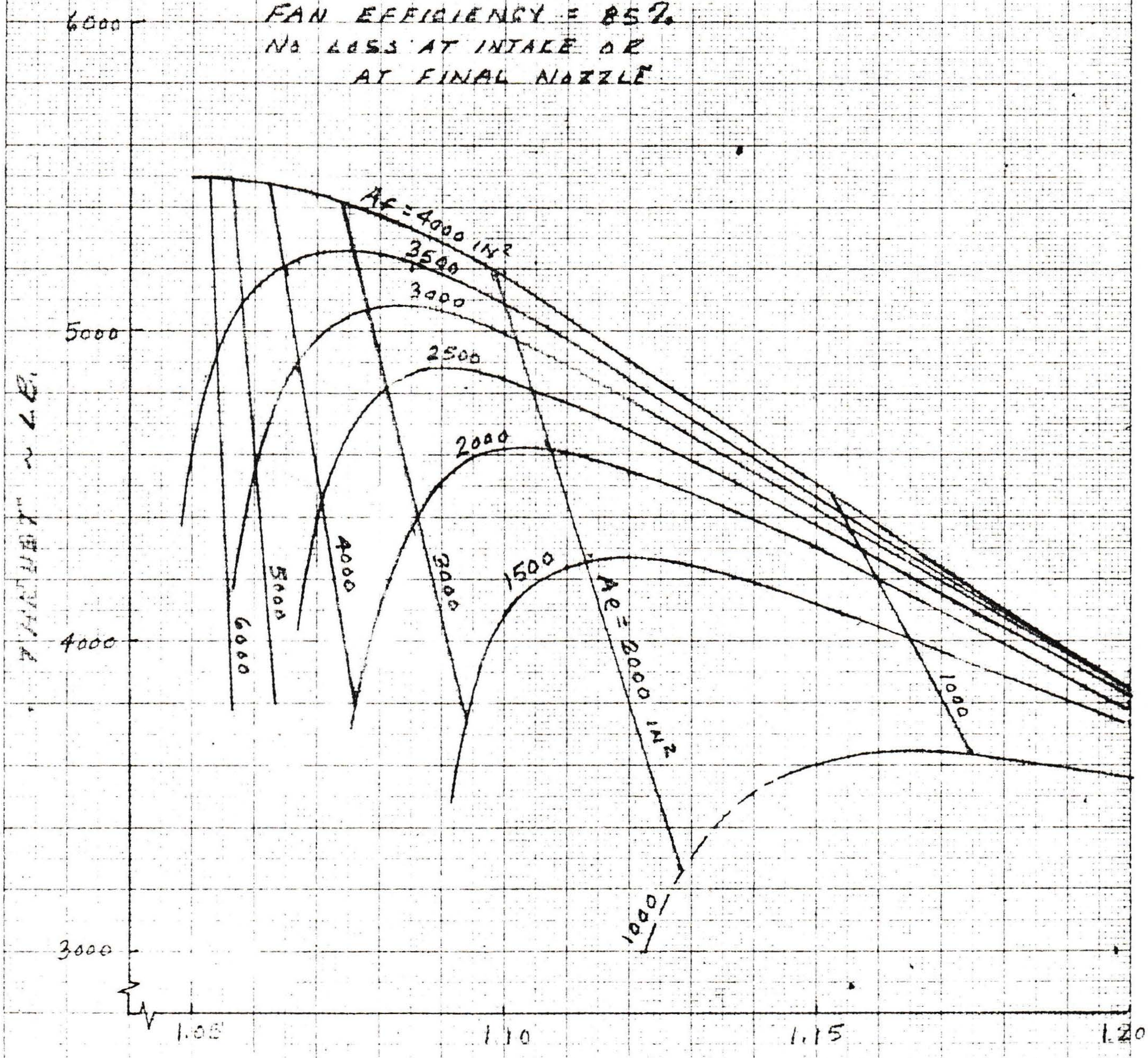

FIG A.11

SPECIFIC FUEL CONSUMPTION VS FAN PRESSURE RATIO

FOR VARIOUS MACH NUMBERS AND DUCT LOSS FACTORS AT SEA LEVEL

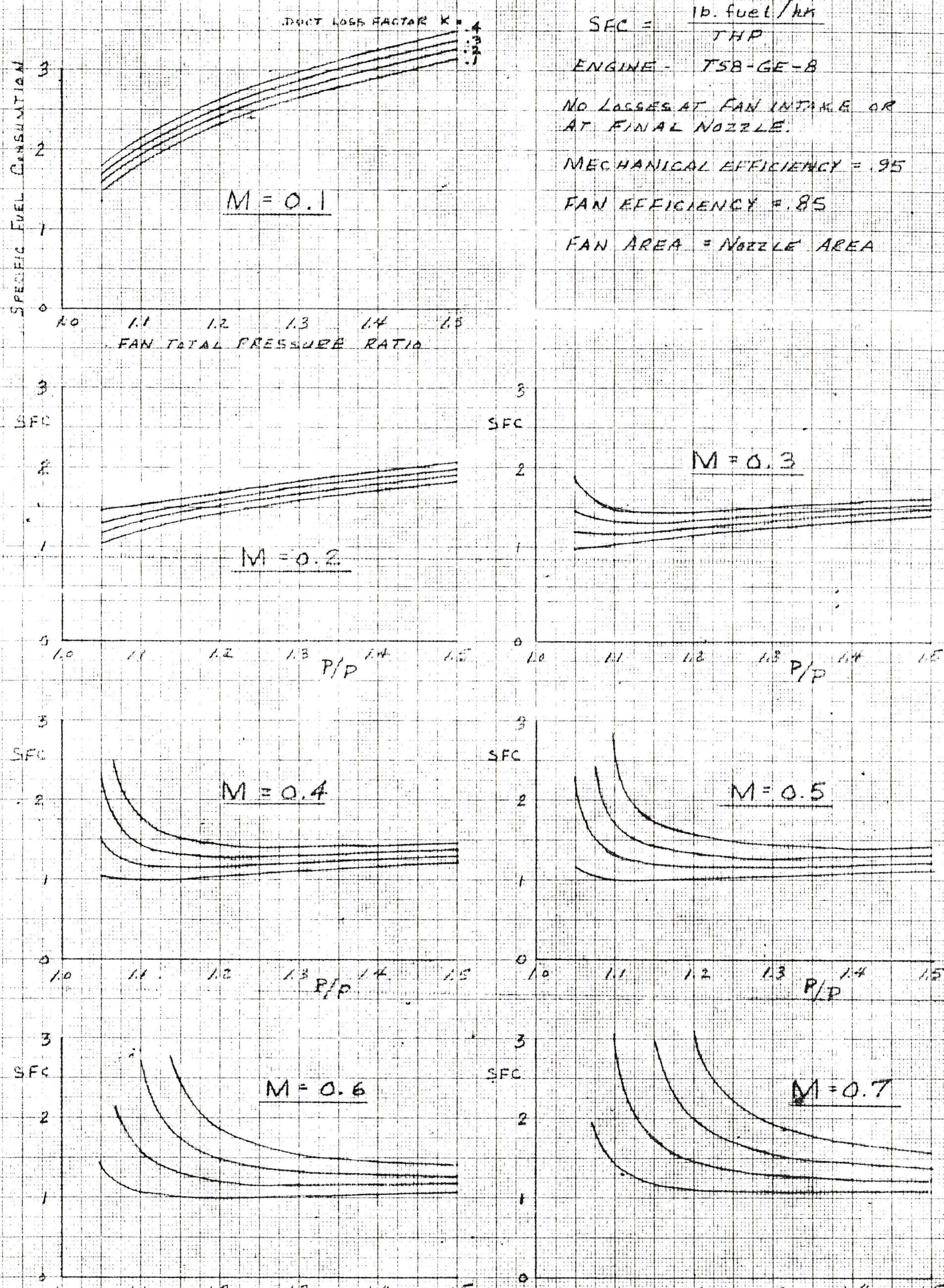

SPECIFIC FUEL CONSUMPTION v FAN PRESSURE RATIO

at various Mach no & duct loss factors AT 10000 ft

MECH EFF = .95

FAN EFF = .85

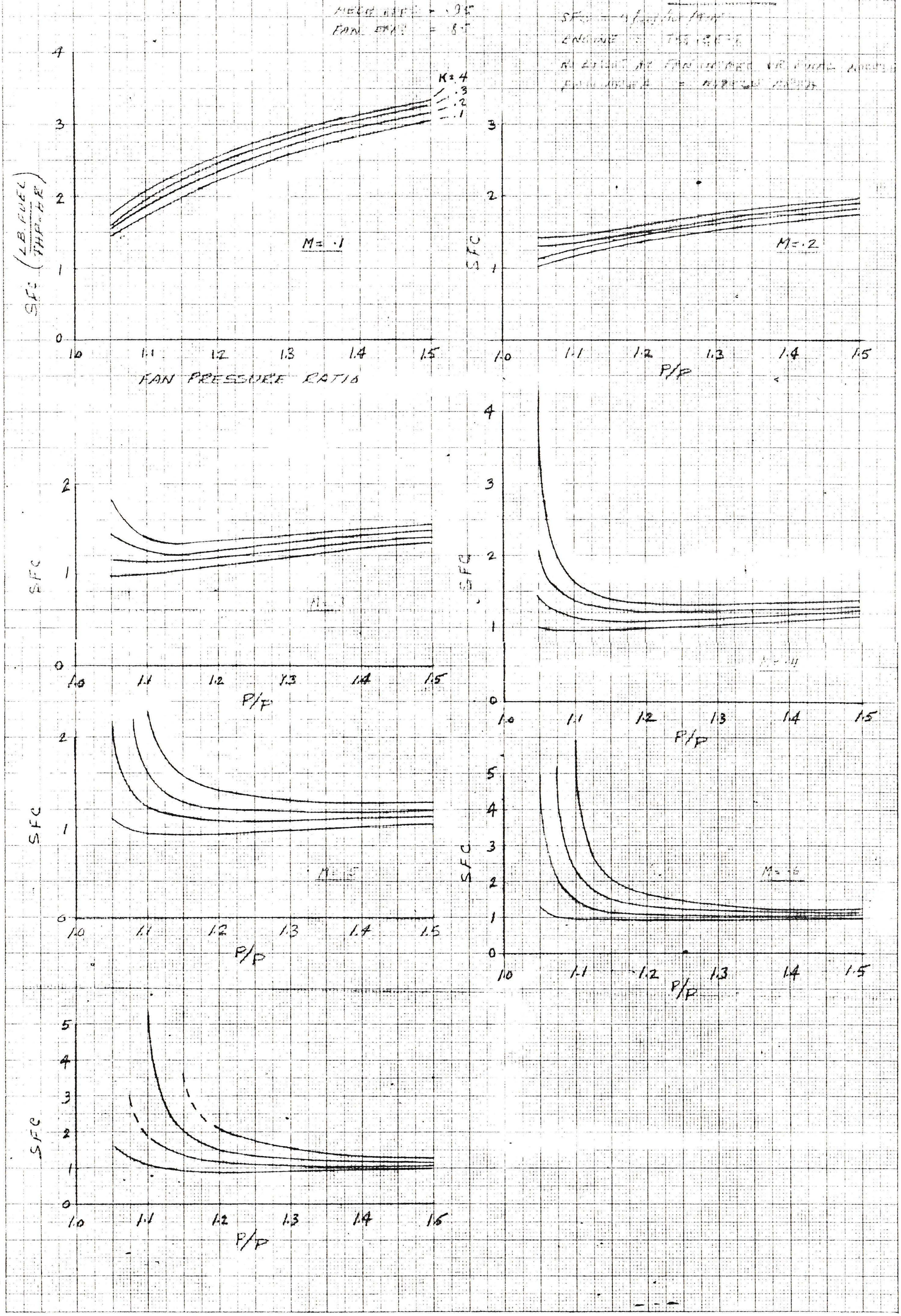

SPECIFIC FUEL CONSUMPTION VS FAN PRESSURE RATIO

FOR VARIOUS MACH NUMBERS AND DUCT LOSS FACTORS AT 20,000 FT.

$SFC = \dfrac{lb\ fuel/hr}{THP}$

ENGINE - T58-GE-8

NO LOSSES AT ENGINE OR FAN INTAKE OR AT FINAL NOZZLE.

MECHANICAL EFFICIENCY = .95

FAN EFFICIENCY = .85

FAN AREA = NOZZLE AREA

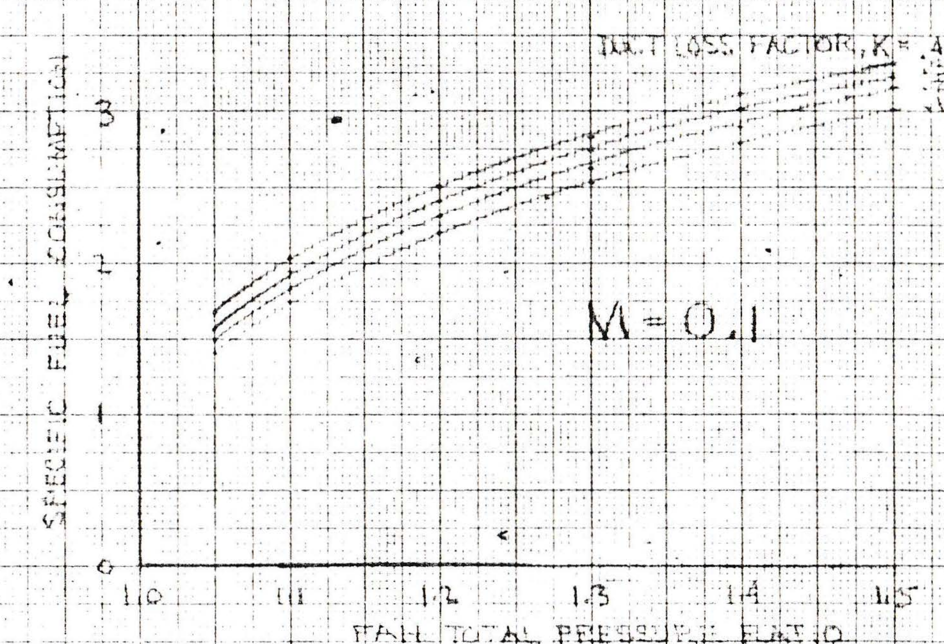

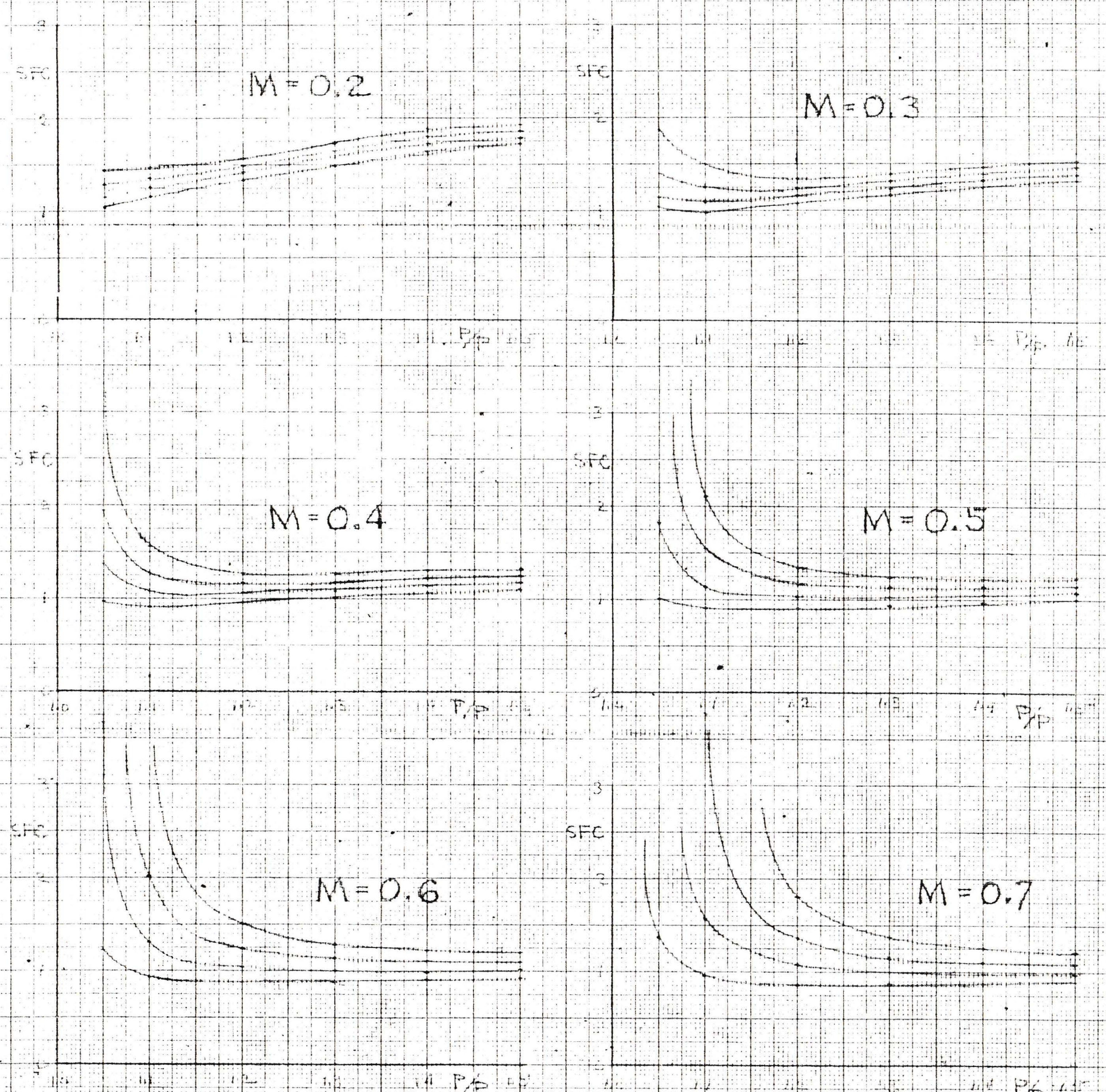

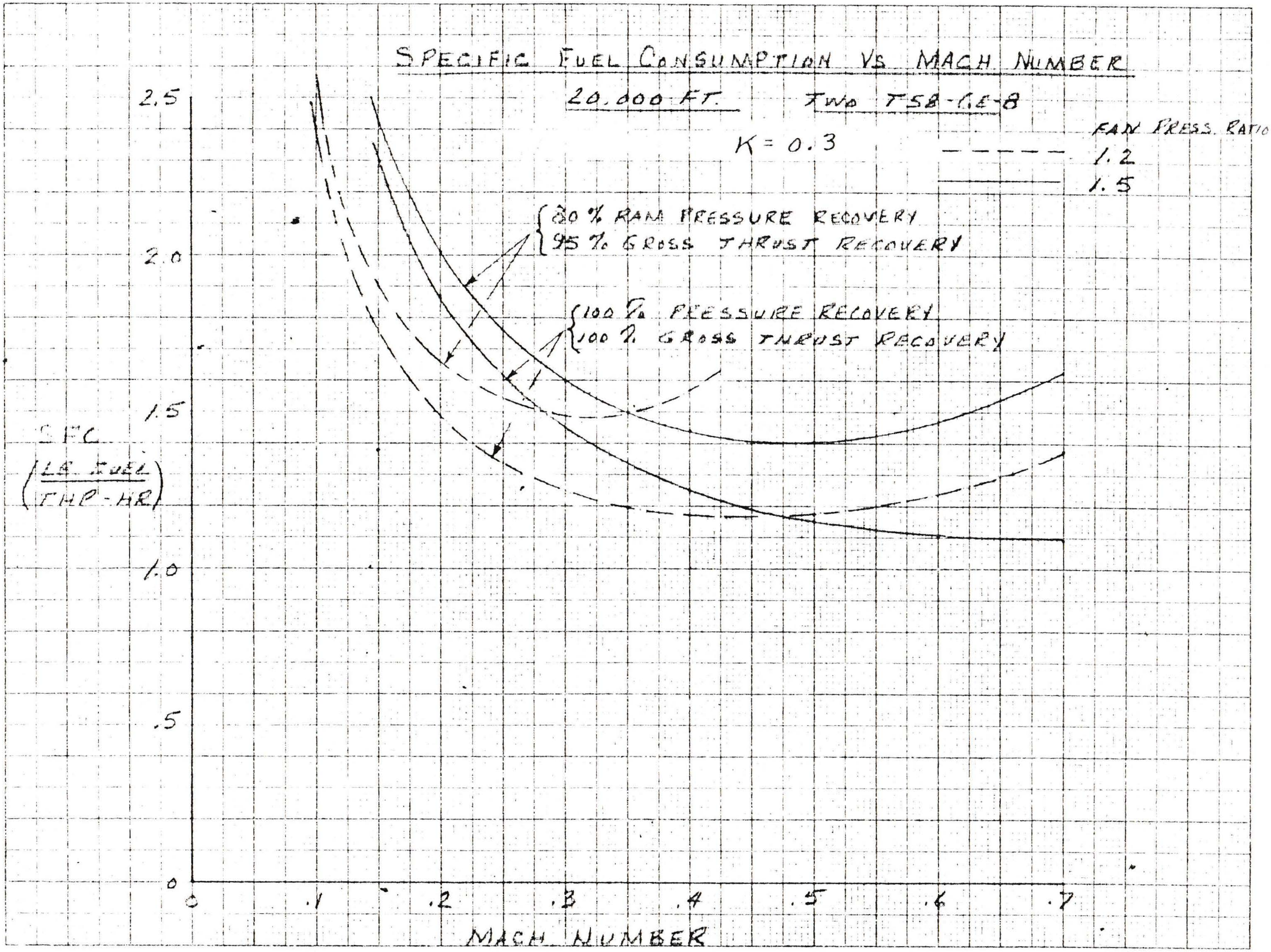
SPECIFIC FUEL CONSUMPTION VS MACH NUMBER
20,000 FT. TWO T58-GE-8
K = 0.3
FAN PRESS. RATIO
1.2
1.5
80 % RAM PRESSURE RECOVERY
95 % GROSS THRUST RECOVERY
100 % PRESSURE RECOVERY
100 % GROSS THRUST RECOVERY
SFC
LB. FUEL / THP-HR
2.5
2.0
1.5
1.0
.5
0
0
.1
.2
.3
.4
.5
.6
.7
MACH NUMBER

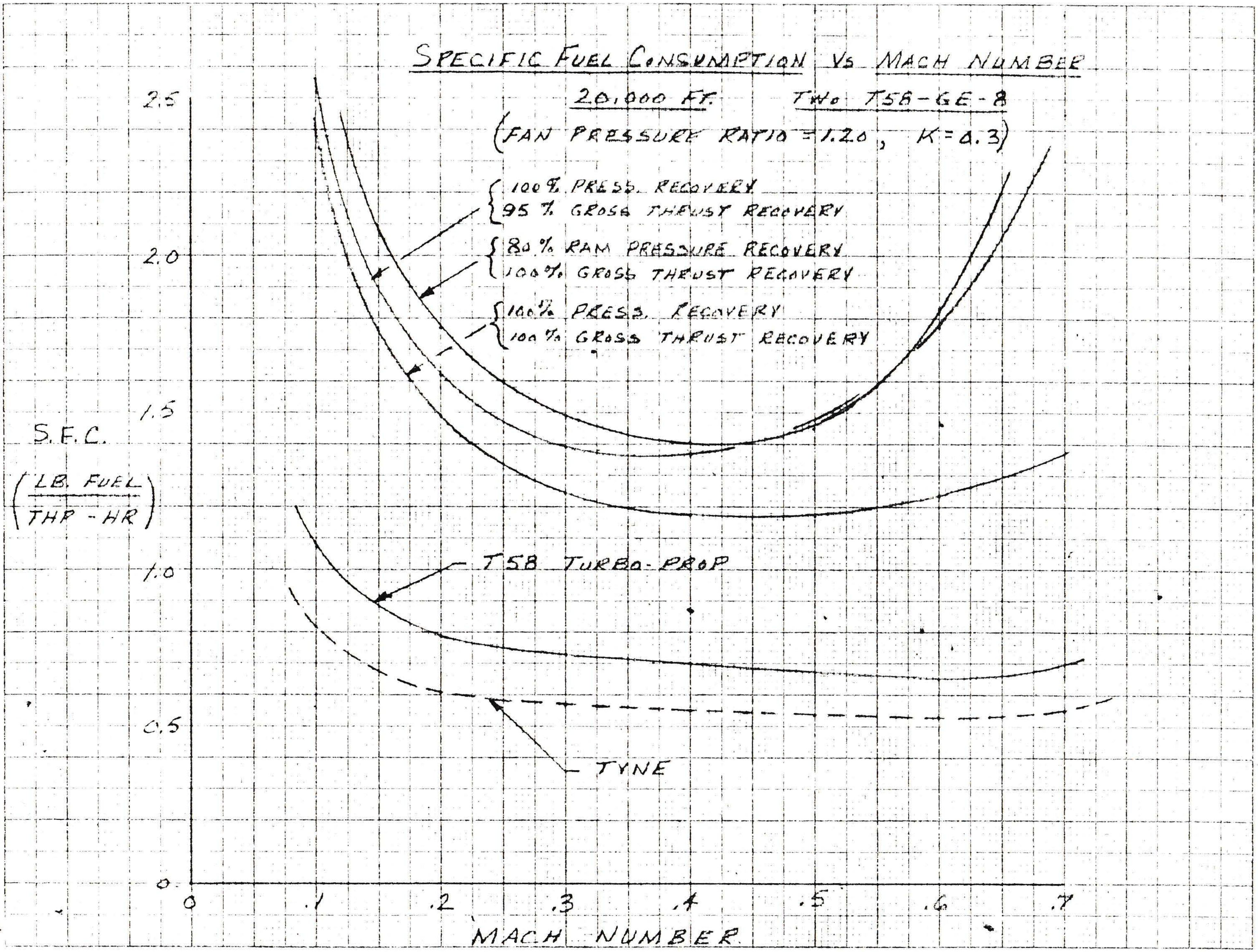

SPECIFIC FUEL CONSUMPTION Vs MACH NUMBER
20,000 FT. TWO T58-GE-8
(FAN PRESSURE RATIO = 1.20, K = 4.3)
100% PRESS. RECOVERY
95% GROSS THRUST RECOVERY
80% RAM PRESSURE RECOVERY
100% GROSS THRUST RECOVERY
100% PRESS. RECOVERY
100% GROSS THRUST RECOVERY
T58 TURBO-PROP
TYNE
S.F.C.
(LB. FUEL / THP - HR)
2.5
2.0
1.5
1.0
0.5
0
0
.1
.2
.3
.4
.5
.6
.7
MACH NUMBER

FIG. A.16

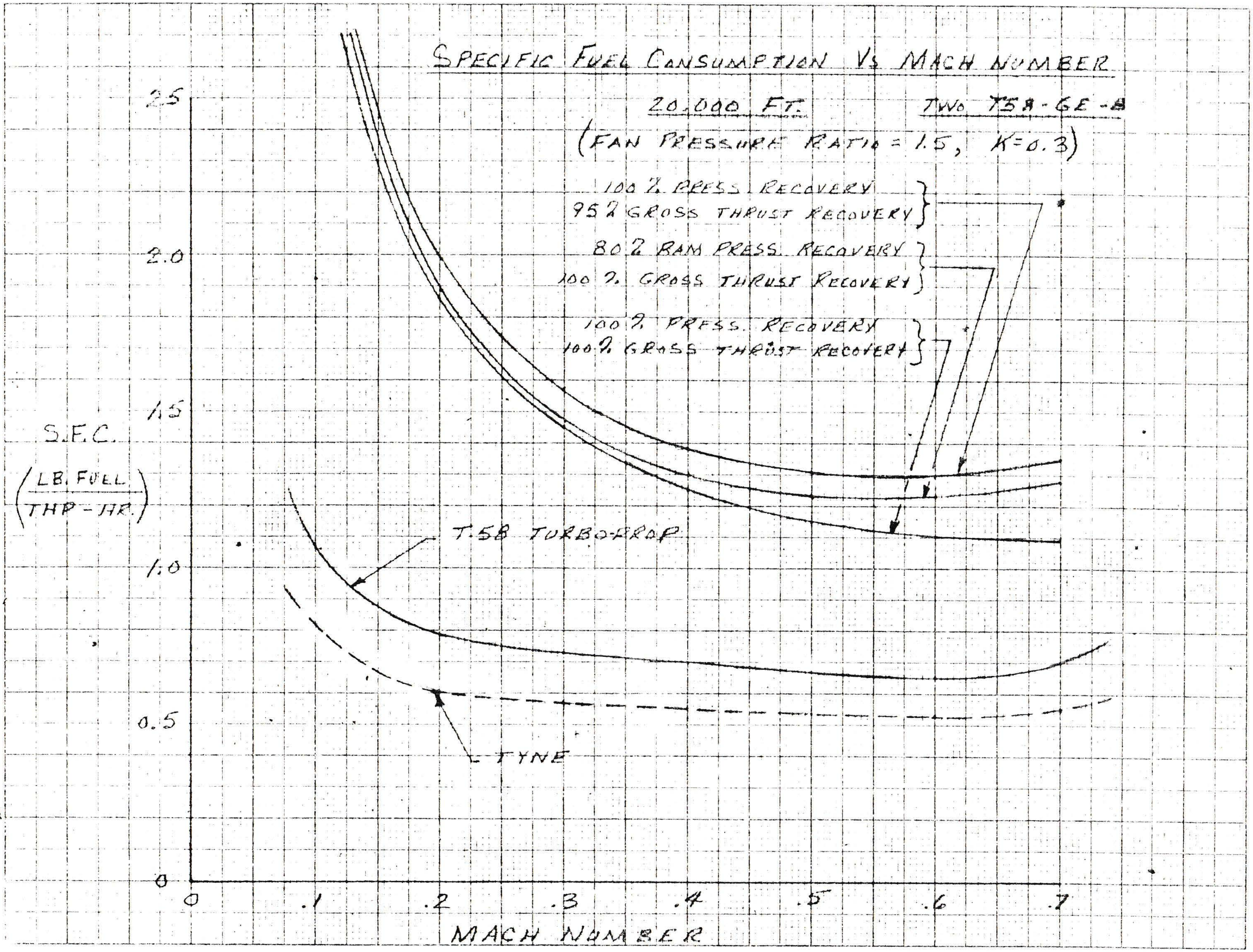
SPECIFIC FUEL CONSUMPTION VS MACH NUMBER
20,000 FT.
TWO T58-GE-8
(FAN PRESSURE RATIO = 1.5, K=0.3)
100 % PRESS. RECOVERY
95 % GROSS THRUST RECOVERY
80 % RAM PRESS. RECOVERY
100 % GROSS THRUST RECOVERY
100 % PRESS. RECOVERY
100 % GROSS THRUST RECOVERY
T-58 TURBO-PROP
TYNE
S.F.C.
(LB. FUEL / THP - HR.)
2.5
2.0
1.5
1.0
0.5
0
0
.1
.2
.3
.4
.5
.6
.7
MACH NUMBER

FIG. A.17

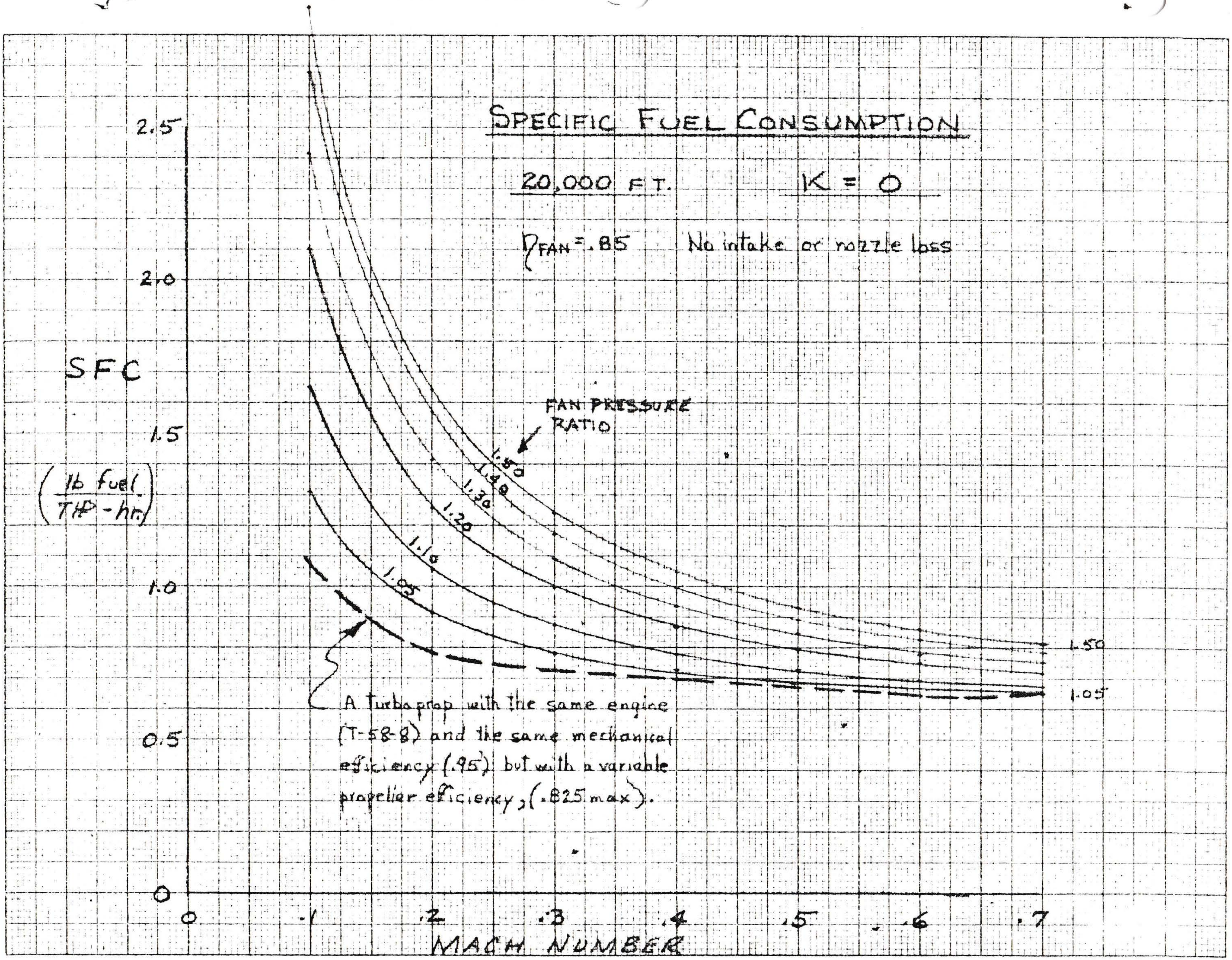
SPECIFIC FUEL CONSUMPTION
20,000 FT.
K = 0
ηFAN = .85
No intake or nozzle loss
SFC
(lb fuel / THP - hr.)
2.5
2.0
1.5
1.0
0.5
0
FAN PRESSURE RATIO
1.50
1.40
1.30
1.20
1.10
1.05
1.50
1.05
A turboprop with the same engine (T-58-8) and the same mechanical efficiency (.95) but with a variable propeller efficiency, (.825 max).
0
.1
.2
.3
.4
.5
.6
.7
MACH NUMBER

Fig. A.18